

2014

## MULTI-SPECIES INTERACTIONS IN FISH POPULATIONS ON THE NORTHWEST ATLANTIC COASTAL SHELF

Minho Kang  
*University of Rhode Island, minhokng@gmail.com*

Follow this and additional works at: <https://digitalcommons.uri.edu/theses>

Terms of Use

All rights reserved under copyright.

---

### Recommended Citation

Kang, Minho, "MULTI-SPECIES INTERACTIONS IN FISH POPULATIONS ON THE NORTHWEST ATLANTIC COASTAL SHELF" (2014). *Open Access Master's Theses*. Paper 356.  
<https://digitalcommons.uri.edu/theses/356>

This Thesis is brought to you by the University of Rhode Island. It has been accepted for inclusion in Open Access Master's Theses by an authorized administrator of DigitalCommons@URI. For more information, please contact [digitalcommons-group@uri.edu](mailto:digitalcommons-group@uri.edu). For permission to reuse copyrighted content, contact the author directly.

MULTI-SPECIES INTERACTIONS IN FISH POPULATIONS ON THE  
NORTHWEST ATLANTIC COASTAL SHELF

BY  
MINHO KANG

A THESIS SUBMITTED IN PARTIAL FULFILMENT OF THE  
REQUIREMENTS FOR THE DEGREE OF  
MASTER OF SCIENCE  
IN  
OCEANOGRAPHY

UNIVERSITY OF RHODE ISLAND

2014

MASTER OF SCIENCE THESIS  
OF  
MINHO KANG

APPROVED:

Major Professor:     Jeremy Collie

Thesis Committee:   Candace Oviatt

Gavino Puggioni

Michael Fogarty

Nasser H. Zawia

DEAN OF THE GRADUATE SCHOOL

UNIVERSITY OF RHODE ISLAND  
2014

## ABSTRACT

Multispecies interactions (predation and competition) are known to have important consequences for the dynamics of marine fish populations. These interactions depend on the spatial overlap among fish species in the community. Several approaches have been used to quantify species interactions, including production models and age- (or length) structured multispecies models. In this study, multi-species biomass dynamics models were extended to account for food-web interactions in multiple spatial areas (Gulf of Maine, Southern New England, and Georges Bank). A total of 15 fish species collected from the study areas were aggregated into four trophic groups: non-migrating benthivores (haddock, yellowtail flounder, winter flounder, and little skate), non-migrating piscivores (Atlantic cod and summer flounder), migrating piscivores (silver hake, spiny dogfish, winter skate, goosefish, pollock, and white hake), and migrating planktivores (Atlantic herring, Atlantic mackerel, longfin squid). The spatial distribution of each species group was determined from trawl-survey data, taking into account distributional shifts. We assumed that the migratory groups (planktivores and piscivores) range over the entire study area, such that their production can be described with a single set of model parameters ( $r$  and  $k$ ). By contrast, production of non-migrating groups (piscivores and benthivores) was assessed with a different set of model parameters ( $r$  and  $k$ ) for each spatial area. A hierarchical model fitting procedure was used to estimate the production parameters ( $r$  and  $k$ ) and interaction coefficients among migrating and non-migrating species groups. In our study, migrating groups (F and P) played a spatially essential role in species interactions across multiple areas, indicating that the three

spatial areas are functionally connected through the high degree of connectivity and direct linkages between migrating groups (F and P) and non-migrating groups (B and S). Our results demonstrate that accounting for trophic interactions improves the model fit and that the strength and direction of these interactions vary among spatial areas. Based on the area-specific interaction effects, this approach can help us understand the functional connections among multiple areas and thus inform current fisheries management.

## **ACKNOWLEDGMENTS**

I would like to thank my advisor, Dr. Jeremy Collie for his patience and helpful feedback throughout my time at GSO, and providing me with the great opportunity to work on this project (CAMEO).

I thank Kiersten Curti and Laurel Col for sharing the bottom trawl survey data for my thesis analysis. I also thank the many scientists who have contributed to the Northeast Fisheries Science Center's (NEFSC) bottom trawl survey.

Finally, I would like to thank my family, whose love and support have made me who I am today.

## TABLE OF CONTENTS

ABSTRACT.....	ii
ACKNOWLEDGMENTS .....	iv
TABLE OF CONTENTS.....	v
LIST OF TABLES .....	vi
LIST OF FIGURES .....	x
INTRODUCTION .....	1
METHODS .....	5
RESULTS .....	25
DISCUSSION .....	82
APPENDICES .....	89
BIBLIOGRAPHY .....	112

## LIST OF TABLES

TABLE	PAGE
<p>Table 1. Results of the linear regressions of the proportion of each species abundance in each area. The final column indicates whether the proportions were considered time varying or constant for a given species. ....</p>	29
<p>Table 2. The best fit parameter estimates for the single-species biomass dynamics models in the GB region. <math>k</math> and <math>B_0</math> are in units of thousand metric tons, and SSR is the sum of squared residuals .....</p>	31
<p>Table 3. The best fit parameter estimates for the single-species biomass dynamics models in the GOM region. <math>k</math> and <math>B_0</math> are in units of thousand metric tons, and SSR is the sum of squared residuals .....</p>	34
<p>Table 4. The best fit parameter estimates for the single-species biomass dynamics models in the SNE region. <math>k</math> and <math>B_0</math> are in units of thousand metric tons, and SSR is the sum of squared residuals .....</p>	37
<p>Table 5. The feeding guild biomass dynamics models with multispecies interactions in the GB region. The feeding guild groups are as follows: Non-migrating Benthivores (B): Haddock, Yellowtail flounder, Winter flounder, Little skate; Non-migrating Piscivores (S): Atlantic cod, Summer flounder; Migrating Piscivores (F): Silver hake, Spiny dogfish, Winter skate, Goosefish, Pollock, White hake; Migrating Planktivores (P): Atlantic herring, Atlantic mackerel, Longfin squid .....</p>	42
<p>Table 6. Result of <math>AIC_c</math> analysis for nine competing models in the GB region. Note that <math>No. par_i</math> is the number of estimated parameters for model <math>i</math>; <math>\log(L_i)</math> is natural logarithm of maximum likelihood for model <math>i</math>; <math>\Delta_i(AIC_c)</math> is AIC differences, relative to</p>	

the smallest AIC value for given models;  $w_i$  ( $AIC_c$ ) is the rounded Akaike weights . 44

Table 7. Multi-species model parameter estimates in the GB region with model-averaged estimate, unconditional standard errors (SE), and the value for 90% confidence intervals (CI)..... 44

Table 8. The parameter values with standard deviations for the trophic grouping in the GB region.  $k$  and  $B_0$  are in units of thousand metric tons ..... 45

Table 9. The maximum sustainable yield (MSY), corresponding harvest rate ( $f_{MSY}$ ), and the stock size at MSY ( $B_{MSY}$ ) for each group in the trophic grouping in the GB region..... 46

Table 10. The feeding guild biomass dynamics models with multispecies interactions in the GOM region. The feeding guild groups are as follows: Non-migrating Benthivores (B): Haddock, Yellowtail flounder, Winter flounder, Little skate; Non-migrating Piscivores (S): Atlantic cod, Summer flounder; Migrating Piscivores (F): Silver hake, Spiny dogfish, Winter skate, Goosefish, Pollock, White hake; Migrating Planktivores (P): Atlantic herring, Atlantic mackerel, Longfin squid ..... 51

Table 11. Result of  $AIC_c$  analysis for five competing models in the GOM region. Note that  $No. par_i$  is the number of estimated parameters for model  $i$ ;  $\log(L_i)$  is natural logarithm of maximum likelihood for model  $i$ ;  $\Delta_i(AIC_c)$  is AIC differences, relative to the smallest AIC value for given models;  $w_i$  ( $AIC_c$ ) is the rounded Akaike weights . 53

Table 12. Multi-species model parameter estimates in the GOM region with model-averaged estimate, unconditional standard errors (SE), and the value for 90% confidence intervals (CI)..... 53

Table 13. The parameter values with standard deviations for the trophic grouping in

the GOM region. $k$ and $B_0$ are in units of thousand metric tons.....	54
Table 14. The maximum sustainable yield (MSY), corresponding harvest rate ( $f_{MSY}$ ), and the stock size at MSY ( $B_{MSY}$ ) for each group in the trophic grouping in the GOM region.....	55
Table 15. The feeding guild biomass dynamics models with multispecies interactions in the SNE region. The feeding guild groups are as follows: Non-migrating Benthivores (B): Yellowtail flounder, Winter flounder, Little skate; Non-migrating Piscivores (S): Summer flounder; Migrating Piscivores (F): Silver hake, Spiny dogfish, Winter skate, Goosefish, Pollock, White hake; Migrating Planktivores (P): Atlantic herring, Atlantic mackerel, and Longfin squid .....	60
Table 16. Result of $AIC_c$ analysis for six competing models in the SNE region. Note that $No. par_i$ is the number of estimated parameters for model $i$ ; $\log(L_i)$ is natural logarithm of maximum likelihood for model $i$ ; $\Delta_i(AIC_c)$ is AIC differences, relative to the smallest AIC value for given models; $w_i (AIC_c)$ is the rounded Akaike weights .	61
Table 17. Multi-species model parameter estimates in the SNE region with model-averaged estimate, unconditional standard errors (SE), and the value for 90% confidence intervals (CI).....	61
Table 18. The parameter values with standard deviations for the trophic grouping in the SNE region. $k$ and $B_0$ are in units of thousand metric tons .....	62
Table 19. The maximum sustainable yield (MSY), corresponding harvest rate ( $f_{MSY}$ ), and the stock size at MSY ( $B_{MSY}$ ) for each group in the trophic grouping in the SNE region.....	63
Table 20. The feeding guild biomass dynamics models with multispecies interactions	

on multiple domains. We assumed that migratory groups range over the entire study area: migrating planktivores (P) and piscivores (F). Production of non-migrating groups was assessed in each domain: non-migrating benthivores (B) and piscivores (S). Note that each non-migrating groups in the boxes indicate Gulf of Maine, Georges Bank, and Southern New England from the top to the bottom ..... 68

Table 21. Result of  $AIC_c$  analysis for nine competing models in multiple spatial areas. Note that  $No. par_i$  is the number of estimated parameters for model  $i$ ;  $\log(L_i)$  is natural logarithm of maximum likelihood for model  $i$ ;  $\Delta_i(AIC_c)$  is AIC differences, relative to the smallest AIC value for given models;  $w_i(AIC_c)$  is the rounded Akaike weights . 71

Table 22. Multi-species model parameter estimates in multiple spatial areas with model-averaged estimate, unconditional standard errors (SE), and the value for 90% confidence intervals (CI)..... 72

Table 23. The parameter values with standard deviations for the trophic grouping in multiple spatial areas.  $k$  and  $B_0$  are in units of thousand metric tons..... 74

## LIST OF FIGURES

FIGURE	PAGE
<p>Figure 1. The proportion of each spatial area to total area species abundance during 1976-2008. Note that the estimated model's slopes are also provided along with their standard error (SE) and the probability (p-value) in Table 1.....</p>	26
<p>Figure 2. Observed biomass (open circle), catch (triangle) and single-species predicted biomass (dashed line) for fifteen species in the GB region. The y-axis has units of thousand metric tons .....</p>	32
<p>Figure 3. Observed biomass (open circle), catch (triangle) and single-species predicted biomass (dashed line) for fifteen species in the GOM region. The y-axis has units of thousand metric tons .....</p>	35
<p>Figure 4. Observed biomass (open circle), catch (triangle) and single-species predicted biomass (dashed line) for thirteen species in the SNE region. The y-axis has units of thousand metric tons .....</p>	38
<p>Figure 5. Observed biomass (closed circle), catch (solid line) and predicted biomass (dashed line) with interaction terms estimated with Type-I and -III functional responses (GB). The y-axis has units of thousand metric tons .....</p>	46
<p>Figure 6. Non-migrating benthivores equilibrium yield (kt) obtained for pairs of harvest rates in the GB region. Broken lines indicate <math>h_{msy}</math> from single-species model. ....</p>	47
<p>Figure 7. Migrating piscivores (above) and planktivores (below) equilibrium yields (kt) obtained for pairs of harvest rates in the GB region. Broken lines indicate <math>h_{msy}</math></p>	

from single-species model.....	48
Figure 8. Observed biomass (closed circle), catch (solid line) and predicted biomass (dashed line) with interaction terms estimated with Type-I and -III functional responses (GOM). The y-axis has units of thousand metric tons .....	55
Figure 9. Non-migrating benthivores equilibrium yields (kt) obtained for pairs of harvest rates in the GOM region. Broken lines indicate $h_{msy}$ from single-species model .....	56
Figure 10. Migrating planktivores equilibrium yields (kt) obtained for pairs of harvest rates in the GOM region. Broken lines indicate $h_{msy}$ from single-species model .....	57
Figure 11. Observed biomass (closed circle), catch (solid line) and predicted biomass (dashed line) with interaction terms estimated with Type-I and -III functional responses (SNE). The y-axis has units of thousand metric tons .....	63
Figure 12. Migrating piscivores (above) and non-migrating benthivores equilibrium yield (kt) obtained for pairs of harvest rates in the SNE region. Broken lines indicate $h_{msy}$ from single-species model .....	64
Figure 13. Observed biomass (closed circle) and predicted biomass from single-species (dotted line), multi-species (dashed line), and multi-species (solid line) models considered spatially in the Georges Bank region. The y-axis has units of thousand metric tons.....	75
Figure 14. Observed biomass (closed circle) and predicted biomass from single-species (dotted line), multi-species (dashed line), and multi-species (solid line) models considered spatially in the Gulf of Maine region. The y-axis has units of thousand metric tons.....	76

Figure 15. Observed biomass (closed circle) and predicted biomass from single-species (dotted line), multi-species (dashed line), and multi-species (solid line) models considered spatially in the Southern New England region. The y-axis has units of thousand metric tons ..... 77

Figure 16. Non-migrating benthivores equilibrium yield (kt) obtained for pairs of harvest rates in the Georges Bank (above) and Gulf of Maine (below) areas. Broken lines indicate  $h_{msy}$  from single-species model ..... 78

Figure 17. Migrating piscivores equilibrium yield (kt) obtained for pairs of harvest rates in the Georges Bank area. Broken lines indicate  $h_{msy}$  from single-species model ..... 79

Figure 18. Non-migrating benthivores (above) and migrating planktivores (below) equilibrium yield (kt) obtained for pairs of harvest rates in the SNE and GB areas. Broken lines indicate  $h_{msy}$  from single-species model ..... 80

Figure 19. Non-migrating benthivores equilibrium yield (kt) obtained for pairs of harvest rates in the Gulf of Maine (a) and Georges Bank (b) areas. Broken lines indicate  $h_{msy}$  from single-species model ..... 81

## INTRODUCTION

Multispecies interactions and spatial considerations can have important consequences for the dynamics of marine fish populations, but there are some limiting factors in developing multispecies models due to the lack of sufficient information on spatial patterns (fish distribution or migration) and in many cases, a lack of knowledge or uncertainty in important parameters (i.e. natural, fishing, and predation mortalities).

Fisheries-induced changes may affect the spatial distribution of fish stocks and fish community structure (Garrison and Link 2000). As heavily exploited species declined in abundance, their spatial ranges and overlap with other species also declined (Atkinson et al. 1997, Garrison and Link 2000). In addition, climate-related factors may dramatically shift spatial distributions of marine fish and their community structure (Murawski 1993, Nye et al. 2009, Rose 2005). Nye et al. (2009) examined the spatial distribution of fish stocks on the northeast Atlantic continental shelf in relation to climate change since the mid 1960s. They suggested that Atlantic Multidecadal Oscillation anomalies have been steadily increasing over the entire North Atlantic Ocean since the early 1970s due to global warming, and these anomalies may contribute significantly to shifts in the spatial distribution of some species. For example, poleward shifts occurred in alewife, American shad, silver hake, red hake (southern stock), and yellowtail flounder (southern stock); conversely, four species, including winter skate, little skate, Atlantic cod (Gulf of Maine stock), and winter flounder (northern stock) showed southward shifts.

These shifts in the spatial distributions of fish stocks due to either exploitation or climate change have likely changed community structure (Planque et al. 2010) and

function by significantly influencing interactions among fish species along the northwest Atlantic coastal shelf. Predation and competition are important processes that regulate interactions among predator and prey species (May et al. 1979, Rose et al. 1996, Steele and Henderson 1981, Spencer and Collie 1995). Various approaches have accounted for the effects of multispecies interactions on fish populations along the coast of the northwest Atlantic Ocean (Grosslein et al. 1980, Sissenwine et al. 1984, Collie and Spencer 1994, Fogarty and Murawski, 1998, Collie and DeLong 1999, Tsou and Collie 2001, Moustahfid et al. 2010, Curti et al. 2013). Collie and Spencer (1994) developed a predator-prey model including a stochastic variable that had first-order autocorrelation, showing that environmental variables are inherently unpredictable but their general pattern can be simulated with a first-order random variable. Spencer and Collie (1995) modified the model incorporating the effect of alternative prey. They found that predator biomass could increase when modeled prey biomass was low due to consumption of alternative prey, and simulations with stochasticity (environmental variables) could also result in shifts between alternative equilibria.

When stomach data for all ages of predator species modeled are available, a multispecies virtual population analysis (MSVPA) approach can be used to estimate the interactions among commercially important fish stocks. MSVPA is an extension of age-structured approaches that are most typically used in single-species assessments (virtual population analysis). The model assumes a constant ration for a predator of a given age-class and year (Gislason and Helgason 1985, Livingston and Jurado-Molina 2000, Tsou and Collie 2001, Tyrrell et al. 2008) and incorporates a Holling Type-II

predator-prey feeding response (Magnusson 1995). To account for time- and age-varying consumption rates for all modeled species, the expanded multispecies virtual population analysis (MSVPA-X) has been developed, which allows a modified functional responses (Type III functional responses) between food availability and predator consumption rates (Tyrrell et al. 2008).

Predation mortality on a species of interest in marine systems is known to vary in time and space. Its magnitude is often equivalent to, or exceeds, harvesting rates and is often regarded as a significant source of fish mortality (Sissenwine et al. 1984, Tsou and Collie 2001, Tyrrell et al. 2011, Curti et al. 2013). Even though spatial considerations on population dynamics may be important when just considering one target species, the question of spatial overlap between the predator and prey species becomes more crucial when biological interactions are considered. Some stock assessment models have been developed to account for the spatial changes in the distribution of fish. For example, Pincin and Wilberg (2012) investigated the ability of spatially explicit and spatially aggregated surplus production models to understand the effects of marine protected areas (MPAs) on estimates from stock assessments. Spatially explicit statistical catch-at-age (SCAA) stock assessments to account for spatial dynamics that included an MPA were also developed by Punt and Methot (2004). Such models are very useful, when additional data such as consumption, migration, or survey information are available.

Collie and DeLong (1999) examined multispecies interactions in the Georges Bank fish community, where 10 species were analyzed to reveal the species interactions during 1963-1993. Based on the taxonomic grouping strategy, they

showed that significant predation occurred by both gadoids and elasmobranchs on pelagics and competition between gadoids and elasmobranchs appeared during 1963-1993. Significant trophic interactions between gadoids, elasmobranchs, and their pelagic prey species were found, but a limitation of these model results was that several of the dominant species have coast-wide seasonal ranges, which implies that processes off Georges Bank may influence their dynamics.

In this paper we extended the multispecies biomass-dynamics model (Collie and DeLong 1999) to multiple spatial areas to account for patterns of connectivity. A group of 15 fish species collected from the Gulf of Maine (GOM), Southern New England (SNE), and Georges Bank (GB) were aggregated into four trophic groups: non-migrating benthivores (B), non-migrating piscivores (S), migrating piscivores (F), and migrating planktivores (P). The spatial distribution of each group was determined from trawl-survey data, taking into account distributional shifts. For example, we assume that the reproduction of migratory groups (migrating planktivores and piscivores) is a function of the entire stock, with the same parameters ( $r$  and  $k$ ), whereas the reproduction of non-migrating groups was assessed as a function of each regional stock separately.

Multispecies dynamics models with interaction effects across multiple domains are necessary to strengthen our understanding of how species interactions, including predation and competition, alter fish populations. This study seeks to improve the models of fish population dynamics by accounting for multispecies interaction effects in three northwest Atlantic ecosystem domains. Once the multispecies biomass dynamics model in multiple areas is developed, the model will

be used to investigate the consequences of different harvest strategies over the study areas. Evaluating model performances with different harvest strategies on predator and prey groups will help the understanding of relationships between fishing mortality and yield of each species and the functional connections among multiple areas.

## METHODS

### I. Bottom trawl survey data

Biomass and catch data for non-migrating species including haddock, yellowtail flounder, winter flounder, and Atlantic cod were available on each domain from the most recent stock assessments, whereas those of migrating species were assessed over a wider geographic area including three domains (GOM, SNE, and GB). For these migrating species, we used bottom trawl-survey data to calculate the proportion of the species biomass and catch found in each area and year. Bottom trawl survey data for target species during 1976-2008 on three domains have been provided by Kiersten Curti (National Marine Fisheries Service, Northeast Fisheries Science Center in Woods Hole). We used spring and fall survey data to quantify distributional patterns in the biomass and catch of target species for the period 1978 to 2008 in each domain.

Based on the bottom trawl-survey data, we used simple linear regression analysis to examine data for a trend, fitting the proportions for each species abundance in each area. In trend analysis, the dependent variable was the proportion in a given year, shown in a trend analysis formula as  $Y$  and the independent variable was years, shown in the analysis formula as  $X$  (Figure 1a-1c). Three basic statistics including the

intercept, the slope, and the probability (P-value) were estimated, and the estimated slopes are provided along with their standard errors (SE) (Table 1). Significance was assigned based on an alpha value of 0.05 ( $P < 0.05$ ) to determine a sloping line (time-varying proportions) or horizontal line (constant proportions) in Figure 1a-1c and Table 1.

## II. Fisheries data

Biomass and catch data in the three domains (Southern New England, Georges Bank, and Gulf of Maine) from 1979 to 2008 were taken from the most recent stock assessments based on different model approaches (Appendix A).

### A. Haddock

#### i. Biomass

Biomass estimates of Georges Bank (Table B16) and Gulf of Maine (Table C.31) haddock (*Melanogrammus aeglefinus*) from 1979 through 2008 were taken from the virtual population analysis (VPA) January 1 biomass provided in the stock assessment (NEFSC 2012).

#### ii. Catch

Total catch of Georges Bank (Table B1) and Gulf of Maine (Table C.1) haddock from 1979 through 2008, including commercial landings and discards, was taken from the stock assessment (NEFSC 2012).

## B. Atlantic cod

### i. Biomass

Georges Bank Atlantic cod (*Gadus morhua*) biomass from 1979 through 2008 was taken from VPA January 1 biomass in the stock assessment (NEFSC 2012). Gulf of Maine Atlantic cod biomass from 1982 through 2008 was taken from VPA January 1 biomass in the stock assessment (NEFSC 2012), and the biomass from 1979 through 1981 was calculated by a modified Collie-Sissenwine Catch-Survey Analysis (modified CSA), as described in Collie and Kruse (1998).

### ii. Catch

Total catch of Georges Bank (Table B1) and Gulf of Maine (Table C.1) Atlantic cod from 1979 through 2008, including commercial and recreational landings with discards, was taken from the stock assessment (NEFSC 2012).

## C. Silver hake

### i. Biomass

Silver hake (*Merluccius bilinearis*) combined northern and southern stocks biomass from 1979 through 2008 was estimated by the Bayesian surplus production (BSP) model (Brodziak et al. 2001). The BSP model was implemented using WINBIGS1.3 software and prior information on the initial values for  $k$ ,  $r$ ,  $q$  (catchability coefficient), process ( $\sigma^2$ ) and observation errors ( $\tau^2$ ) was taken directly from the pre-existing work (Brodziak et al. 2001). Silver hake biomass combined was

then multiplied by the time-varying proportions to determine each regional stock biomass.

ii. Catch

Nominal landings of combined silver hake were taken from Table A1 in the stock assessment (NEFSC 2011) and the estimates were scaled by the time-varying proportions to calculate landings in each area.

D. Pollock

i. Biomass

Biomass estimates for Gulf of Maine/Georges Bank pollock (*Pollachius virens*) from 1979 through 2008 were taken from the results for January 1 biomass (Table C11) estimated by the Age Structured Assessment Program base model in the stock assessment (NEFSC 2010). And then biomass estimates were multiplied by the mean proportions to calculate each regional stock biomass (GOM: 0.7901, GB: 0.1790, and SNE: 0.0309).

ii. Catch

The commercial and recreational catch information including landings and discards was taken from Table C2 in the stock assessment (NEFSC 2011) and the catch was multiplied by the mean proportions to calculate each regional stock biomass (GOM: 0.7901, GB: 0.1790, and SNE: 0.0309).

## E. White hake

### i. Biomass

Biomass estimates for Gulf of Maine/Georges Bank white hake (*Urophycis tenuis*) were calculated by multiplying the January 1 stock size numbers generated from the Age Structured Production Model (Table L23 in NEFSC 2008) by the 1989-2007 average values for January 1 stock weights at age derived using the Rivard equation (Table L14 in NEFSC 2008). In the absence of other data, 2008 biomass was assumed equal to 2007 biomass. The biomass estimates were then multiplied by the time-varying proportions to calculate each regional stock biomass.

### ii. Catch

Nominal catch of combined silver hake including landings and otter trawl discards was taken from Table H10 in the stock assessment (NEFSC 2012) and was multiplied by the time-varying proportions to determine each regional catch.

## F. Yellowtail flounder

### i. Biomass

Georges Bank yellowtail flounder (*Limanda ferruginea*) biomass from 1979 through 2008 was taken from VPA January 1 biomass in the stock assessment (Table c12b in NEFSC 2008). Gulf of Maine yellowtail flounder biomass from 1985 through 2008 was taken from VPA January 1 biomass in the stock assessment (NEFSC 2008), and the biomass from 1979 through 1984 was calculated by a modified CSA method, as described in Collie and Kruse (1998). Southern New England yellowtail flounder

January 1 biomass from 1979 through 2008 was taken from the Age Structured Assessment Program Base Run model results in the stock assessment (NEFSC 2012).

ii. Catch

Total catch of Georges Bank (Table C1) and Southern New England (Table D1) yellowtail flounder from 1979 through 2008, including commercial landings and discards, was taken from the stock assessment (NEFSC 2008), and the catch of the Cape Cod-Gulf of Maine stock from 1979 through 2008 was taken from Table D1 in NEFSC 2012.

G. Winter flounder

i. Biomass

Georges Bank winter flounder (*Pseudopleuronectes americanus*) biomass from 1979 through 2000 was taken from the population biomass estimated by the standard forward projection methods for statistical catch-at-age analyses (Table 1 in NEFSC 2002). Georges Bank winter flounder biomass from 2001 through 2008 was calculated by multiplying the January 1 stock size numbers generated from the VPA analysis (Table B24 in NEFSC 2011) by the 2006-2010 average values for January 1 stock weights at age (Table B31 in NEFSC 2011) and the 2003-2007 average values for January 1 stock weights at age (Table K24 in NEFSC 2008). Gulf of Maine winter flounder biomass from 1979 through 1981 was calculated by a modified CSA, as described in Collie and Kruse (1998). Gulf of Maine winter flounder biomass from 1982 through 2008 was calculated by multiplying the January 1 stock size numbers

generated from the VPA analysis (Table I29 in NEFSC 2008) by the January 1 stock weights at age (Table A3c in NEFSC 2011). Southern New England winter flounder biomass from 1979 through 1980 was calculated by a modified CSA. Southern New England winter flounder biomass from 1981 through 2008 was calculated by multiplying the January 1 stock size numbers generated from the VPA analysis (Table J29 in NEFSC 2008) by the January 1 stock weights at age (Table A3c in NEFSC 2011).

## ii. Catch

Total catch of Georges Bank winter flounder, including commercial landings and discards, was taken from Table B3 in NEFSC (2011). Total catch for Gulf of Maine winter flounder, including commercial landings and discards, was taken from Table C1 in NEFSC (2011). Finally, total catch of the Southern New England/Mid-Atlantic winter flounder stock complex, including commercial and recreational landings with discards, is provided by Table A15 in NEFSC (2011).

## H. Summer flounder

### i. Biomass

Biomass estimates of summer flounder (*Paralichthys dentatus*) from 1982 through 2007 were taken from VPA January 1 biomass in the stock assessment (NEFSC 2008). Summer flounder biomass from 1979 through 1981 was calculated by a modified CSA, as described in Collie and Kruse (1998). And then the biomass

estimates were multiplied by the mean proportions to calculate each regional stock biomass (GOM: 0.0067, GB: 0.0666, and SNE: 0.9267).

## ii. Catch

Total catch of summer flounder, including commercial and recreational landings with estimated discards, was taken from the stock assessment (Table 28 in NEFSC 2011) and then was scaled by the mean proportions (GOM: 0.0067, GB: 0.0666, and SNE: 0.9267) to determine each regional catch.

## I. Spiny dogfish

### i. Biomass

Biomass estimates for spiny dogfish (*Squalus acanthias*) from 1979 through 2008 were taken from the results of stock assessment (NEFSC 2010) based on area swept by NEFSC trawl surveys. Estimates were based on a nominal survey trawl footprint of 0.01 nm<sup>2</sup> for the R/V Albatross. Spiny dogfish biomass was multiplied by the time-varying proportions to determine each regional stock biomass.

### ii. Catch

Spiny dogfish commercial landings and recreational landings with discards from 1979 through 2005 were taken from Table B4.1 in NEFSC (2006) and from 2005 through 2008 were provided in the stock assessment (DFO 2010). Table 4.13 in NEFSC (2006) provides whole stock dead discards from U.S. commercial fisheries from 1981 through 1988. Dead discards from the U.S. commercial fisheries during

1979 and 1980 are assumed to be equal to dead discards during 1981. Table B4.8 in NEFSC (2006) provides whole stock live plus dead discards from the U.S. commercial fisheries from 1989 through 2005. Dead discards from 1989 through 2005 were calculated by multiplying total discards from each sector of the commercial fishery by the discard mortality rate in Table 4.13 in NEFSC (2006). Total catch of spiny dogfish was then multiplied by the time-varying proportions to determine each regional catch

## J. Atlantic herring

### i. Biomass

The Atlantic herring (*Clupea harengus*) total Gulf of Maine-Georges Bank stock complex January 1 biomass from 1979 through 2008, as estimated by the Age Structured Assessment Program (ASAP) Base model, was taken from the results from the stock assessment (Table A5-2 in NEFSC 2012). Atlantic herring biomass was then multiplied by the time-varying proportions to determine each regional stock biomass.

### ii. Catch

The total Gulf of Maine-Georges Bank Atlantic herring stock complex landings are given in Table 1 of Shepherd et al. (2009). Total landings were multiplied by the time-varying proportions to determine each regional landing.

## K. Atlantic mackerel

### i. Biomass

The total Northwest Atlantic mackerel (*Scomber scombrus*) stock biomass from 1979 through 2003 was taken from the VPA results (Jonathan Deroba, NEFSC, personal communication, and DFO 2010, Table B3 in NEFSC 2006). 2004 through 2008 Atlantic mackerel biomass was calculated by a modified CSA, as described in Collie and Kruse (1998). Atlantic mackerel biomass was multiplied by the mean proportions to calculate each regional stock biomass (GOM: 0.0283, GB: 0.1525, and SNE: 0.8192).

ii. Catch

The total Atlantic mackerel Northwest Atlantic stock landings, including commercial and recreational landings, were taken from Table B1 in NEFSC 2006 and in Table 5 in Grégoire and Maguire (2010). The catch data were multiplied by the mean proportions to calculate each regional stock biomass (GOM: 0.0283, GB: 0.1525, and SNE: 0.8192).

L. Longfin squid

i. Biomass

Annualized biomass for longfin squid (*Loligo pealeii*) from 1979 through 2008 was taken from the results of catchability-adjusted spring and fall NEFSC surveys swept-area biomass (NEFSC 2011). Longfin squid biomass was scaled by the mean proportions to determine each regional stock biomass (GOM: 0.0141, GB: 0.1188, and SNE: 0.8671).

ii. Catch

Longfin squid commercial landings and discards from 1979 through 2008 are given in Table B4 and B7 in NEFSC (2011). The catch data were multiplied by the mean proportions (GOM: 0.0141, GB: 0.1188, and SNE: 0.8671) to calculate each regional catch.

M. Goosefish

i. Biomass

Biomass estimates for the goosefish (*Lophius americanus*) combined stock from 1980 through 2008 were taken from the population biomass estimated by the statistical catch-at-length model (Table A35 in NEFSC 2010). In the absence of other data, 1979 biomass was assumed equal to 1980 biomass. Goosefish biomass was scaled by the mean proportions to calculate each regional stock biomass (GOM: 0.5495, GB: 0.1042, and SNE: 0.3462).

ii. Catch

Goosefish commercial landings and discards from 1980 through 2008 are given in Table A10 in NEFSC (2010), and commercial landing data with discard for 1979 was taken in Table A3 in NEFSC (2010). Note that the landing data for 1979 was from the general canvass data, which contains landings data collected by NMFS port agents or reported by states not included in the weigh-out system. Finally the catch data were multiplied by the mean proportions (GOM: 0.5495, GB: 0.1042, and SNE: 0.3462) to calculate each regional catch.

## N. Little skate and winter skate

### i. Biomass

Biomass estimates of little skate (*Leucoraja erinacea*) and winter skate (*Leucoraja ocellata*) were calculated based on the area-swept biomass methods, where little skate and winter skate catchability were assumed constant at 0.15 and 0.2, respectively (Michael Fogarty, NEFSC, personal communication). The fall survey area-swept biomass estimates from 1979 through 2007 were taken from in Table 19 (winter skate) and Table 22 (little skate) in NEFSC (2009). Note that the total survey areas used for areas-swept biomass methods are 71,915 nmi<sup>2</sup> (offshore strata 1-30, 33-40, and 61-76) for winter skate and 73,679 nmi<sup>2</sup> (offshore strata 1-30, 33-40, 61-76, and inshore strata 1-66) for little skate.

In the absence of other data, 2008 biomass estimate was assumed equal to 2007 biomass. Little skate and winter skate biomass were scaled by the time-varying proportions to determine each regional stock biomass.

### ii. Catch

Total commercial landings and discards of skate complex from 1979 through 2008 are given in Table 1 in NEFSC (2009). The proportions of little skate (0.201) and winter skate (0.445) were calculated by multiplying all skate species landings by the proportions of each species observed in the whole stock area fall survey (Table 19 and 22 in NEFSC 2009). The calculated landings of little skate and winter skate for the

whole stock area were multiplied by the time-varying proportions to calculate each regional catch.

### III. Model formulation and analyses

#### A. Single-species models

The discrete-time biomass dynamics model (Graham 1935, Schaefer 1954, Walters and Hilborn 1976, Quinn and Deriso 1999) is the basic model in this study.

$$\hat{B}_{i,t+1} = \hat{B}_{i,t} + r_i \cdot \hat{B}_{i,t} \left( 1 - \frac{\hat{B}_{i,t}}{k_i} \right) - Y_{i,t} \quad (1)$$

where a “^” denotes a predicted quantity.  $\hat{B}_{i,t}$  is the predicted biomass of species  $i$  in year  $t$ ,  $\hat{B}_{i,t+1}$  is the biomass of species  $i$  in year  $t+1$ , and  $Y_{i,t}$  is the observed catch of species  $i$  in year  $t$ . There are two species-specific population parameters: the intrinsic population growth rate ( $r_i$ ) of species  $i$  and the equilibrium population size in the absence of catch ( $k_i$ ) of species  $i$ . Initial biomass ( $B_{i=0}$ ) of species  $i$  is also an estimated parameter.

#### B. Multispecies models with interactions

Single-species biomass dynamics models (Schaefer 1954, Quinn and Deriso 1999) were extended to multispecies models with the addition of interaction terms (May et al. 1979, Collie and DeLong 1999). A group of 15 fish species collected from the Gulf of Maine, Southern New England, and Georges Bank were aggregated into four trophic groups: non-migrating benthivores (B), non-migrating piscivores (S), migrating piscivores (F), and migrating planktivores (P). Multispecies models were fit by the trophic grouping strategy, but we also looked at two other grouping strategies

(taxonomic and predator-prey grouping), to determine the significant interaction effects in each domain. The biomass dynamics models were of the form:

$$\hat{B}_{a,g,t+1} = \hat{B}_{a,g,t} + r_{a,g} \cdot \hat{B}_{a,g,t} \left( 1 - \frac{\hat{B}_{a,g,t}}{k_{a,g}} \right) - Y_{a,g,t} \pm \text{interaction terms} \quad (2)$$

where a “^” denotes a predicted quantity,  $\hat{B}_{a,g,t}$  is the predicted biomass of group  $g$  in area  $a$ , in year  $t$ , and  $Y_{a,g,t}$  is the observed catch of group  $g$  in area  $a$ , in year  $t$ .

Equation (2) is a discrete form of the Schaefer model with intrinsic growth rate ( $r_{a,g}$ ), carrying capacity ( $k_{a,g}$ ), and initial biomass ( $B_{t=0}$ ) of group  $g$  in area  $a$ .

Multispecies interaction terms consist of two types of interaction effects: predation and competition.

$$- \alpha_{a,g,h} \cdot \hat{B}_{a,g,t} \cdot \hat{B}_{a,h,t} \quad (3)$$

where  $-\alpha_{a,g,h}$  term can be either the competition or predation parameter representing the negative interaction effect of group  $h$  on group  $g$  in area  $a$ .  $\hat{B}_{a,g,t}$  is the predicted biomass of group  $g$  at time  $t$  in area  $a$  and  $\hat{B}_{a,h,t}$  is the predicted biomass of group  $h$  at time  $t$  in area  $a$ . For example, if  $g$  and  $h$  represent prey and predator items respectively, the interaction term ( $-\alpha_{a,g,h}$ ) is called a predation coefficient. On the other hand, if both  $g$  and  $h$  are competing groups, the interaction term is regarded as a competition coefficient.

The interaction term (Equation 3) describes a linear (Type I) functional response (Holling 1959, May et al. 1979, Collie and DeLong 1999). However, these interaction terms were also examined with nonlinear functional responses (Type II and III).

### C. Multispecies models in multiple areas

The spatial distribution of each group was determined from the bottom trawl-survey data, taking into account distributional shifts. For example, we assumed that the reproduction of migratory groups (migrating planktivores and piscivores) is a function of the entire stock, with the same parameters ( $r$  and  $k$ ), whereas the reproduction of non-migrating groups was assessed as a function of each regional stock with different parameters ( $r$  and  $k$ ) separately. The multispecies models for migratory groups ( $P$  and  $F$ ) were of the form below.

$$\hat{P}_{\bullet,t+1} = \hat{P}_{\bullet,t} + r_p \cdot \hat{P}_{\bullet,t} \left( 1 - \frac{\hat{P}_{\bullet,t}}{k_p} \right) - Y_{\bullet,t} \pm \alpha_{a,P,B} \cdot \hat{P}_{a,t} \cdot \hat{B}_{a,t} \quad (4)$$

where dot notation indicates the sum over study areas.  $Y_{\bullet,t}$  is the observed total catch of group  $P$  in mass units and  $\hat{P}_{\bullet,t+1}$  is the predicted total biomass of migrating planktivores in year  $t+1$ .  $\hat{P}_{a,t}$  is the predicted biomass of migrating planktivores in area  $a$ , in year  $t$ . Each regional biomass ( $\hat{P}_{a,t}$ ) was calculated by multiplying the predicted total biomass of migrating planktivores ( $\hat{P}_{\bullet,t}$ ) by the calculated time-varying proportions ( $p$ ) of biomass in each domain.

$$\hat{P}_{a,t} = p_{a,t} \cdot \hat{P}_{\bullet,t} \quad (5)$$

The time-varying proportions ( $p$ ) represent the proportions of the total stock that occupy each domain (GOM, SNE, and GB) and were calculated from the observed biomass.

$$P_{a,t} = \frac{P_{a,t}}{\sum_{a=1}^3 P_{a,t}} \quad (6)$$

where  $P_{a,t}$  is the observed biomass of migrating planktivores in area  $a$  (GOM, SNE, and GB) in year  $t$ .

The  $\pm \alpha_{a,P,B}$  term (Equation 4) can be either the competition or predation parameter representing the negative or positive interaction effect of group  $P$  on group  $B$  in area  $a$ . In addition, the multispecies models for non-migratory groups ( $B$  and  $S$ ) were of the form below.

$$\hat{S}_{a,t+1} = \hat{S}_{a,t} + r_{a,S} \cdot \hat{S}_{a,t} \left( 1 - \frac{\hat{S}_{a,t}}{k_{a,S}} \right) - Y_{a,S,t} \pm \alpha_{a,S,B} \cdot \hat{S}_{a,t} \cdot \hat{B}_{a,t} \quad (7)$$

where  $\hat{S}_{a,t}$  is the predicted biomass of non-migrating piscivores ( $S$ ) in area  $a$ , in year  $t$ .

And  $Y_{a,S,t}$  is the observed catch of group  $S$  in area  $a$ , in year  $t$ . The  $\pm \alpha_{a,S,B}$  term can be either the competition or predation parameter representing the negative or positive interaction effect of group  $S$  on group  $B$  in area  $a$ . The interaction terms (Equation 4 and Equation 7) with a linear (Type I) functional response were also examined with nonlinear functional responses (Type II and III).

#### D. Model parameterization

Automatic Differentiation Model Builder (ADMB), a computer software program for rapid development and fitting of general nonlinear statistical models, was used to estimate model parameters. We estimated model parameters based on the maximum likelihood method, and the predicted biomass for each group was estimated

by minimizing the sum of squared residuals (*SSR*) based on observation error fitting methods.

$$SSR = \sum_{i=1}^G \sum_{j=1}^T (Ln(B_{i,j,a}) - Ln(\hat{B}_{i,j,a}))^2 \quad (8)$$

where  $B_{i,j,a}$  is the observed biomass of group  $g$  in year  $t$ , in area  $a$ , and  $\hat{B}_{i,j,a}$  is the predicted biomass of group  $g$  in year  $t$ , in area  $a$ . The number of groups ( $G$ ) and years ( $T$ ) depended on each grouping strategy, and each area ( $a$ ) or multiple areas were separately examined based on three domains (Southern New England, Georges Bank, and Gulf of Maine). A sample ADMB code for the multi-species biomass dynamics model in multiple areas is presented in Appendix B.

#### E. Model selection

Model selection was based on the information-theoretic approach (Burnham and Anderson 2002). The Akaike Information Criterion (AIC) was chosen as the selection criterion. Since the number of observations was small, the  $AIC_c$  (“corrected AIC”) was used (Equation 9) to select models with significant interaction values (Burnham and Anderson 2004).

$$AIC_c = -2 \times LL < \theta | x > + 2k + \left( \frac{2n(n+1)}{n-k-1} \right) \quad (9)$$

where  $n$  is the number of parameters and  $y$  the sample size in the estimated model.

$LL < \theta | x >$  is the log-likelihood of a particular set of parameter values ( $\theta$ ) given the data ( $x$ ). Note that the sample size ( $y$ ) in single-species biomass dynamics models without interaction terms indicates the number of years of data ( $T$ ). The sample size

( $y$ ) in multispecies models corresponding to each grouping strategy was calculated by multiplying the number of years of data ( $T$ ) by the number of species groups ( $G$ ).

$$LL < \theta | x > = -\frac{1}{2} \cdot G \cdot T \cdot Ln \left( \sum_{i=1}^G \sum_{j=1}^T (Ln(x_{i,j}) - Ln(\hat{x}_{i,j}))^2 \right) \quad (10)$$

$LL < \theta | x >$  is the log-likelihood of a particular set of parameter values ( $\theta$ ) given the data ( $x$ ), and the variable of interest ( $x$ ) in this study is biomass ( $B$ ). Note that this study used the most simplified version of the log-likelihood (Equation 10), which is derived from the probability function for lognormal residual errors (Hastings and Peacock, 1975).

#### H. Model selections using Akaike weights ( $w_i$ )

It is important to assess the weight of evidence in favor of the best model when a binary decision is made and the other candidate models are simply discarded. In particular, when the AIC differences are very small, the acceptance of a single model may lead to a false sense of confidence. We selected the best model in terms of Kullback-Leibler information using the Akaike weights ( $w_i$ ), which can be interpreted as the probability that model  $i$  is the actual expected K-L best model given the sampling sets (Burnham and Anderson 2002).

$$w_i = \frac{\exp(-0.5 \times \Delta_i)}{\sum_{r=1}^R \exp(-0.5 \times \Delta_r)} \quad (11)$$

where  $\Delta_i$  is the difference between the AIC of the best fitting model and that of model  $i$  and  $w_i$  are Akaike weights for model  $i$ . The denominator is simply the sum of the relative likelihoods for all candidate models.

## I. Model averaging for prediction

In the case where no single model is superior to some of others in all candidate models (i.e.  $w_i < 0.9$ ), model averaging is performed (Burnham and Anderson 2002, Johnson and Omland 2004). We computed a weighted estimate of the predicted value, weighting the predictions by the Akaike weights ( $w_i$ ).

$$\hat{\theta} = \sum_{i=1}^R w_i \times \hat{\theta}_i \quad (12)$$

where  $\hat{\theta}$  is a model averaged estimate of parameter ( $\theta$ ) and the  $\hat{\theta}_i$  differ across all  $R$  models. The unconditional sampling variance of the estimator ( $\theta$ ) can be calculated by the equation (13) below.

$$\text{var}(\hat{\theta}) = \left[ \sum_{i=1}^R w_i \times \sqrt{\text{var}(\hat{\theta}_i | g_i) + (\hat{\theta}_i - \hat{\theta})^2} \right]^2 \quad (13)$$

where  $\text{var}(\hat{\theta}_i | g_i)$  is the estimate of the variance of  $\theta$  from the  $i$ th model (Buckland et al. 1997, Burnham and Anderson 2002, Johnson and Omland 2004).

## RESULTS

### I. Spatial distribution patterns of each species

Slope was the most important part of a trend model. It represented the proportional rate at which change occurs over time. In order to quantify distributional patterns in the biomass and catch of target species among the three spatial domains, for example, we took the constant proportions from the regression line (Figure 1a-1c), if the linear trend test was statistically non-significant in all areas (e.g. summer flounder) or significant only one area (e.g. mackerel, pollock, goosefish, and longfin squid) in Table 1. By contrast, we used the time-varying proportions obtained from the regression line (Figure 1a-1c), if the line slope was significantly different from zero ( $P < 0.05$ ) in all areas (e.g. white hake), or even in two areas in order to constrain the predicted proportions to sum to one (e.g. herring, little skate, silver hake, spiny dogfish, and winter skate) in Table 1.

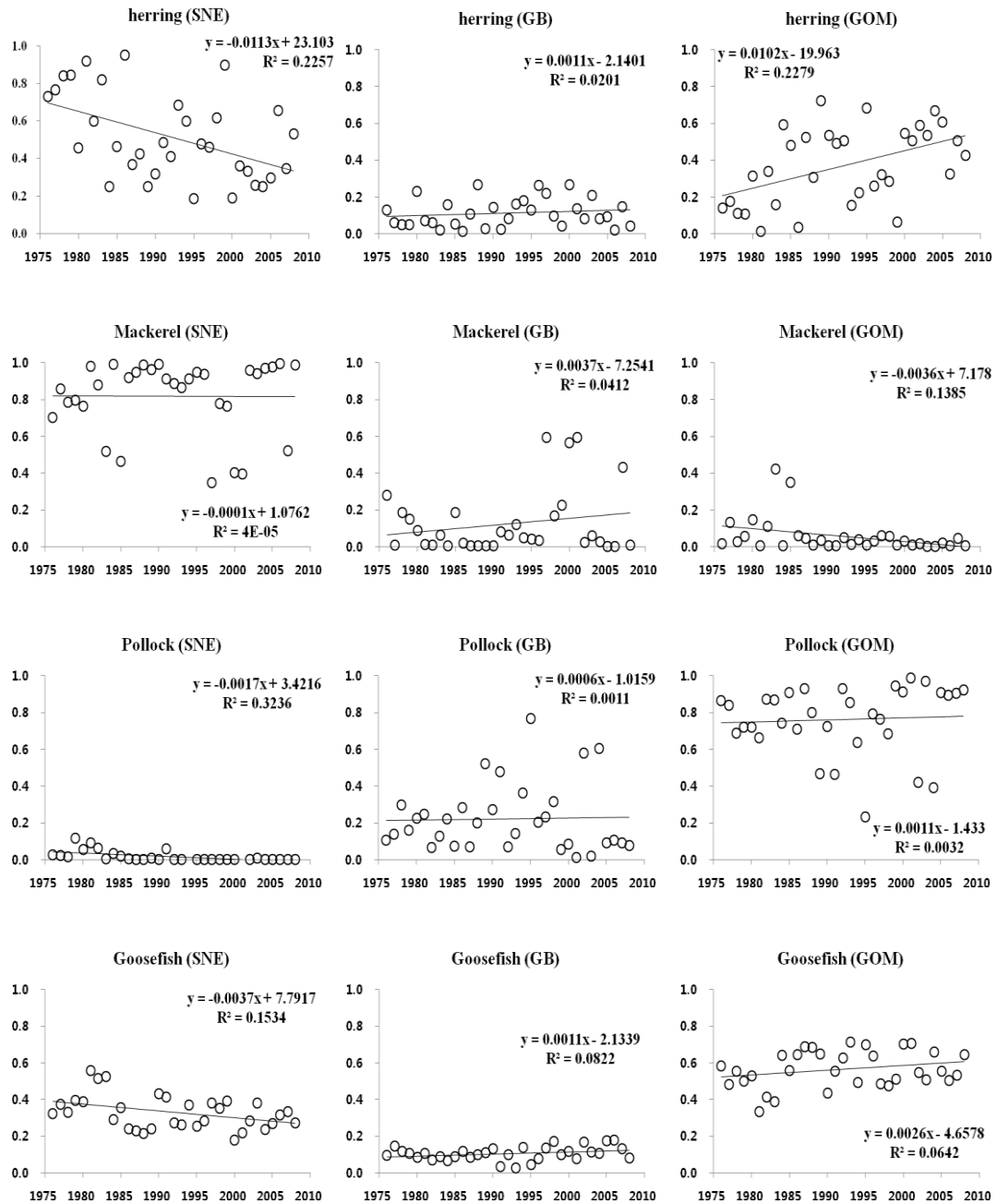


Figure 1a. The proportion of each spatial area to total area species abundance during 1976-2008. Note that the estimated model's slopes are also provided along with their standard error (SE) and the probability (p-value) in Table 1.

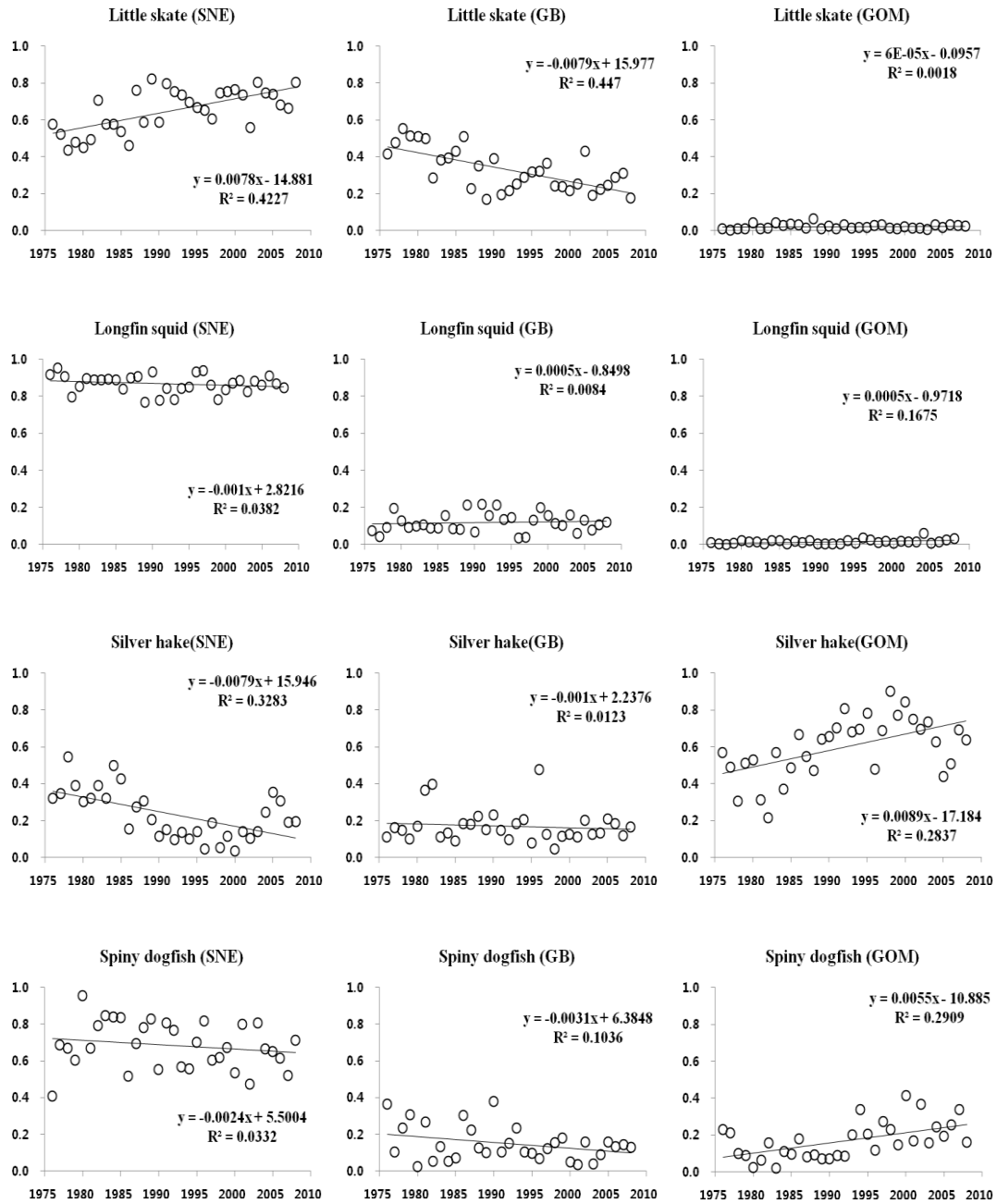


Figure 1b. The proportion of each spatial area to total area species abundance during 1976-2008. Note that the estimated model's slopes are also provided along with their standard error (SE) and the probability (p-value) in Table 1.

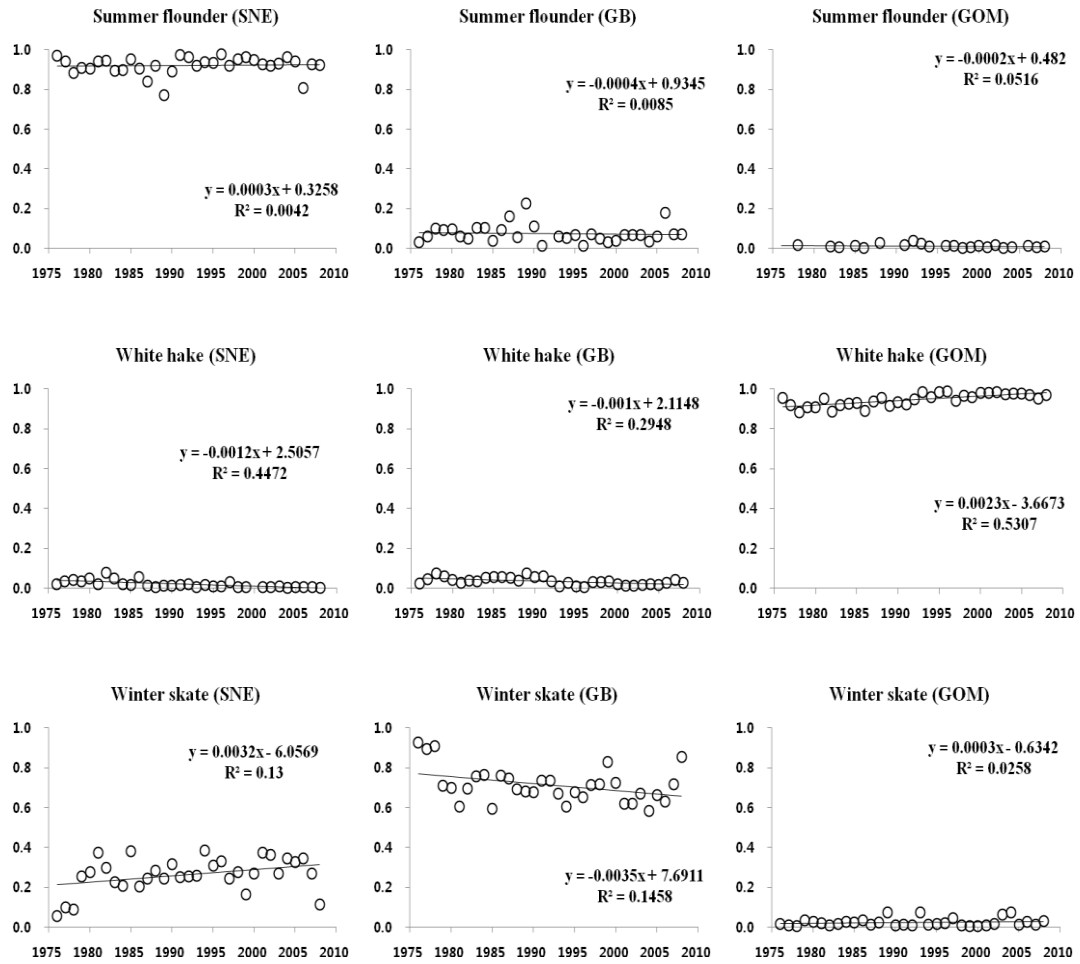


Figure 1c. The proportion of each spatial area to total area species abundance during 1976-2008. Note that the estimated model's slopes are also provided along with their standard error (SE) and the probability (p-value) in Table 1.

Table 1. Results of the linear regressions of the proportion of each species abundance in each area. The final column indicates whether the proportions were considered time varying or constant for a given species.

Species	Region	Slope	SE	R <sup>2</sup>	p-value	Proportion
Herring	SNE	-0.011	0.004	0.226	0.005	Time-varying
Herring	GB	0.001	0.001	0.020	0.432	Time-varying
Herring	GoM	0.010	0.003	0.228	0.005	Time-varying
Mackerel	SNE	0.000	0.004	0.000	0.972	Constant
Mackerel	GB	0.004	0.003	0.041	0.257	Constant
Mackerel	GoM	-0.004	0.002	0.139	0.033	Constant
Pollock	SNE	-0.002	0.000	0.324	0.001	Constant
Pollock	GB	0.001	0.003	0.001	0.858	Constant
Pollock	GoM	0.001	0.003	0.003	0.753	Constant
Goosefish	SNE	-0.004	0.002	0.153	0.024	Constant
Goosefish	GB	0.001	0.001	0.082	0.106	Constant
Goosefish	GoM	0.003	0.002	0.064	0.155	Constant
Little skate	SNE	0.008	0.002	0.423	<0.0001	Time-varying
Little skate	GB	-0.008	0.002	0.447	<0.0001	Time-varying
Little skate	GoM	0.000	0.000	0.002	0.815	Time-varying
Longfin squid	SNE	-0.001	0.001	0.038	0.276	Constant
Longfin squid	GB	0.000	0.001	0.008	0.611	Constant
Longfin squid	GoM	0.000	0.000	0.168	0.018	Constant
Silver hake	SNE	-0.008	0.002	0.328	0.000	Time-varying
Silver hake	GB	-0.001	0.002	0.012	0.539	Time-varying
Silver hake	GoM	0.009	0.003	0.284	0.001	Time-varying
Spiny dogfish	SNE	-0.002	0.002	0.033	0.310	Time-varying
Spiny dogfish	GB	-0.003	0.002	0.104	0.048	Time-varying
Spiny dogfish	GoM	0.006	0.002	0.291	0.001	Time-varying
Summer flounder	SNE	0.000	0.001	0.004	0.721	Constant
Summer flounder	GB	0.000	0.001	0.009	0.616	Constant
Summer flounder	GoM	0.000	0.000	0.052	0.309	Constant
White hake	SNE	-0.001	0.000	0.447	<0.0001	Time-varying
White hake	GB	-0.001	0.000	0.295	0.001	Time-varying
White hake	GoM	0.002	0.000	0.531	<0.0001	Time-varying
Winter skate	SNE	0.003	0.001	0.130	0.039	Time-varying
Winter skate	GB	-0.004	0.002	0.146	0.028	Time-varying
Winter skate	GoM	0.000	0.000	0.026	0.372	Time-varying

## II. Single-species models

The biomass dynamics models were developed for three main categories: single-species and multi-species models in each area (GOM, SNE, and GB) separately and multi-species in multiple areas. This section summarizes the single-species biomass dynamics models for individual fish stocks in the three domains.

### A. Georges Bank

The biomass dynamics model captured the major trends in biomass over time in the GB region, but some species resulted in poor fits (Figure 2). Each single-species model provided an acceptable fit to the observed biomass data with reasonable estimates of parameters, but little skate had a very high  $k$  (22,025 thousand metric tons) and spiny dogfish had a high  $r$  (2.296) (Table 2). In addition, silver hake, one of dominant species in the area, had a very low  $k$  and  $r$  values in the GB region (Table 2).

The total biomass of Georges Bank Atlantic cod, a transboundary stock harvested by both USA and Canadian fishing fleets, declined during the 1970s and 1990s, and still remained below 30,000 metric tons since 2000 (Figure 2). Total biomasses of herring and mackerel, the most important pelagic species of the Georges Bank region, increased steadily from the 1980s and have declined recently. Biomass and catch for longfin squid and spiny dogfish were highly variable, making it difficult to discern trends (Figure 2).

Table 2. The best fit parameter estimates for the single-species biomass dynamics models in the GB region.  $k$  and  $B_0$  are in units of thousand metric tons, and SSR is the sum of squared residuals.

Georges Bank				
Species	Parameter values			
	$r$	$k$	$B_0$	SSR
Haddock	0.275	600*	67	1.601
Yellowtail flounder	0.560	57	20	0.852
Winter flounder	0.461	22	19	1.038
Little skate	0.079	22025	80	4.113
Atlantic cod	0.355	551	170	0.799
Summer flounder	0.914	6	2	1.344
Silver hake	0.010	228	289	0.919
Spiny dogfish	2.296	72	19	5.900
Winter skate	0.234	450	213	5.529
Goosefish	0.875	24	24	0.495
Pollock	0.107	176	32	1.170
White hake	0.142	5*	3	0.369
Atlantic herring	0.540	189	22	0.741
Mackerel	0.135	560	100	1.456
Longfin squid	0.638	15	11	7.737

\* Fixed value

The corresponding sum of squared residuals (SSR) ranged from 0.369 (white hake) to 7.737 (longfin squid). The carrying capacity ( $k$ ) for haddock and white hake on Georges Bank was fixed due to the near exponential increase (or decrease) in biomass during the period (Figure 2, Table 2).

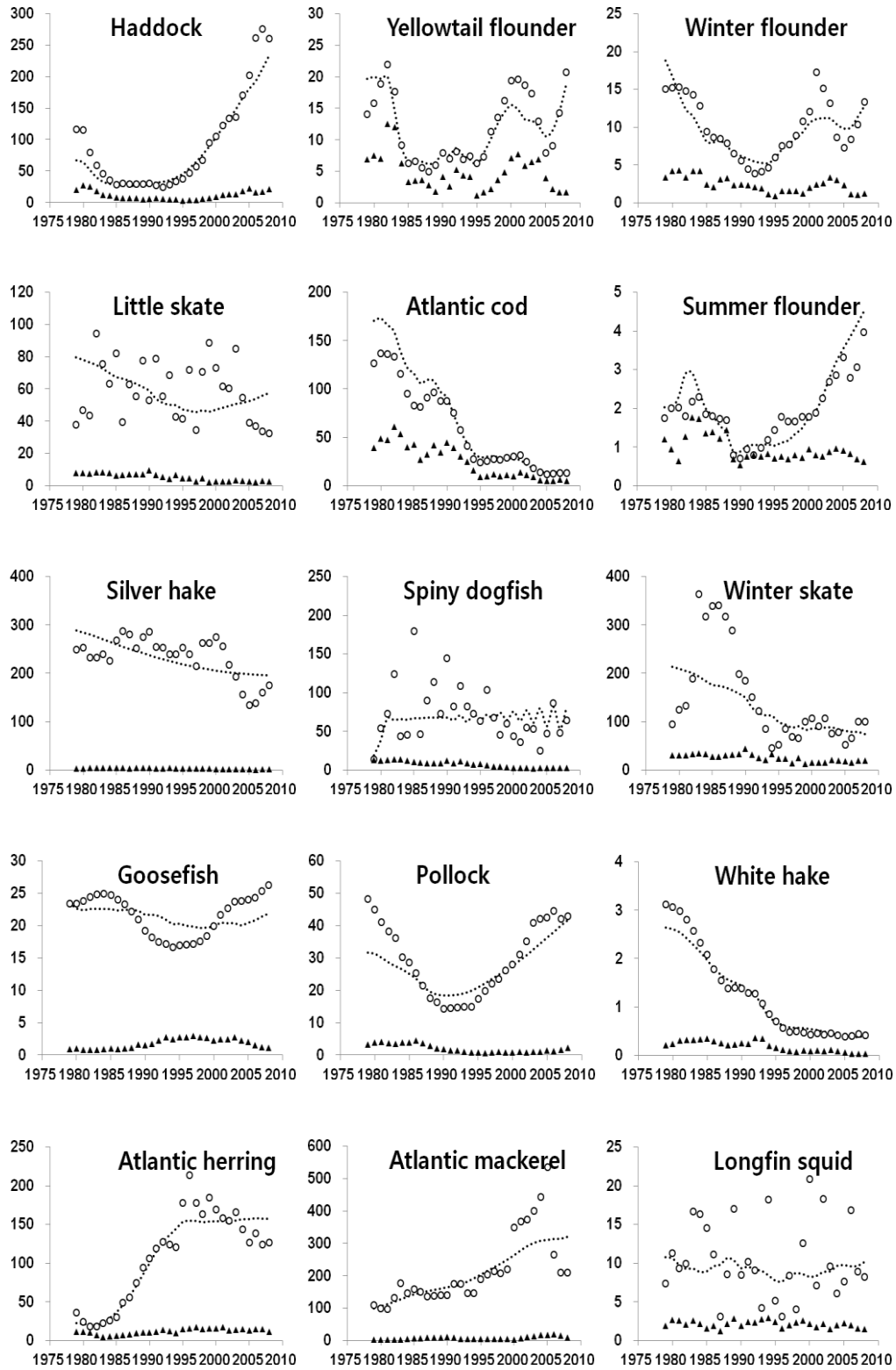


Figure 2. Observed biomass (open circle), catch (triangle) and single-species predicted biomass (dashed line) for fifteen species in the GB region. The y-axis has units of thousand metric tons.

## B. Gulf of Maine

When the single-species models were fit to each of the fifteen Gulf of Maine fish stocks separately, the corresponding sum of squared residuals ranged from 0.495 (goosefish) to 9.642 (longfin squid) (Table 3). Each model provided an acceptable fit to the observed biomass data (Figure 3) with reasonable estimates of parameters.

The total biomass of silver hake, the most dominant species in the Gulf of Maine, peaked in 2000 with 1,146,834 metric tons and was again low in 2005 at 616,106 metric tons. Unlike Georges Bank mackerel, mackerel in the Gulf of Maine suffered severe declines in stock biomass since the mid-1980s and remained below 10,000 metric tons during 2006 and 2008. Longfin squid and spiny dogfish biomasses were highly variable and fluctuated in the Gulf of Maine (Figure 3). The two species including yellowtail flounder and winter flounder in the Gulf of Maine had fixed values for the carrying capacity ( $k$ ) (Figure 3, Table 3).

Table 3. The best fit parameter estimates for the single-species biomass dynamics models in the GOM region.  $k$  and  $B_0$  are in units of thousand metric tons, and SSR is the sum of squared residuals.

Gulf of Maine				
Species	Parameter values			
	$r$	$k$	$B_0$	SSR
Haddock	0.435	22	29	4.896
Yellowtail flounder	0.583	20*	13	2.591
Winter flounder	0.370	90*	9	1.021
Little skate	0.428	3.6	2.5	4.136
Atlantic cod	0.628	99	37	1.401
Summer flounder	0.931	0.6	0.2	1.352
Silver hake	0.286	923	595	0.633
Spiny dogfish	0.656	115	20	5.466
Winter skate	0.346	9.2	6.0	4.870
Goosefish	0.875	125	124	0.495
Pollock	0.107	774	140	1.170
White hake	0.259	69	63	0.211
Atlantic herring	0.532	718	56	0.583
Mackerel	0.135	104	19	1.456
Longfin squid	0.297	6.1	0.8	9.642

\* Fixed value

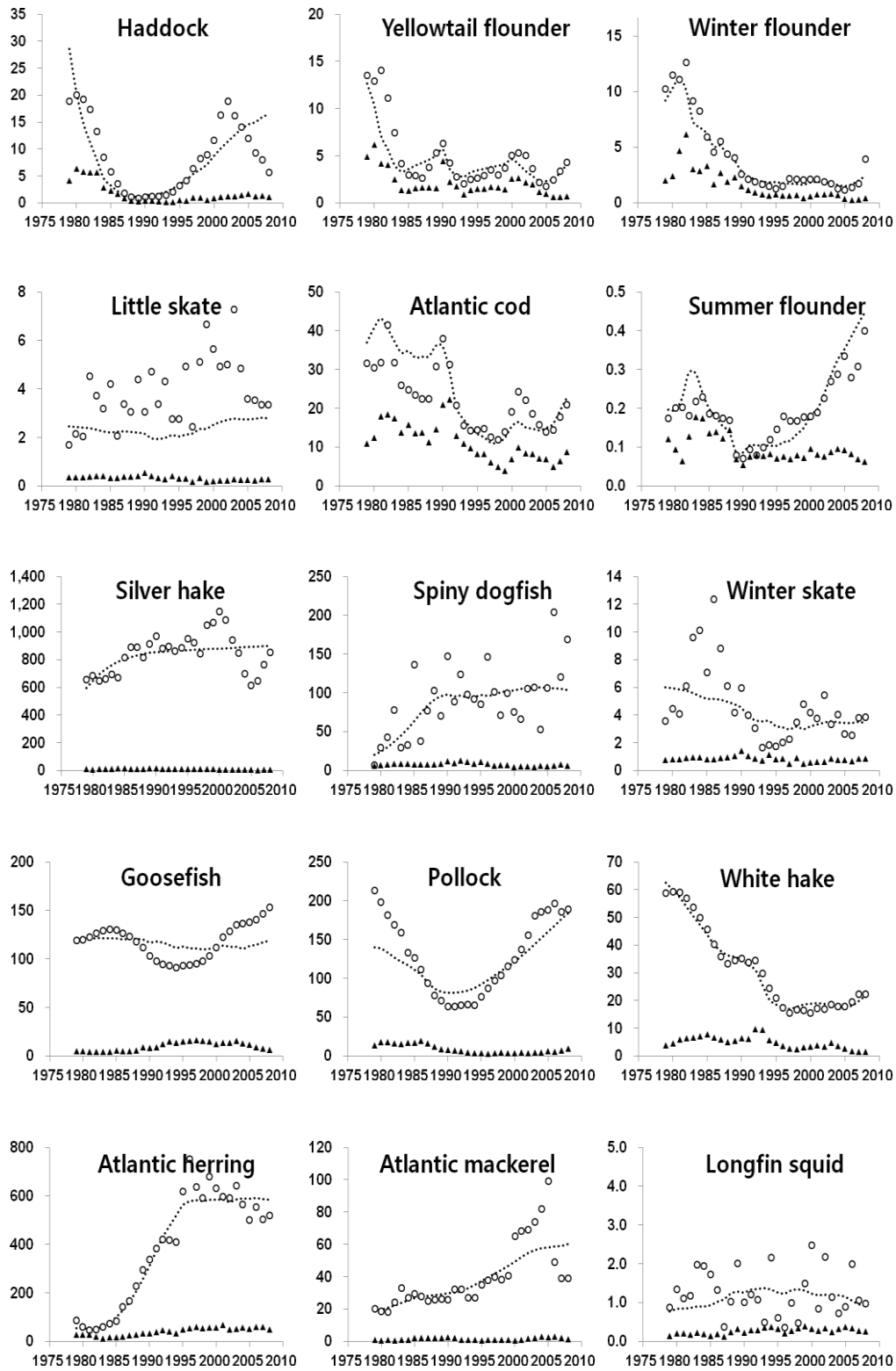


Figure 3. Observed biomass (open circle), catch (triangle) and single-species predicted biomass (dashed line) for fifteen species in the GOM region. The y-axis has units of thousand metric tons.

### C. Southern New England

The single-species biomass-dynamics models reproduced the general biomass patterns for each species except for four species, including silver hake, spiny dogfish, winter skate, and longfin squid (Figure 4). Summer flounder had a very high  $r$  (1.172) and two species, including silver hake and white hake had very low  $r$  (0.01 – 0.045) estimates in the Southern New England area (Table 4).

Silver hake (*Merluccius bilinearis*), a migrating piscivore, is an important commercial species along the northwest Atlantic coastal shelf. It suffered a gradual decline since the mid-1980s in the SNE region. Total biomasses of Atlantic herring and mackerel peaked in 1996 with 862,369 metric tons and in 2005 with 2,867,729 metric tons, respectively (Figure 4). Longfin squid and spiny dogfish biomasses were highly variable and fluctuated over the study periods (Figure 4).

The two species including silver hake and white hake had fixed values for the carrying capacity ( $k$ ) (Figure 4, Table 4). The corresponding sum of squared residuals ranged from 0.495 (goosefish) to 11.028 (yellowtail flounder) in the SNE region (Table 4).

Table 4. The best fit parameter estimates for the single-species biomass dynamics models in the SNE region.  $k$  and  $B_0$  are in units of thousand metric tons, and SSR is the sum of squared residuals.

Southern New England				
Species	Parameter values			
	$r$	$k$	$B_0$	SSR
Yellowtail flounder	0.800	46	37	11.028
Winter flounder	0.373	187	44	0.789
Little skate	0.372	183	62	2.298
Summer flounder	1.172	60	27	1.815
Silver hake	0.010	1000*	314	4.685
Spiny dogfish	0.896	391	133	5.907
Winter skate	0.338	104	68	4.885
Goosefish	0.875	78	78	0.495
Pollock	0.107	30	5.5	1.170
White hake	0.045	5*	2.4	1.503
Atlantic herring	0.608	644	145	1.950
Mackerel	0.135	3006	536	1.456
Longfin squid	0.563	115	83	7.753

\* Fixed value

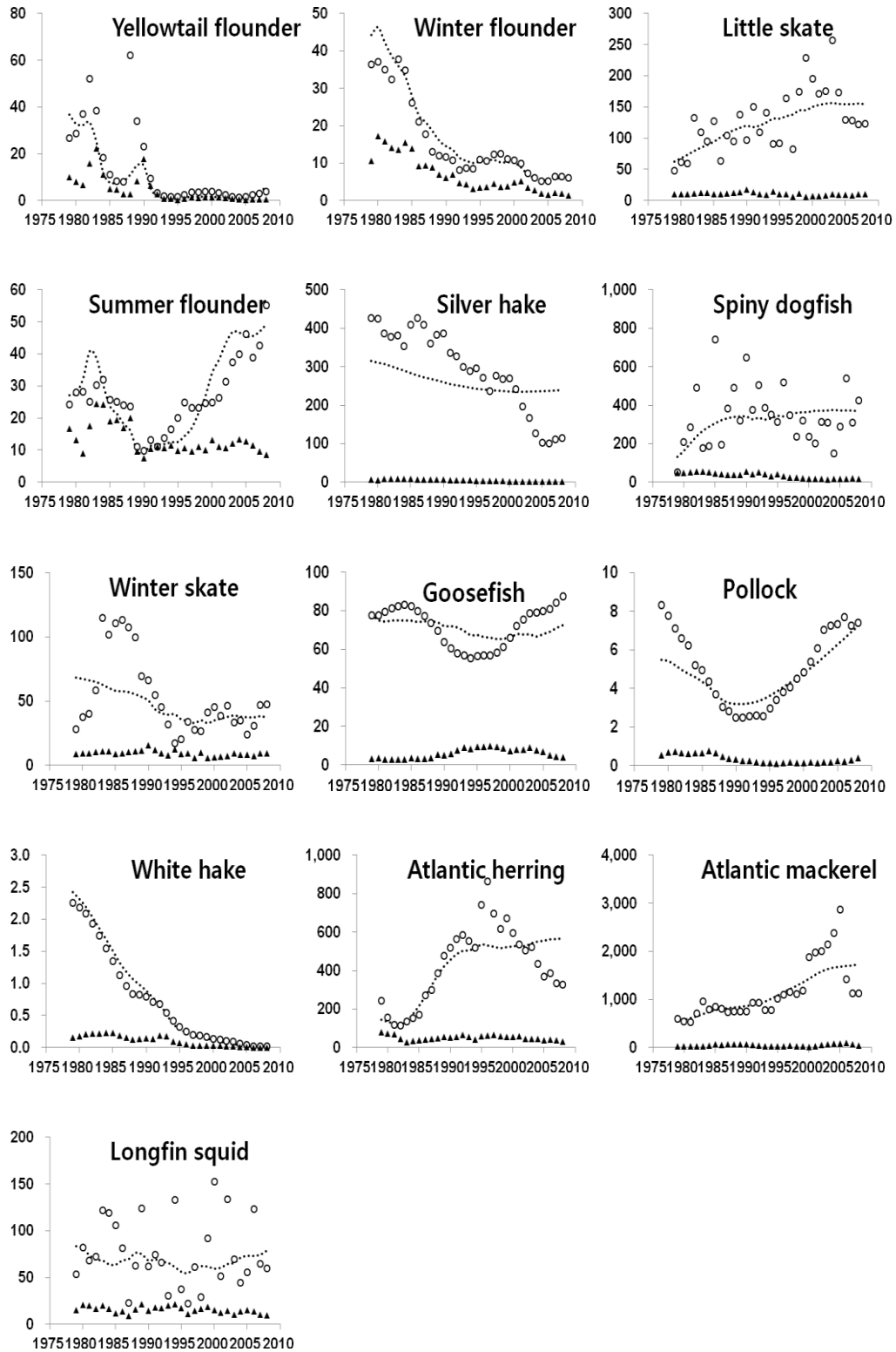


Figure 4. Observed biomass (open circle), catch (triangle) and single-species predicted biomass (dashed line) for thirteen species in the SNE region. The y-axis has units of thousand metric tons.

### III. Multi-species models with interactions

This section summarizes the parameterized candidate models for multi-species biomass dynamics models with interactions based on each single domain, separately. The biomasses and catches of the 15 fish species were aggregated into four trophic groups to simplify the model and to reduce the number of interaction terms: non-migrating benthivores (B), non-migrating piscivores (S), migrating piscivores (F), and migrating planktivores (P). Note that the multi-species interaction parameters are named to indicate the type and sign of the interactions. For example,  $c_{PB}$  is Type-I competition effect of  $B$  (non-migrating benthivores) on  $P$  (migrating planktivores), which is always negative. In addition,  $n_{FP}$  is negative Type-III predation effect of  $F$  (migrating piscivores) on  $P$  (migrating planktivores) and  $p_{FP}$  is positive Type-III predation effect of  $F$  on  $P$ .

The types of the interactions are also graphically presented through the use of arrows in Table 5. For example, a line segment with a triangle affixed to one end is used to point its direction of an interaction and indicate Type-I interaction, and a line segment with a closed circle indicates its direction of a Type- III interaction between two groups. Refer to Methods III, Section B. for additional description of the multi-species interactions.

## A. Georges Bank

There were five candidate multi-species model configurations of the trophic grouping strategy (M1-M5), resulting in a lower Akaike Information Criterion ( $AIC_c$ ) than the trophic grouping without interactions (M6) in Table 5. The conclusion from the raw  $AIC_c$  values was that model M1 is the preferred model (Table 5). Based on the Akaike weights, the relative likelihood of the model, it can be inferred that the best model (M1) is approximately 4.1 times (i.e.,  $w_1/w_2=4.11$ ) more likely to be the best model in terms of Kullback-Leibler discrepancy than the second model (M2) in Table 6. This is not strong evidence that model 1 is likely best if other replicate samples were available. We computed a weighted estimate of the predicted value, weighting the predictions by the Akaike weights ( $w_i$ ) with the unconditional sampling variance of the estimator ( $\theta$ ) in Table 7.

Based on the models (M1-M5), the predation effect (Type-III) of migrating piscivores (F) on non-migrating benthivores (B) and negative Type-I competition effect of non-migrating benthivores (B) on migrating planktivores (P) resulted in the largest reduction in the  $AIC_c$  values and the sum of squared residuals from the single-species fit (Table 5-6). The other negative predation effect (Type-III) of non-migrating piscivores (S) on non-migrating benthivores (B) was also important interaction, but negative Type-I competition effect of non-migrating piscivores (S) on migrating piscivores (F) did not reduce the  $AIC_c$  values (Table 5). The predation effect (Type-III) between migrating piscivores (F) and migrating planktivores (P) and the interaction (Type-III predation) between non-migrating piscivores (S) and migrating

planktivores (P) were not important in the multi-species biomass dynamics models on Georges Bank.

For each of the four primary biomass dynamics models on Georges Bank, the largest changes in parameter values and improvements in predicted biomass were observed in migrating piscivores and planktivores (Table 8, Figure 5). The maximum sustainable yield (MSY), corresponding harvest rate ( $f_{MSY}$ ), and the stock size at MSY ( $B_{MSY}$ ) for each group based on single-species biomass dynamics models are calculated in Table 9.

The equilibrium yields of non-migrating benthivores in the Georges Bank area depend on the harvest of non-migrating piscivores, and the change of migrating piscivore harvest rates does not greatly affect the equilibrium yields of non-migrating benthivores in the Georges Bank (Figure 6). The equilibrium yields of migrating piscivores increases with decreasing non-migrating benthivores harvest rate (Figure 7).

Table 5. The feeding guild biomass dynamics models with multispecies interactions in the GB region. The feeding guild groups are as follows: Non-migrating Benthivores (B): Haddock, Yellowtail flounder, Winter flounder, Little skate; Non-migrating Piscivores (S): Atlantic cod, Summer flounder; Migrating Piscivores (F): Silver hake, Spiny dogfish, Winter skate, Goosefish, Pollock, White hake; Migrating Planktivores (P): Atlantic herring, Atlantic mackerel, Longfin squid.

Model	Multi-species interaction	Total # of parameters	SSR	AIC <sub>c</sub>
M1		18	2.362	145.916
M2		12	2.362	148.744
M3		12	3.110	163.06

Model	Multi-species interaction	Total # of parameters	SSR	AIC <sub>c</sub>
M4		15	2.917	163.075
M5		14	3.552	184.098
M6	Without interactions	11	4.103	193.84

Table 6. Result of AIC<sub>c</sub> analysis for nine competing models in the GB region. Note that No. par<sub>i</sub> is the number of estimated parameters for model *i*; log(L<sub>i</sub>) is natural logarithm of maximum likelihood for model *i*; Δ<sub>i</sub>(AIC<sub>c</sub>) is AIC differences, relative to the smallest AIC value for given models; w<sub>i</sub> (AIC<sub>c</sub>) is the rounded Akaike weights.

Model	No. par <sub>i</sub>	log(L <sub>i</sub> )	AIC <sub>i</sub>	Δ <sub>i</sub>	exp(-1/2*Δ <sub>i</sub> )	w <sub>i</sub> (AIC <sub>c</sub> )
M1	18	-51.6	145.9	0.00	1.000	0.8042
M2	19	-51.6	148.7	2.83	0.243	0.1955
M3	12	-68.1	163.1	17.1	0.000	0.0002
M4	15	-64.2	163.1	17.2	0.000	0.0002
M5	14	-76.0	184.1	38.2	0.000	0.0000
M6	11	-84.7	193.8	47.9	0.000	0.0000

Table 7. Multi-species model parameter estimates in the GB region with model-averaged estimate, unconditional standard errors (SE), and the value for 90% confidence intervals (CI).

Parameter	Estimate	SE	90% CI	
			Upper	Lower
r_B	0.255	0.079	0.385	0.125
k_B	1001	690	2133	-131
B0_B	200	51	284	116
r_S	0.497	0.028	0.543	0.451
k_S	300*	-	-	-
B0_S	184	23	222	147
r_F	0.041	0.036	0.100	-0.019
k_F	3360	2386	7274	-553
B0_F	451	216	805	97
r_P	0.302	0.095	0.457	0.146
k_P	2126	1487	4565	-313
B0_P	108	26	150	66
n_PB	0.001	0.001	0.002	-2.06x10 <sup>-4</sup>
c_sb	0.007	0.117	0.198	-0.185
alpha_sb	0.100	1.752	2.973	-2.774
alpha_sp	1.80x10 <sup>-7</sup>	2.89x10 <sup>-4</sup>	4.75x10 <sup>-4</sup>	-4.75x10 <sup>-4</sup>
c_fb	1.15x10 <sup>-7</sup>	1.75x10 <sup>-6</sup>	2.99x10 <sup>-6</sup>	-2.76x10 <sup>-6</sup>
d_fb	0.006	0.088	0.151	-1.390
alpha_fb	1.69x10 <sup>-7</sup>	1.98x10 <sup>-4</sup>	3.24x10 <sup>-4</sup>	-3.24x10 <sup>-4</sup>
alpha_fp	0.100	1.530	2.609	-2.409

\* Fixed value

Table 8. The parameter values with standard deviations for the trophic grouping in the GB region.  $k$  and  $B_0$  are in units of thousand metric tons.

Georges Bank				
Parameters	Single-species	std. dev.	Multi-species	std. dev.
$r_b$	0.217	0.040	0.255	0.079
$k_b$	1072	703.71	1001	690
$B_{0_b}$	175	23	200	51
$r_s$	0.497	0.028	0.497	0.028
$k_s$	300*		300*	
$B_{0_s}$	184	23	184	23
$r_f$	0.069	0.023	0.041	0.036
$k_f$	3477	2408	3360	2386
$B_{0_f}$	718	144.370	451	216
$r_p$	0.197	0.072	0.302	0.095
$k_p$	1291	1241	2126	1487
$B_{0_p}$	107	32.100	108	26
$n_{pb}$			$7.48 \times 10^{-4}$	$5.82 \times 10^{-4}$
$c_{sb}$			0.007	0.119
$\alpha_{sb}$			0.100	1.793
$\alpha_{sp}$			$1.75 \times 10^{-7}$	$2.73 \times 10^{-4}$
$d_{fb}$			$5.76 \times 10^{-3}$	0.092
$\alpha_{fb}$			$1.59 \times 10^{-7}$	$1.79 \times 10^{-4}$
$\alpha_{fp}$			0.100	1.586
Number of observations	120		120	
Number of parameters	11		18	
Sum of squares	4.103		2.362	
AICc	194		146	

\* Fixed value

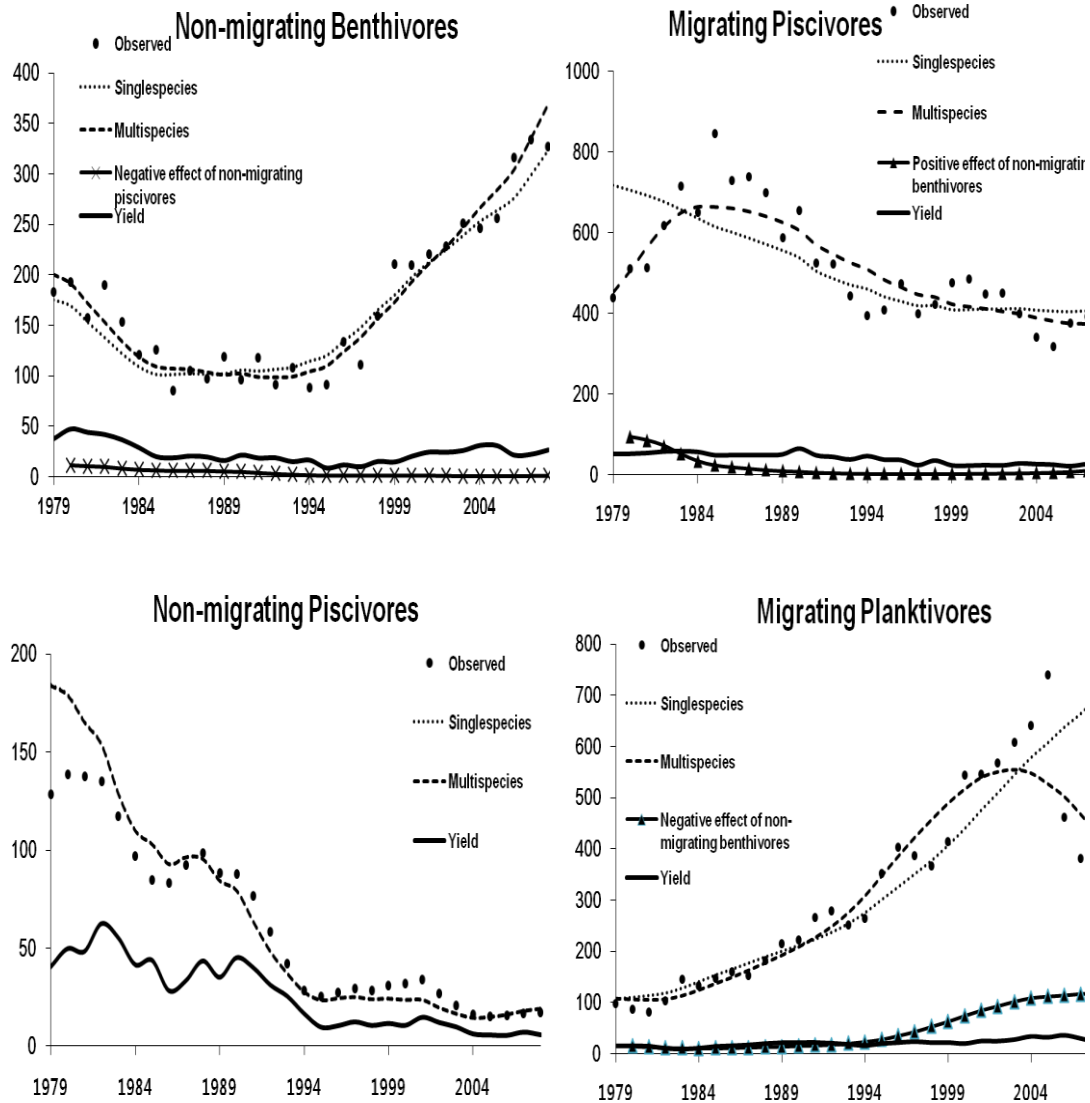


Figure 5. Observed biomass (closed circle), catch (solid line) and predicted biomass (dashed line) with interaction terms estimated with Type-I and -III functional responses (GB). The y-axis has units of thousand metric tons.

Table 9. The maximum sustainable yield (MSY), corresponding harvest rate ( $f_{MSY}$ ), and the stock size at MSY ( $B_{MSY}$ ) for each group in the trophic grouping in the GB region.

Model	Group	MSY (kt)	$f_{MSY}$	$B_{MSY}$
Single-species	P	63.5	0.098	645
	B	58.1	0.108	536
	S	37.3	0.248	150
	F	60.0	0.034	1739

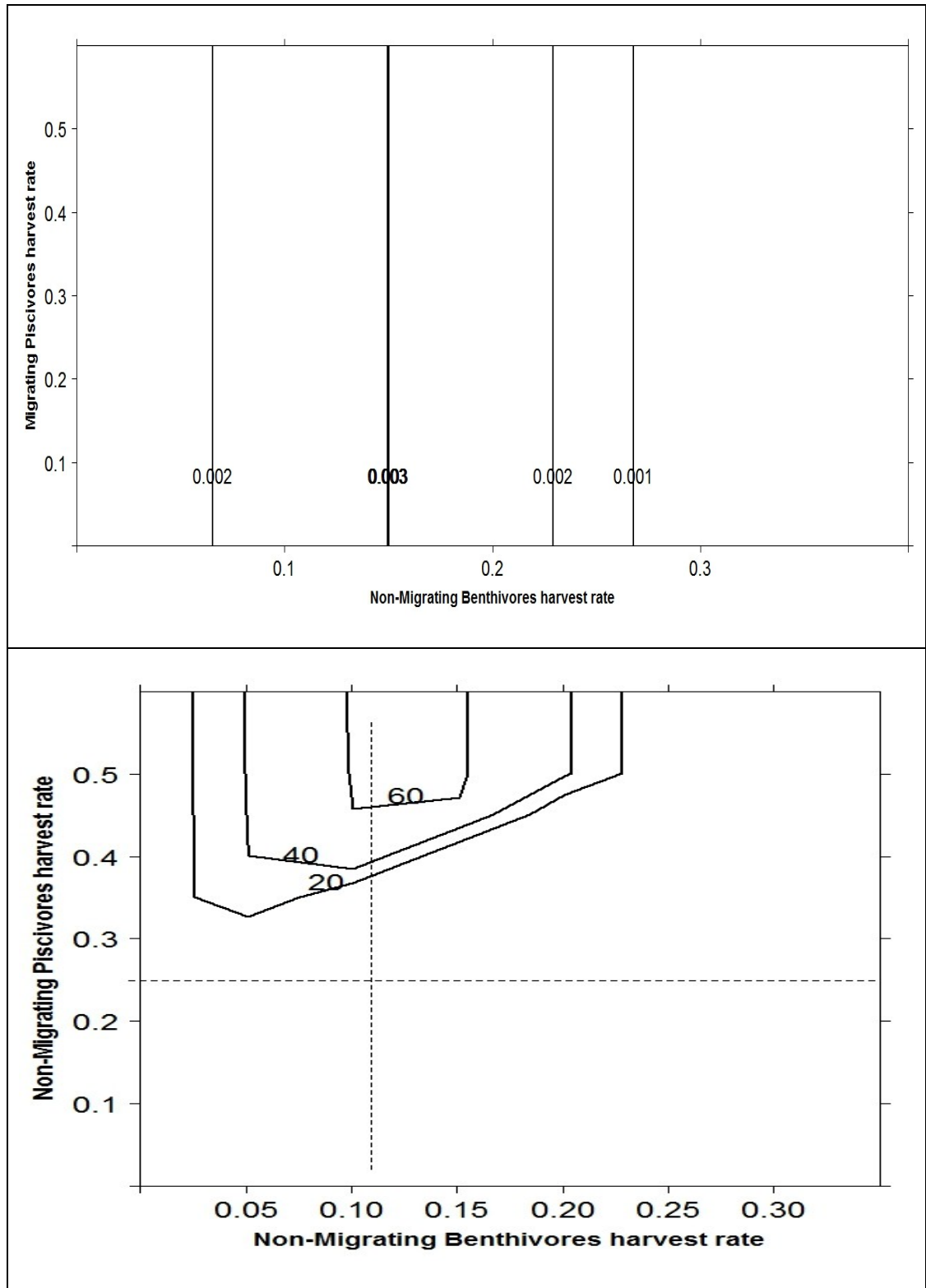


Figure 6. Non-migrating benthivores equilibrium yield (kt) obtained for pairs of harvest rates in the GB region. Broken lines indicate  $h_{msy}$  from single-species model.

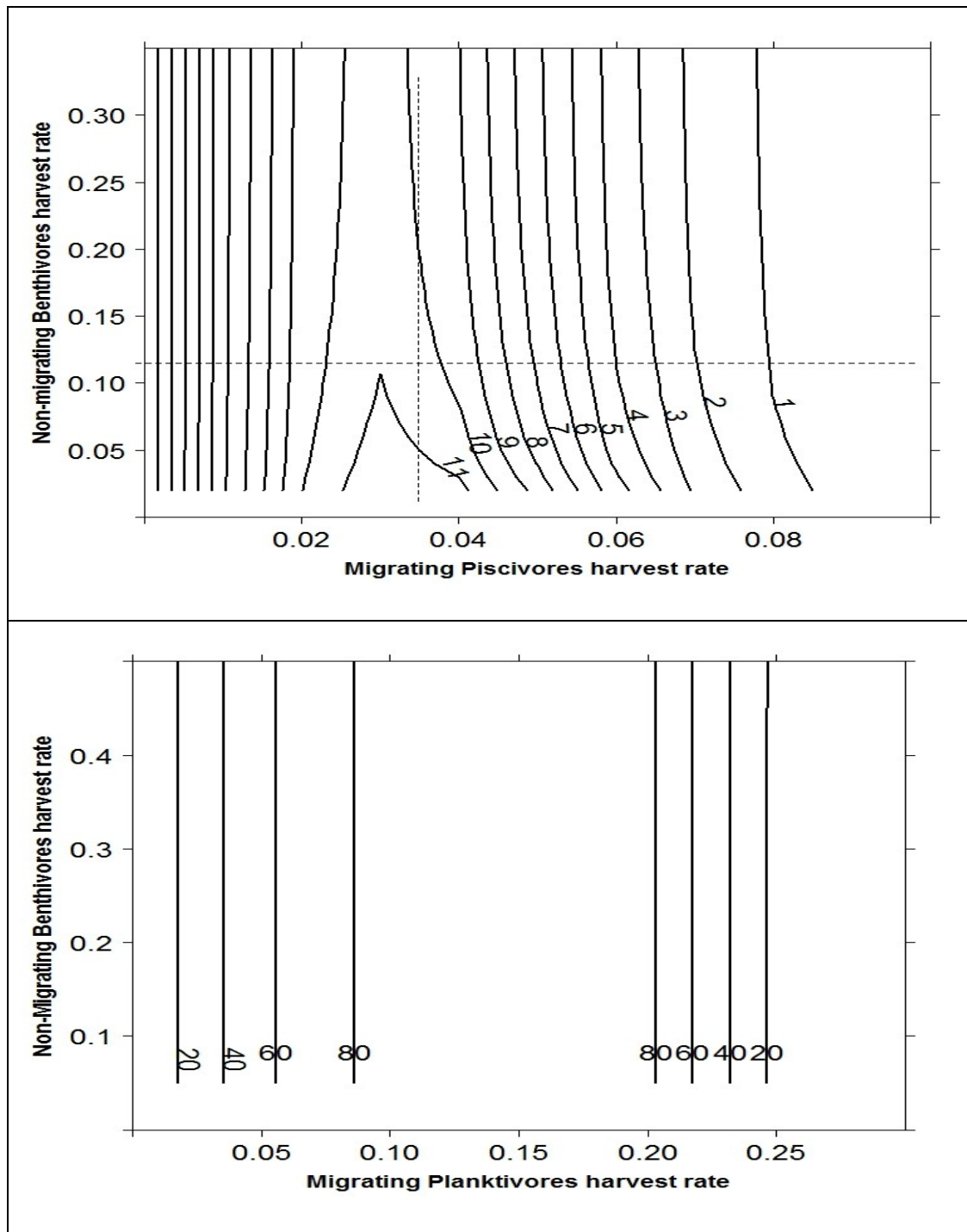


Figure 7. Migrating piscivores (above) and planktivores (below) equilibrium yields (kt) obtained for pairs of harvest rates in the GB region. Broken lines indicate  $h_{msy}$  from single-species model.

## ii. Gulf of Maine

Three multi-species candidate models (M1-M3) resulted in a lower  $AIC_c$  values than the trophic grouping without interactions (M4) in Table 10. The conclusion from the raw  $AIC_c$  values was that model M1 is the preferred model (Table 11). Based on the Akaike weights, the evidence ratio between the best and second-best model is approximately 407 ( $0.9954/0.0024$ ), suggesting that the evidence is 407 times stronger for the best model relative to the second-best model. We also computed a weighted estimate of the predicted value, weighting the predictions by the Akaike weights ( $w_i$ ) with the unconditional sampling variance of the estimator ( $\theta$ ) in Table 12.

The negative Type-III predation effect of migrating piscivores (F) on non-migrating benthivores (B) and negative Type-I competition effects between non-migrating benthivores (B) and migrating planktivores (P) resulted in the largest reduction in the  $AIC_c$  value and the sum of squared residuals from the single-species fit based on Model M1 (Table 10-11). The Type-III predation interactions between migrating piscivores (F) and migrating planktivores (P) and between non-migrating piscivores (S) and migrating planktivores (P) were not important in the multi-species biomass dynamics models in the GOM region (Table 10).

For each of the four primary biomass dynamics models in the Gulf of Maine, the largest changes in parameter values and improvements in predicted biomass were observed in migrating piscivores and planktivores (Table 13, Figure 8). The maximum sustainable yield (MSY), corresponding harvest rate ( $f_{MSY}$ ), and the stock size at MSY

( $B_{MSY}$ ) for each group based on single-species biomass dynamics models are calculated in Table 14.

The equilibrium yields of non-migrating benthivores in the Gulf of Maine depend on the harvest of migrating piscivores and planktivores (Figure 9). In addition, the yield of migrating planktivores increases as the non-migrating benthivore harvest rate is increased due to the negative effect of competition (Figure 10).

Table 10. The feeding guild biomass dynamics models with multispecies interactions in the GOM region. The feeding guild groups are as follows: Non-migrating Benthivores (B): Haddock, Yellowtail flounder, Winter flounder, Little skate; Non-migrating Piscivores (S): Atlantic cod, Summer flounder; Migrating Piscivores (F): Silver hake, Spiny dogfish, Winter skate, Goosefish, Pollock, White hake; Migrating Planktivores (P): Atlantic herring, Atlantic mackerel, Longfin squid.

Model	Multi-species interaction	Total # of parameters	SSR	AIC <sub>c</sub>
M1	<p>Diagram for Model M1: Guild B (left) has a diagonal arrow labeled III pointing to Guild F (top). Guild B has two horizontal arrows labeled I pointing to Guild P (right). Guild S (bottom) is present but has no arrows.</p>	16	3.765	196.364
M2	<p>Diagram for Model M2: Guild B (left) has one horizontal arrow labeled I pointing to Guild P (right). Guild F (top) and Guild S (bottom) are present but have no arrows.</p>	12	4.537	208.383
M3	<p>Diagram for Model M3: Guild B (left) has two horizontal arrows labeled I pointing to Guild P (right). Guild F (top) and Guild S (bottom) are present but have no arrows.</p>	13	4.455	208.727

Model	Multi-species interaction	Total # of parameters	SSR	AIC <sub>c</sub>
M4	Without interactions	11	4.861	214.204

Table 11. Result of  $AIC_c$  analysis for five competing models in the GOM region. Note that No. par<sub>*i*</sub> is the number of estimated parameters for model *i*; log( $L_i$ ) is natural logarithm of maximum likelihood for model *i*;  $\Delta_i(AIC_c)$  is AIC differences, relative to the smallest AIC value for given models;  $w_i(AIC_c)$  is the rounded Akaike weights.

Model	No. par <sub><i>i</i></sub>	log( $L_i$ )	$AIC_i$	$\Delta_i$	exp(-1/2* $\Delta_i$ )	$w_i(AIC_c)$
M1	16	-79.5	196.4	0.000	1.000	0.9954
M2	12	-90.7	208.4	12.019	0.002	0.0024
M3	13	-89.6	208.7	12.363	0.002	0.0021
M4	11	-94.9	214.2	17.840	0.000	0.0001

Table 12. Multi-species model parameter estimates in the GOM region with model-averaged estimate, unconditional standard errors (SE), and the value for 90% confidence intervals (CI).

Parameter	Estimate	SE	90% CI	
			Upper	Lower
$r_b$	0.893	0.005	0.902	0.885
$k_b$	97	52	181	12
$B_{0\_b}$	52	24	92	13
$r_s$	0.744	0.053	0.831	0.656
$k_s$	80*	-	-	-
$B_{0\_s}$	36	9	50	21
$r_f$	0.082	0.050	0.165	$2.67 \times 10^{-4}$
$k_f$	2924	2078	6332	-484
$B_{0\_f}$	1051	286	1519	582
$r_p$	0.486	0.239	0.878	0.094
$k_p$	980	286	1448	511
$B_{0\_p}$	146	72	265	28
$n_{pb}$	0.005	0.008	0.018	-0.008
$n_{bp}$	$4.34 \times 10^{-4}$	0.001	0.002	-0.001
$c_{fb}$	$2.31 \times 10^{-4}$	$4.82 \times 10^{-4}$	0.001	-0.001
$\alpha_{fb}$	0.024	0.060	0.122	-0.075
$\alpha_{fp}$	$4.54 \times 10^{-5}$	$4.52 \times 10^{-5}$	$1.20 \times 10^{-4}$	$2.87 \times 10^{-5}$

\* Fixed value

Table 13. The parameter values with standard deviations for the trophic grouping in the GOM region.  $k$  and  $B_0$  are in units of thousand metric tons.

Gulf of Maine				
Parameters	Single-species	std. dev.	Multi-species	std. dev.
$r_b$	0.326	0.068	0.896	0.001
$k_b$	92	52	97	52
$B_{0\_b}$	56	17	52	24
$r_s$	0.744	0.053	0.744	0.053
$k_s$	80*		80*	
$B_{0\_s}$	36	9	36	9
$r_f$	0.075	0.048	0.083	0.050
$k_f$	2901	2097	2924	2078
$B_{0\_f}$	1123	282	1050	286
$r_p$	0.368	0.091	0.486	0.239
$k_p$	858	186	980	286
$B_{0\_p}$	111	31	146	7
$n_{pb}$			$4.93 \times 10^{-3}$	$7.71 \times 10^{-3}$
$n_{bp}$			$4.45 \times 10^{-4}$	$5.01 \times 10^{-4}$
$c_{fb}$			$2.31 \times 10^{-4}$	$4.26 \times 10^{-4}$
$\alpha_{fb}$			0.024	0.055
$\alpha_{fp}$			$4.54 \times 10^{-5}$	$2.78 \times 10^{-7}$
Number of observations	120		120	
Number of parameters	11		16	
Sum of squares	4.861		3.765	
AICc	214		196	

\* Fixed value

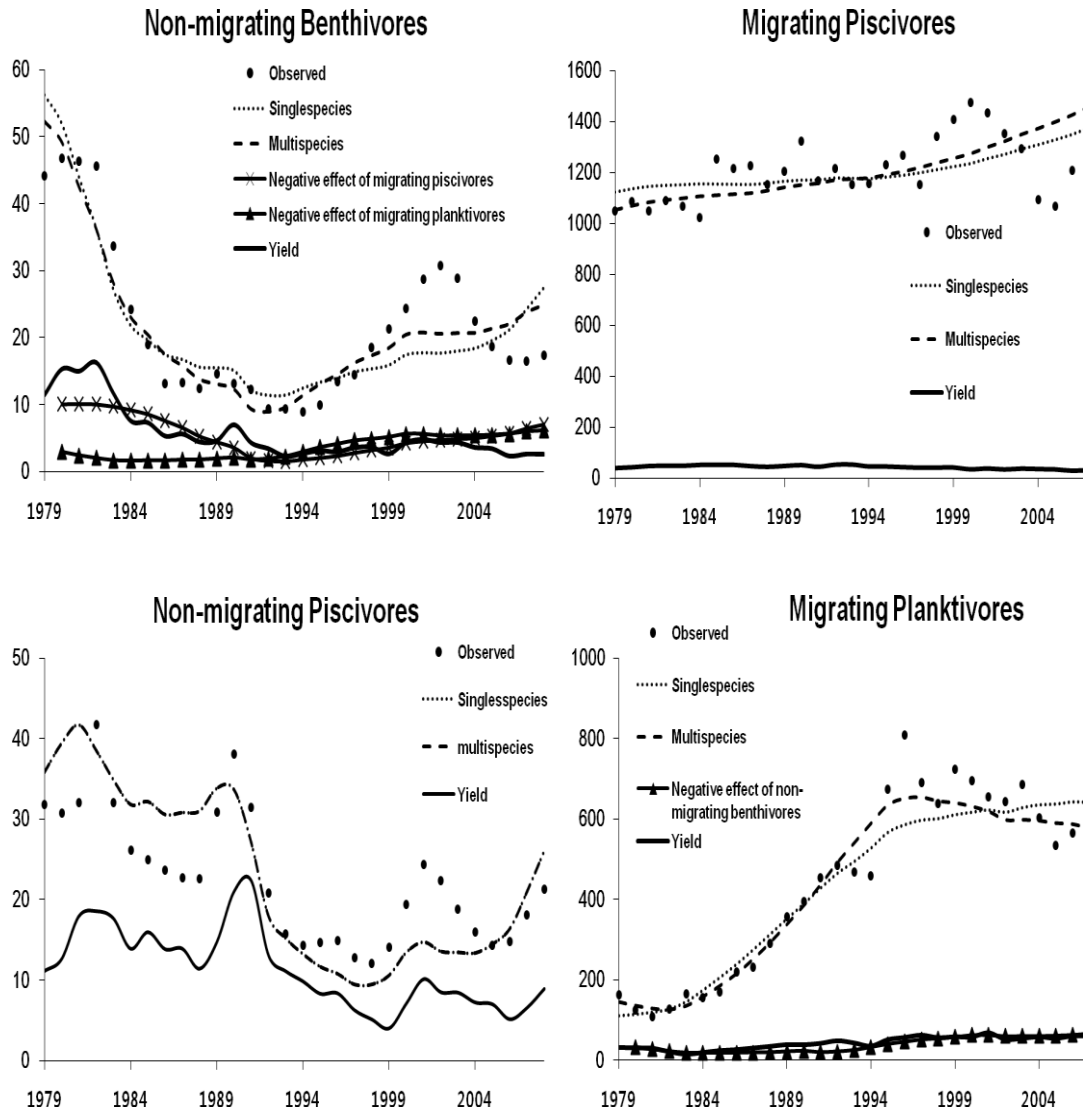


Figure 8. Observed biomass (closed circle), catch (solid line) and predicted biomass (dashed line) with interaction terms estimated with Type-I and -III functional responses (GOM). The y-axis has units of thousand metric tons.

Table 14. The maximum sustainable yield (MSY), corresponding harvest rate ( $f_{MSY}$ ), and the stock size at MSY ( $B_{MSY}$ ) for each group in the trophic grouping in the GOM region.

Model	Group	MSY (kt)	$f_{MSY}$	$B_{MSY}$
Single-species	P	78.8	0.184	429
	B	7.5	0.163	45.8
	S	14.9	0.372	40
	F	54.3	0.037	1451

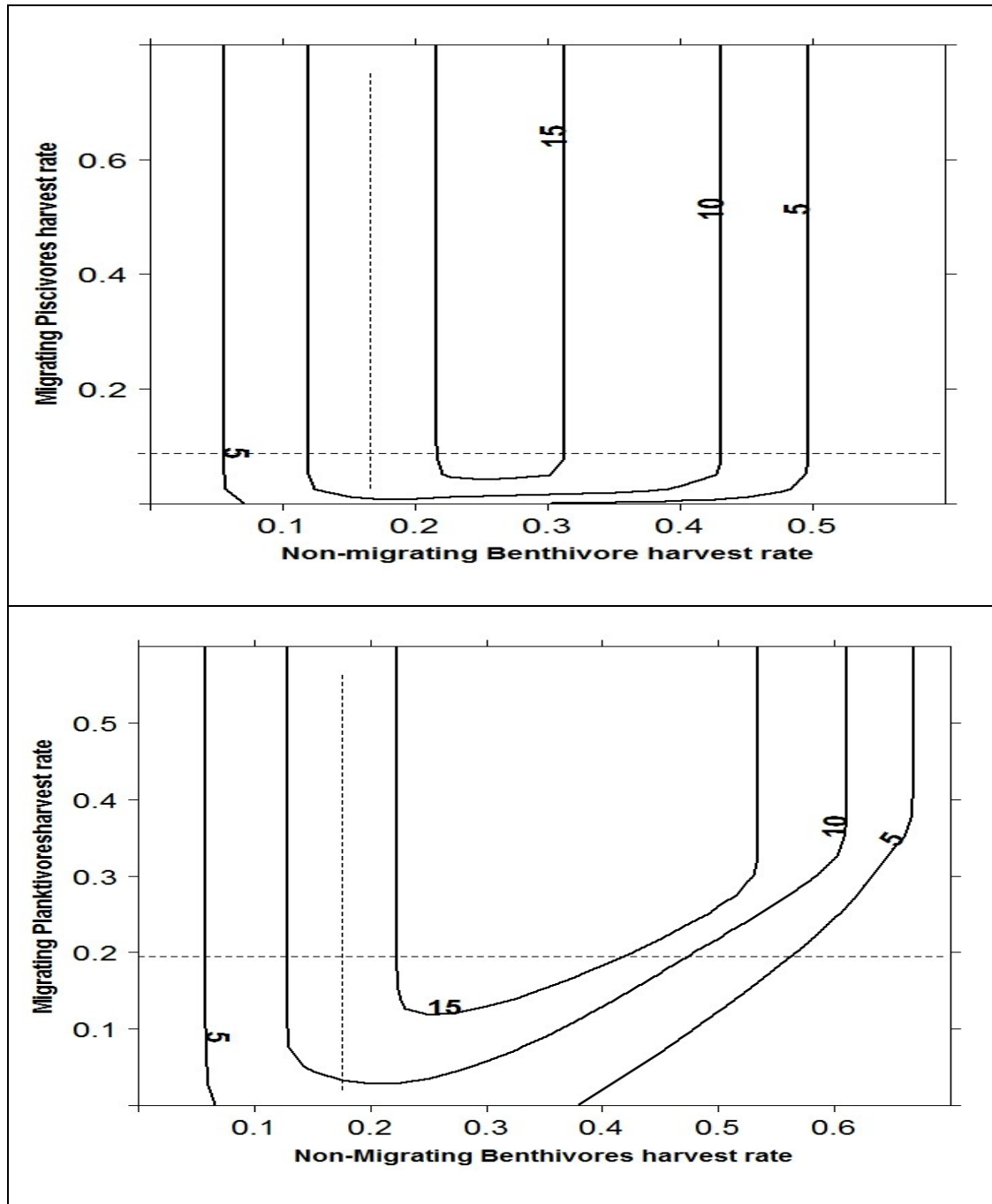


Figure 9. Non-migrating benthivores equilibrium yields (kt) obtained for pairs of harvest rates in the GOM region. Broken lines indicate  $h_{msy}$  from single-species model.

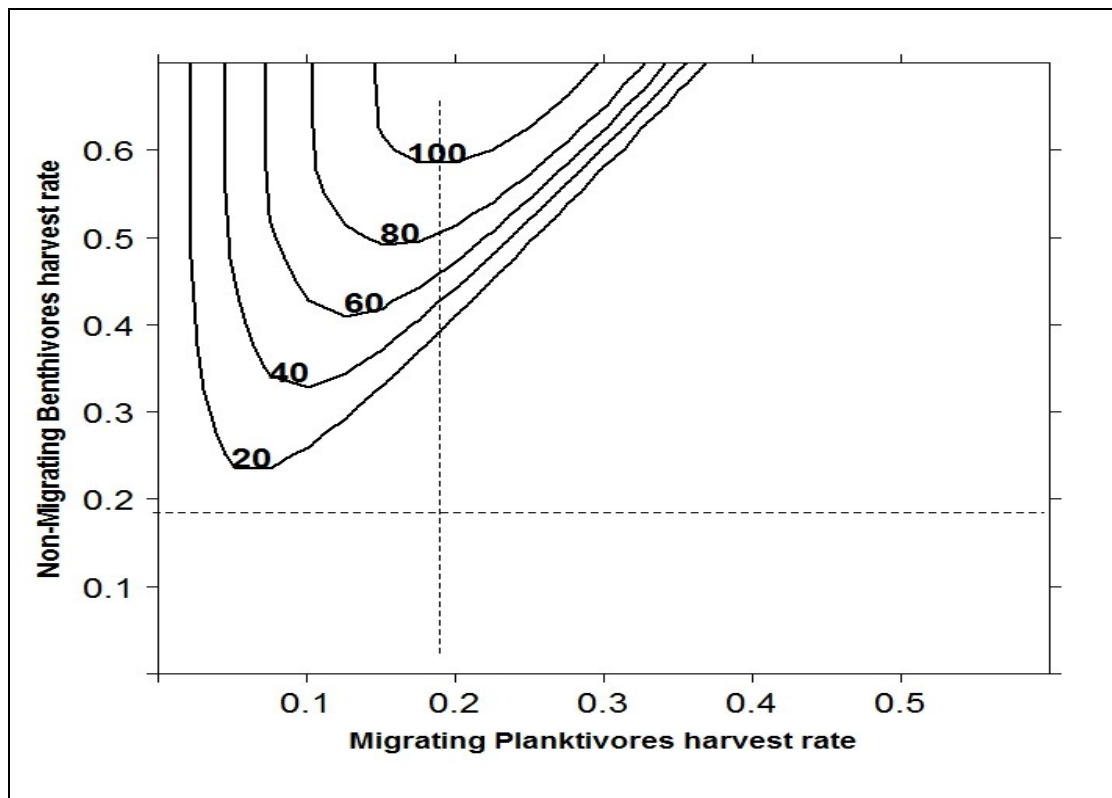


Figure 10. Migrating planktivores equilibrium yields (kt) obtained for pairs of harvest rates in the GOM region. Broken lines indicate  $h_{msy}$  from single-species model.

### iii. Southern New England

Two multi-species candidate models (M1-M2) resulted in a lower  $AIC_c$  values than the trophic grouping without interactions (M3) in Table 15. The conclusion from the raw  $AIC_c$  values was that model M1 is the preferred model (Table 16). It can be inferred that Model M1 has the only chance of being the best one among those considered in the set of candidate models based on the Akaike weights. The evidence ratio between the best and second-best model is approximately 15 (0.9383/0.0617). We also computed a weighted estimate of the predicted value, weighting the predictions by the Akaike weights ( $w_i$ ) with the unconditional sampling variance of the estimator ( $\theta$ ) in Table 17.

The multi-species model includes only two significant multi-species interactions: the positive Type-III predation effect of migrating piscivores (F) on non-migrating benthivores (B) and negative Type-I competition effect of migrating planktivores (P) on non-migrating benthivores (B). The predation effects (Type-III) of non-migrating piscivores (S) on migrating planktivores (P) and non-migrating benthivores (B) were not important in the multi-species biomass dynamics models in the SNE region (Table 15).

For each of the four primary biomass dynamics models in the Southern New England area, the largest changes in parameter values and improvements in predicted biomass were observed in migrating piscivores and non-migrating benthivores (Table 18, Figure 11). The maximum sustainable yield (MSY), corresponding harvest rate ( $f_{MSY}$ ), and the stock size at MSY ( $B_{MSY}$ ) for each group based on single-species biomass dynamics models are calculated in Table 19. The equilibrium yields of migrating piscivores increases with decreasing non-migrating benthivore harvest rate

(Figure 12). The equilibrium yields of non-migrating benthivores in the Southern New England depend on the harvest of migrating planktivores. The yield of non-migrating benthivores is maximized when migrating planktivore harvest rates increase (Figure 12).

Table 15. The feeding guild biomass dynamics models with multispecies interactions in the SNE region. The feeding guild groups are as follows: Non-migrating Benthivores (B): Yellowtail flounder, Winter flounder, Little skate; Non-migrating Piscivores (S): Summer flounder; Migrating Piscivores (F): Silver hake, Spiny dogfish, Winter skate, Goosefish, Pollock, White hake; Migrating Planktivores (P): Atlantic herring, Atlantic mackerel, and Longfin squid.

Model	Multi-species interaction	Total # of parameters	SSR	AIC <sub>c</sub>
M1	<p>Diagram for Model M1: A box labeled 'B' is connected to a box labeled 'P' by a horizontal line with a solid black dot at the 'B' end. Below this line is the label 'I'. Above 'B' is a box labeled 'F', with an arrow pointing from 'B' to 'F' labeled 'III'. Below 'B' and 'P' is a box labeled 'S'.</p>	15	4.911	225.581
M2	<p>Diagram for Model M2: A box labeled 'B' is connected to a box labeled 'P' by a horizontal line with a solid black dot at the 'B' end. Below this line is the label 'I'. Above 'B' is a box labeled 'F'. Below 'B' and 'P' is a box labeled 'S'.</p>	12	5.479	231.025
M3	Without interactions	11	7.023	258.355

Table 16. Result of  $AIC_c$  analysis for six competing models in the SNE region. Note that No. par<sub>*i*</sub> is the number of estimated parameters for model *i*; log( $L_i$ ) is natural logarithm of maximum likelihood for model *i*;  $\Delta_i(AIC_c)$  is AIC differences, relative to the smallest AIC value for given models;  $w_i(AIC_c)$  is the rounded Akaike weights.

Model	No. par <sub><i>i</i></sub>	log( $L_i$ )	$AIC_i$	$\Delta_i$	exp(-1/2* $\Delta_i$ )	$w_i(AIC_c)$
M1	15	-95.5	225.6	0.000	1.000	0.9383
M2	12	-102.1	231.0	5.444	0.066	0.0617
M3	11	-117.0	258.4	32.774	0.000	0.0000

Table 17. Multi-species model parameter estimates in the SNE region with model-averaged estimate, unconditional standard errors (SE), and the value for 90% confidence intervals (CI).

Parameter	Estimate	SE	90% CI	
			Upper	Lower
$r_b$	0.471	0.170	0.750	0.193
$k_b$	558	372	1169	-53
$B_{0_b}$	143	43	214	73
$r_s$	0.807	0.076	0.932	0.683
$k_s$	100*	-	-	-
$B_{0_s}$	28	5	36	20
$r_f$	0.013	0.007	0.024	0.003
$k_f$	4053	2863	8748	-643
$B_{0_f}$	738	266	1173	302
$r_p$	0.246	0.094	0.401	0.091
$k_p$	3047	1108	4864	1231
$B_{0_p}$	785	226	1155	415
$n_{bp}$	$1.19 \times 10^{-4}$	$1.39 \times 10^{-4}$	$3.46 \times 10^{-4}$	$1.09 \times 10^{-4}$
$d_{fb}$	0.097	8.593	14.2	-14.0
$\alpha_{fb}$	$1.40 \times 10^{-6}$	0.003	0.005	-0.005
$\alpha_{fp}$	0.023	2.07	3.4	-3.4

\* Fixed value

Table 18. The parameter values with standard deviations for the trophic grouping in the SNE region.  $k$  and  $B_0$  are in units of thousand metric tons.

Southern New England				
Parameters	Single-species	std. dev.	Multi-species	std. dev.
$r_b$	0.896	0.004	0.470	0.169
$k_b$	193	20	558	372
$B_{0\_b}$	127	60	143	43
$r_s$	0.807	0.076	0.807	0.076
$k_s$	100*		100*	
$B_{0\_s}$	28	4.92	28	5
$r_f$	0.064	0.024	0.010	$3.17 \times 10^{-4}$
$k_f$	4227	2892	4041	2861
$B_{0\_f}$	1038	214	718	258
$r_p$	0.250	0.100	0.247	0.094
$k_p$	2988	1069	3043	1101
$B_{0\_p}$	784	241	784	225
$n_{bp}$			$1.18 \times 10^{-4}$	$7.15 \times 10^{-5}$
$d_{fb}$			0.097	9.2
$\alpha_{fb}$			$1.40 \times 10^{-6}$	0.003
$\alpha_{fp}$			0.023	2.206
Number of observations	120		120	
Number of parameters	11		15	
Sum of squares	7.023		4.911	
AICc	258		226	

\* Fixed value

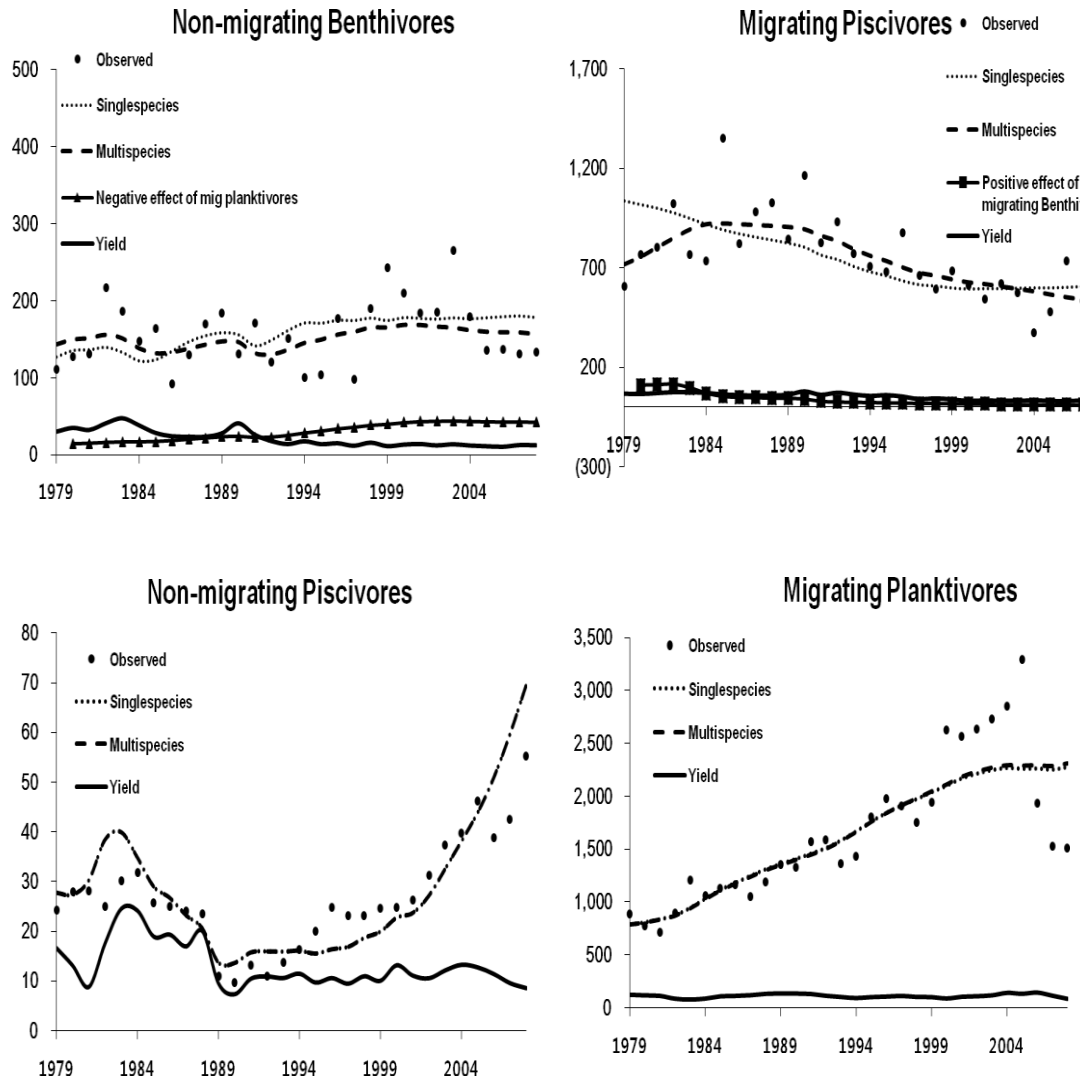


Figure 11. Observed biomass (closed circle), catch (solid line) and predicted biomass (dashed line) with interaction terms estimated with Type-I and -III functional responses (SNE). The y-axis has units of thousand metric tons.

Table 19. The maximum sustainable yield (MSY), corresponding harvest rate ( $f_{MSY}$ ), and the stock size at MSY ( $B_{MSY}$ ) for each group in the trophic grouping in the SNE region.

Model	Group	MSY (kt)	$f_{MSY}$	$B_{MSY}$
Single-species	P	186.6	0.125	1494
	B	43.3	0.448	97
	S	20.2	0.404	50
	F	67.4	0.032	2113

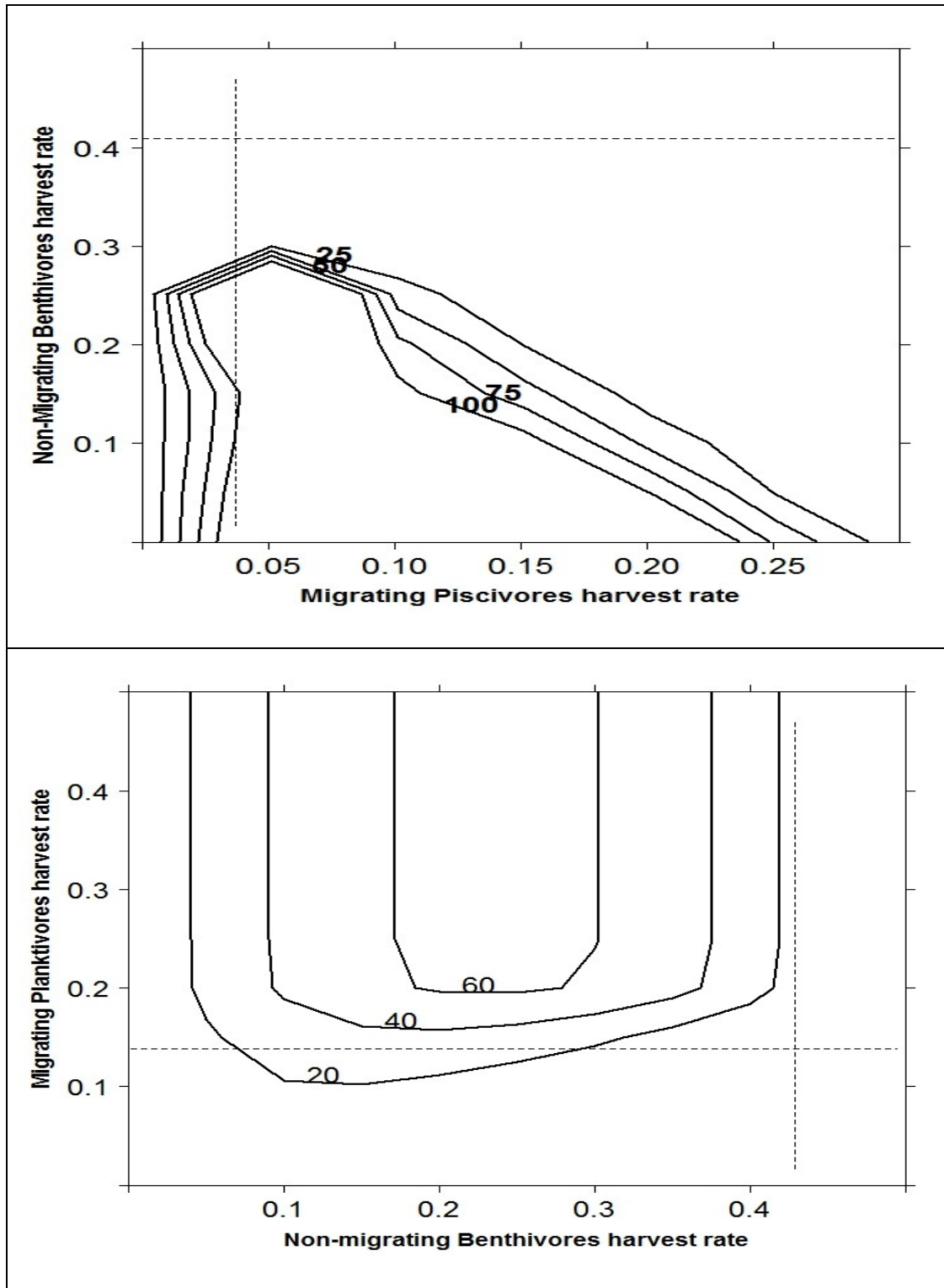


Figure 12. Migrating piscivores (above) and non-migrating benthivores equilibrium yield (kt) obtained for pairs of harvest rates in the SNE region. Broken lines indicate  $h_{msy}$  from single-species model.

#### IV. Multispecies models on multiple domains

This section summarizes the parameterized candidate models for multi-species biomass dynamics models with interactions based on multiple spatial areas. The biomasses and catches of the 15 fish species were aggregated into four trophic groups to simplify the model and to reduce the number of interaction terms: non-migrating benthivores (B), non-migrating piscivores (S), migrating piscivores (F), and migrating planktivores (P). In addition, we assumed that the migratory groups (planktivores and piscivores) range over the entire study area, such that their production can be described with a single set of model parameters ( $r$  and  $k$ ) in the entire area. By contrast, production of non-migrating groups (piscivores and benthivores) was assessed with a different set of model parameters ( $r$  and  $k$ ) for each spatial area. Refer to Methods III, Section C. for additional description of the multi-species interactions on multiple spatial areas.

There were eight candidate multi-species models spatially structured (M1-M8) with a lower Akaike Information Criterion ( $AIC_c$ ) than the trophic grouping without interactions (M9) in Table 20. The conclusion from the raw  $AIC_c$  values was that model M1 is the preferred model but it can be inferred that Model M1 has the relatively strong support based on the Akaike weights for each model (Table 21). The evidence ratio between the best and second-best model is approximately 2.83 ( $0.5282/0.1866$ ). Therefore, we computed a weighted estimate of the predicted value, weighting the predictions by the Akaike weights ( $w_i$ ) with the unconditional sampling variance of the estimator ( $\theta$ ) in Table 22.

The multi-species model on multiple domains includes five multi-species interactions (Model 1 in Table 20). The Type-III predation effects of migrating piscivores (F) on non-migrating benthivores (B) were important at the regional level (GOM and GB). The competition effects (Type-I) between migrating planktivores (P) and non-migrating benthivores (B) were significant in the SNE and GB areas (Model 1 in Table 20). In addition, the Southern New England area had strong predation effects of non-migrating piscivores (S) on migrating planktivores (P) and non-migrating benthivores (B) (Model 4 in Table 20).

For each of the four primary biomass dynamics models based on multiple spatial areas, the largest changes in parameter values and improvements in predicted biomass were observed in migrating piscivores and planktivores (Table 23, Figures 13-15).

The equilibrium yields of non-migrating benthivores (B) in the Georges Bank and Gulf of Maine areas depend on the harvest of migrating piscivores (Figure 16). The yields of benthivores in the Georges Bank and Gulf of Maine areas are maximized, by eliminating predators, when migrating piscivore harvest rates increase. Conversely, the yield of migrating piscivores increases with decreasing non-migrating benthivore harvest rate in the Georges Bank because migrating piscivores prey on non-migrating benthivores (Figure 17).

In addition, the yield of non-migrating benthivores depends on the harvest of migrating planktivores in the Southern New England. Non-migrating benthivore yields increase as the migrating planktivore harvest rate is increased due to the negative effect of competition from migrating planktivore in the area. On the other hand,

migrating planktivore yields in the Georges Bank are maximized as the non-migrating benthivore harvest rate is increased due to the negative competition effect (Figure 18).

Table 20. The feeding guild biomass dynamics models with multispecies interactions on multiple domains. We assumed that migratory groups range over the entire study area: migrating planktivores (P) and piscivores (F). Production of non-migrating groups was assessed in each domain: non-migrating benthivores (B) and piscivores (S). Note that each non-migrating groups in the boxes indicate Gulf of Maine, Georges Bank, and Southern New England from the top to the bottom.

Model	Multi-species interaction	Total # of parameters	SSR	AIC <sub>c</sub>
M1		30	8.128	571.786
M2		31	8.110	573.867
M3		26	8.588	574.688

Model	Multi-species interaction	Total # of parameters	SSR	AIC <sub>c</sub>
M4	<p>The diagram for Model M4 shows four boxes labeled F, B, S, and P. Box F is on the left, B is in the middle, S is below B, and P is on the right. There are two arrows pointing from B to F. A horizontal line with a dot at its right end connects B and P, labeled 'I' above it. A horizontal line with a dot at its left end connects B and S, labeled 'I' above it. A diagonal line with a dot at its top end points from the top-left of B to the top-left of S. Another diagonal line with a dot at its top end points from the top-right of S to the top-right of P.</p>	34	7.907	575.861
M5	<p>The diagram for Model M5 is identical to Model M4, showing interactions between F, B, S, and P with arrows and lines labeled 'I'.</p>	33	8.011	576.284
M6	<p>The diagram for Model M6 is identical to Model M4, showing interactions between F, B, S, and P with arrows and lines labeled 'I'.</p>	33	8.041	577.192

Model	Multi-species interaction	Total # of parameters	SSR	AIC <sub>c</sub>
M7		37	7.889	583.644
M8		23	9.878	600.78
M9	Without interactions	21	11.696	636.449

Table 21. Result of AIC<sub>c</sub> analysis for nine competing models in multiple spatial areas. Note that No. par<sub>*i*</sub> is the number of estimated parameters for model *i*; log(L<sub>*i*</sub>) is natural logarithm of maximum likelihood for model *i*; Δ<sub>*i*</sub>(AIC<sub>c</sub>) is AIC differences, relative to the smallest AIC value for given models; w<sub>*i*</sub> (AIC<sub>c</sub>) is the rounded Akaike weights.

Model	No. par <sub><i>i</i></sub>	log(L <sub><i>i</i></sub> )	AIC <sub><i>i</i></sub>	Δ <sub><i>i</i></sub>	exp(-1/2*Δ <sub><i>i</i></sub> )	w <sub><i>i</i></sub> (AIC <sub>c</sub> )
M1	30	-251.443	571.786	0.000	1.000	0.5282
M2	31	-251.164	573.867	2.081	0.353	0.1866
M3	26	-258.048	574.688	2.902	0.234	0.1238
M4	34	-248.125	575.861	4.075	0.130	0.0689
M5	33	-249.696	576.284	4.498	0.106	0.0557
M6	33	-250.15	577.192	5.406	0.067	0.0354
M7	37	-247.862	583.644	11.858	0.003	0.0014
M8	23	-274.834	600.78	28.994	0.000	0.0000
M9	21	-251.443	636.449	64.663	0.000	0.0000

Table 22. Multi-species model parameter estimates in multiple spatial areas with model-averaged estimate, unconditional standard errors (SE), and the value for 90% confidence intervals (CI).

Parameter	Estimate	SE	90% CI	
			Upper	Lower
r <sub>p</sub> Total	0.258	0.077	0.385	0.132
k <sub>p</sub> Total	7214	4645	14832	-404
B <sub>0_p</sub> Total	1039	273	1486	592
r <sub>f</sub> Total	0.032	0.219	0.391	-0.328
k <sub>f</sub> Total	5192	3663	11199	-815
B <sub>0_f</sub> Total	2229	1024	3908	549
r <sub>b</sub> GB	0.269	0.173	0.552	-0.014
k <sub>b</sub> GB	1020	700	2169	-128
B <sub>0_b</sub> GB	199	70	313	85
r <sub>b</sub> GoM	0.896	0.001	0.897	0.894
k <sub>b</sub> GoM	114	61	213	14
B <sub>0_b</sub> GoM	55	23	92	17
r <sub>b</sub> SNE	0.471	0.177	0.761	0.181
k <sub>b</sub> SNE	576	380	1199	-46
B <sub>0_b</sub> SNE	145	43	217	74
r <sub>s</sub> GB	0.497	0.028	0.543	0.452
k <sub>s</sub> GB	300*	-	-	-
B <sub>0_s</sub> GB	184	23	222	147
r <sub>s</sub> GoM	0.744	0.053	0.831	0.656
k <sub>s</sub> GoM	80*	-	-	-
B <sub>0_s</sub> GoM	36	9	50	21
r <sub>s</sub> SNE	0.808	0.076	0.932	0.683
k <sub>s</sub> SNE	100*	-	-	-
B <sub>0_s</sub> SNE	28	5	36	20
n <sub>pb</sub> GB	0.002	0.003	0.007	-0.003
n <sub>bp</sub> SNE	1.14x10 <sup>-4</sup>	7.27x10 <sup>-5</sup>	2.34x10 <sup>-4</sup>	-5.03x10 <sup>-6</sup>
c <sub>fb</sub> GB	4.03x10 <sup>-4</sup>	0.141	0.231	-0.231
d <sub>fb</sub> GB	0.005	1.618	2.658	-2.648
α <sub>fb</sub> GB	0.017	5.879	9.658	-9.625
α <sub>fp</sub> GB	0.006	1.943	3.192	-3.181
c <sub>fb</sub> GOM	6.12x10 <sup>-5</sup>	5.15x10 <sup>-5</sup>	1.46x10 <sup>-4</sup>	-2.32x10 <sup>-5</sup>
d <sub>fb</sub> GOM	7.57x10 <sup>-5</sup>	1.78x10 <sup>-4</sup>	3.68x10 <sup>-4</sup>	-2.16x10 <sup>-4</sup>
α <sub>fb</sub> GOM	0.004	0.005	0.011	-0.004
α <sub>fp</sub> GOM	1.60x10 <sup>-6</sup>	3.37x10 <sup>-6</sup>	7.12x10 <sup>-6</sup>	-3.63x10 <sup>-6</sup>
c <sub>sb</sub> SNE	0.005	0.016	0.031	-0.020

$c_{sp}$ SNE	$5.43 \times 10^{-4}$	$2.91 \times 10^{-3}$	0.005	-0.004
$\alpha_{sb}$ SNE	0.016	0.074	0.138	-0.106
$\alpha_{sp}$ SNE	$1.84 \times 10^{-8}$	$8.76 \times 10^{-7}$	$1.45 \times 10^{-6}$	$-1.42 \times 10^{-6}$
$c_{FP}$ Total	$4.39 \times 10^{-8}$	$5.55 \times 10^{-6}$	$9.15 \times 10^{-6}$	$-9.07 \times 10^{-6}$
$\alpha_{fb}$ Total	$1.36 \times 10^{-4}$	0.017	0.028	-0.028
$\alpha_{fp}$ Total	$1.65 \times 10^{-9}$	$2.47 \times 10^{-8}$	$4.06 \times 10^{-8}$	$-4.03 \times 10^{-8}$

\* Fixed value

Table 23. The parameter values with standard deviations for the trophic grouping in multiple spatial areas.  $k$  and  $B_0$  are in units of thousand metric tons.

Multiple areas including the Southern New England, Georges Bank and Gulf of Maine				
Parameters	Single-species	std. dev.	Multi-species	std. dev.
$r_p$ Total	0.246	0.091	0.254	0.072
$k_p$ Total	5039	1535	7265	4729
$B_{0_p}$ Total	1011	292	1048	270
$r_f$ Total	0.089	0.055	0.023	0.293
$k_f$ Total	5606	3594	5164	3671
$B_{0_f}$ Total	2954	698	2162	1090
$r_b$ GB	0.217	0.040	0.281	0.205
$k_b$ GB	1072	704	1014	700
$B_{0_b}$ GB	175	23	203	78
$r_b$ GoM	0.326	0.068	0.896	0.001
$k_b$ GoM	92	52	113	61
$B_{0_b}$ GoM	56	17	54	23
$r_b$ SNE	0.896	0.004	0.463	0.170
$k_b$ SNE	193	20	570	379
$B_{0_b}$ SNE	127	60	144	43
$r_s$ GB	0.497	0.028	0.497	0.028
$k_s$ GB	300*		300	
$B_{0_s}$ GB	184	23	184	23
$r_s$ GoM	0.744	0.053	0.744	0.053
$k_s$ GoM	80*		80	
$B_{0_s}$ GoM	36	9	36	9
$r_s$ SNE	0.807	0.076	0.807	0.076
$k_s$ SNE	100*		100	
$B_{0_s}$ SNE	28	5	28	5
$n_{pb}$ GB			0	0
$n_{bp}$ SNE			0	0
$c_{fb}$ GB			$2.95 \times 10^{-6}$	$1.09 \times 10^{-5}$
$d_{fb}$ GB			$4.37 \times 10^{-5}$	$1.60 \times 10^{-4}$
$\alpha_{fb}$ GB			$6.22 \times 10^{-5}$	$3.85 \times 10^{-4}$
$\alpha_{fp}$ GB			$1.88 \times 10^{-5}$	$1.24 \times 10^{-4}$
$c_{fb}$ GOM			$5.81 \times 10^{-5}$	$4.77 \times 10^{-5}$
$\alpha_{fb}$ GOM			0.0032373	0.004
$\alpha_{fp}$ GOM			$1.49 \times 10^{-6}$	$3.21 \times 10^{-6}$
Number of observations	240		240	
Number of parameters	21		30	
Sum of squares	11.696		8.128	

AICc	636	572
------	-----	-----

\* Fixed value

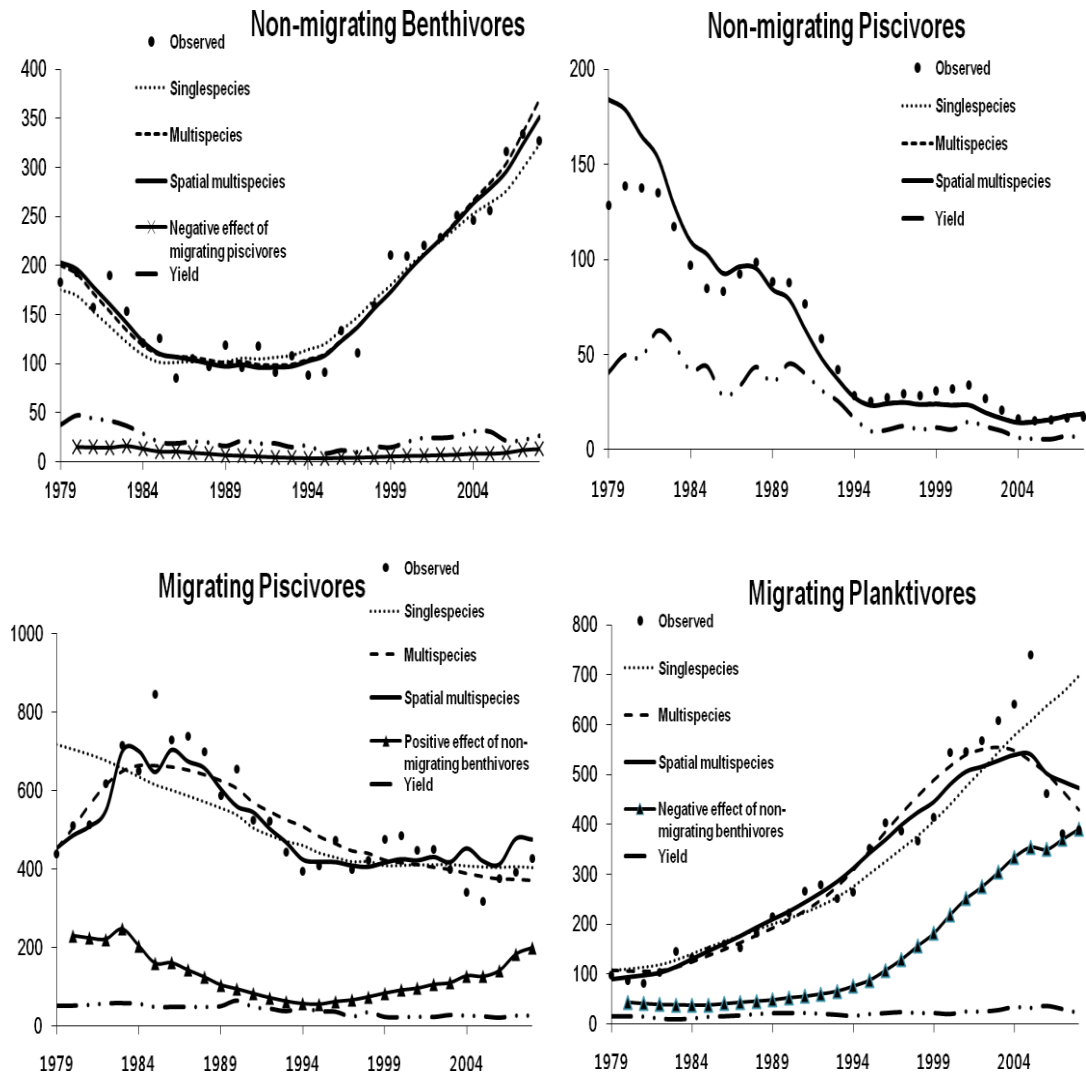


Figure 13. Observed biomass (closed circle) and predicted biomass from single-species (dotted line), multi-species (dashed line), and multi-species (solid line) models considered spatially in the Georges Bank region. The y-axis has units of thousand metric tons.

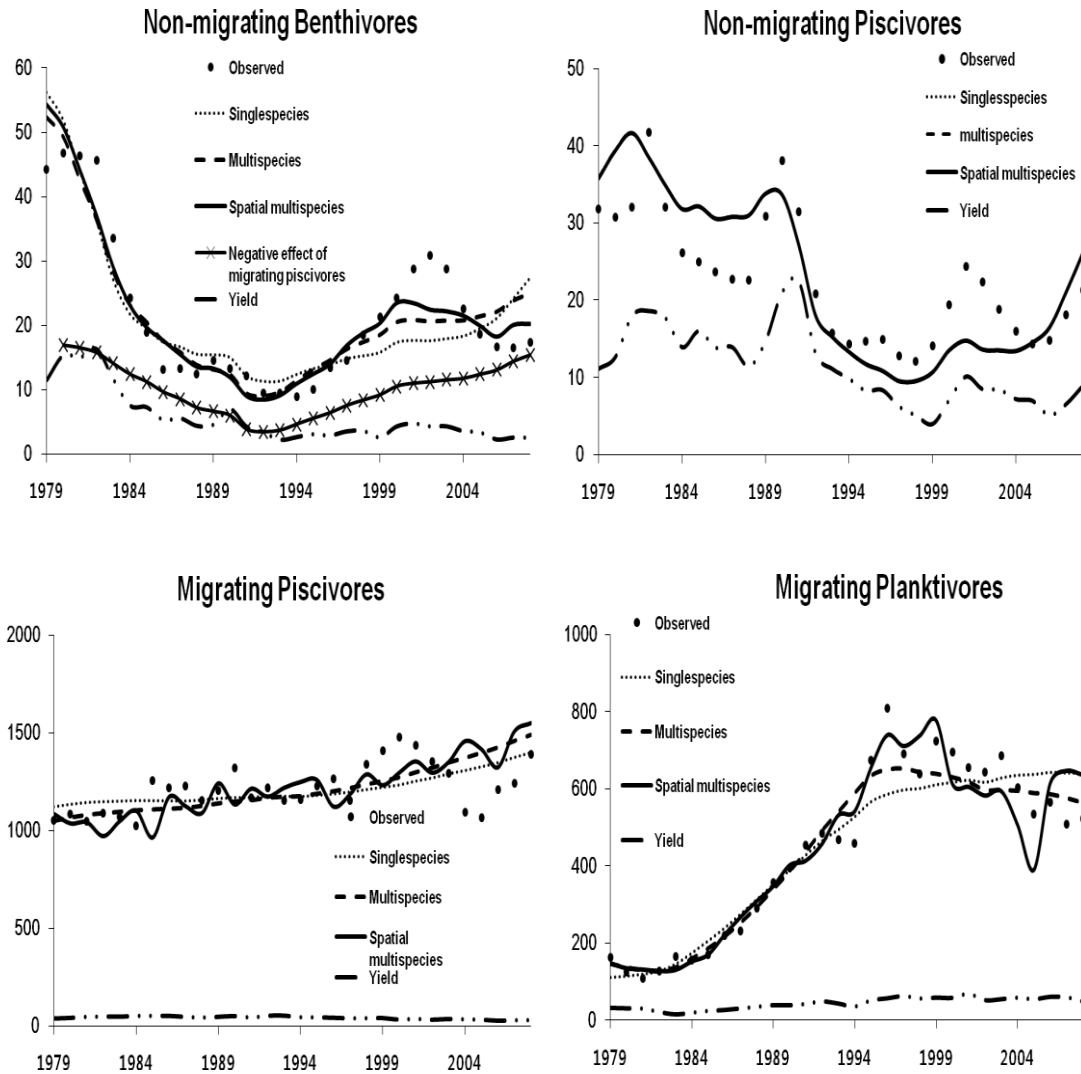


Figure 14. Observed biomass (closed circle) and predicted biomass from single-species (dotted line), multi-species (dashed line), and multi-species (solid line) models considered spatially in the Gulf of Maine region. The y-axis has units of thousand metric tons.

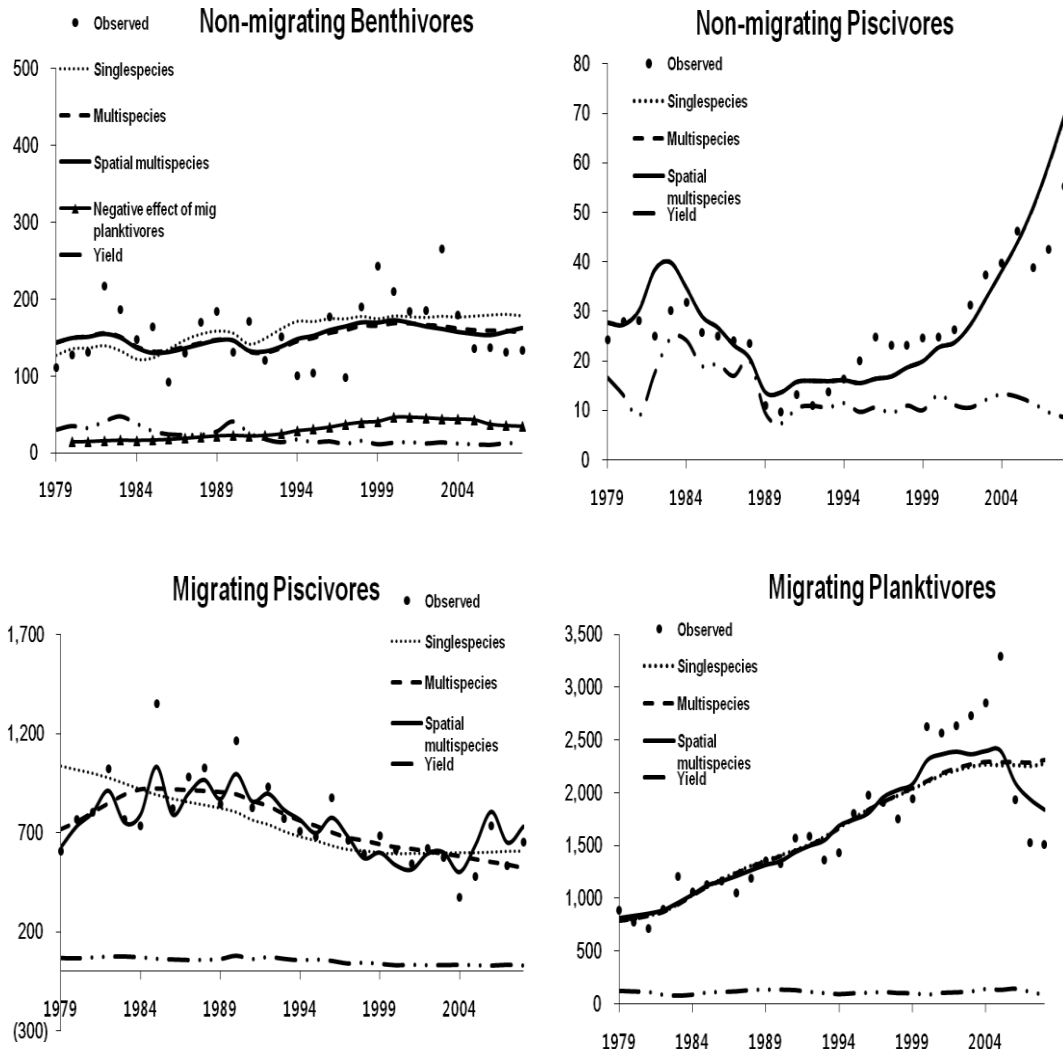


Figure 15. Observed biomass (closed circle) and predicted biomass from single-species (dotted line), multi-species (dashed line), and multi-species (solid line) models considered spatially in the Southern New England region. The y-axis has units of thousand metric tons.

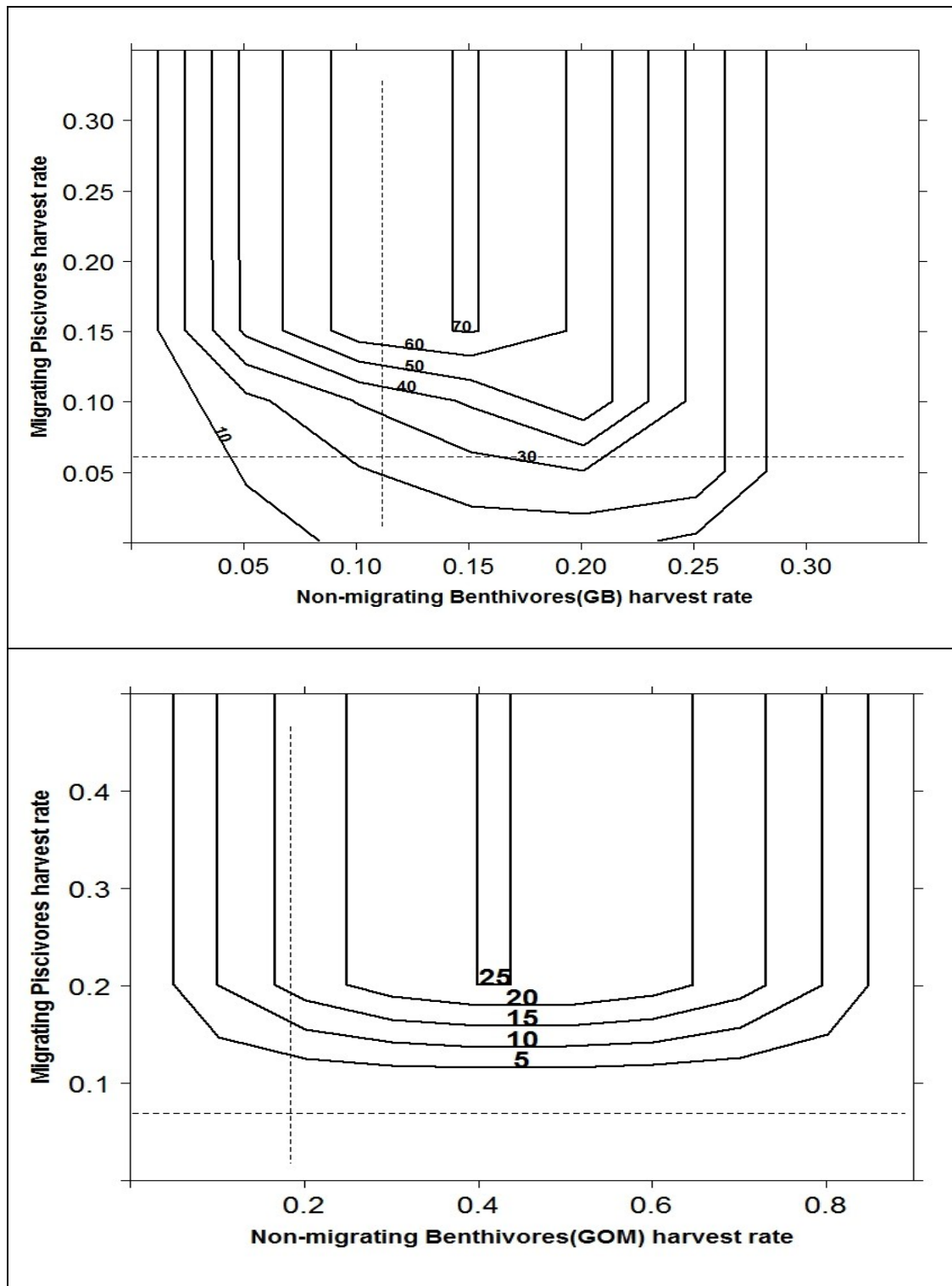


Figure 16. Non-migrating benthivores equilibrium yield (kt) obtained for pairs of harvest rates in the Georges Bank (above) and Gulf of Maine (below) areas. Broken lines indicate  $h_{msy}$  from single-species model.

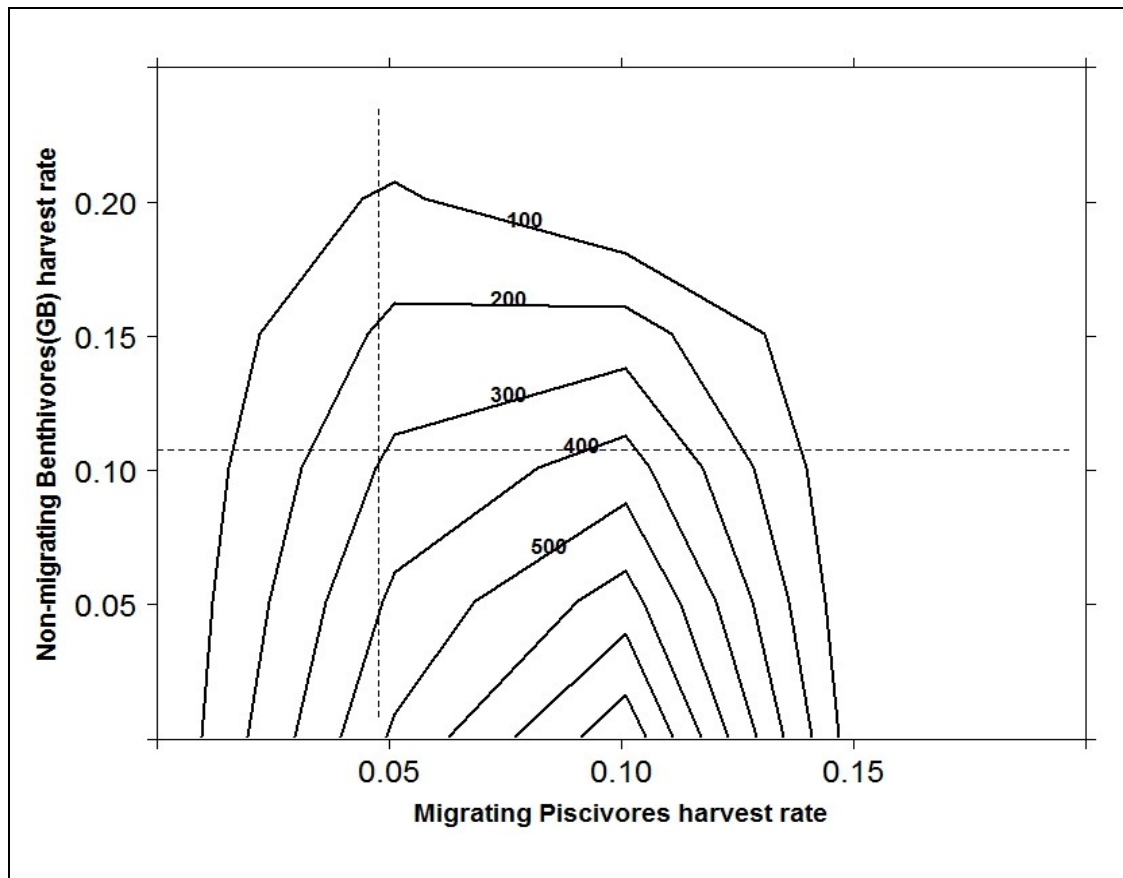


Figure 17. Migrating piscivores equilibrium yield (kt) obtained for pairs of harvest rates in the Georges Bank area. Broken lines indicate  $h_{msy}$  from single-species model.

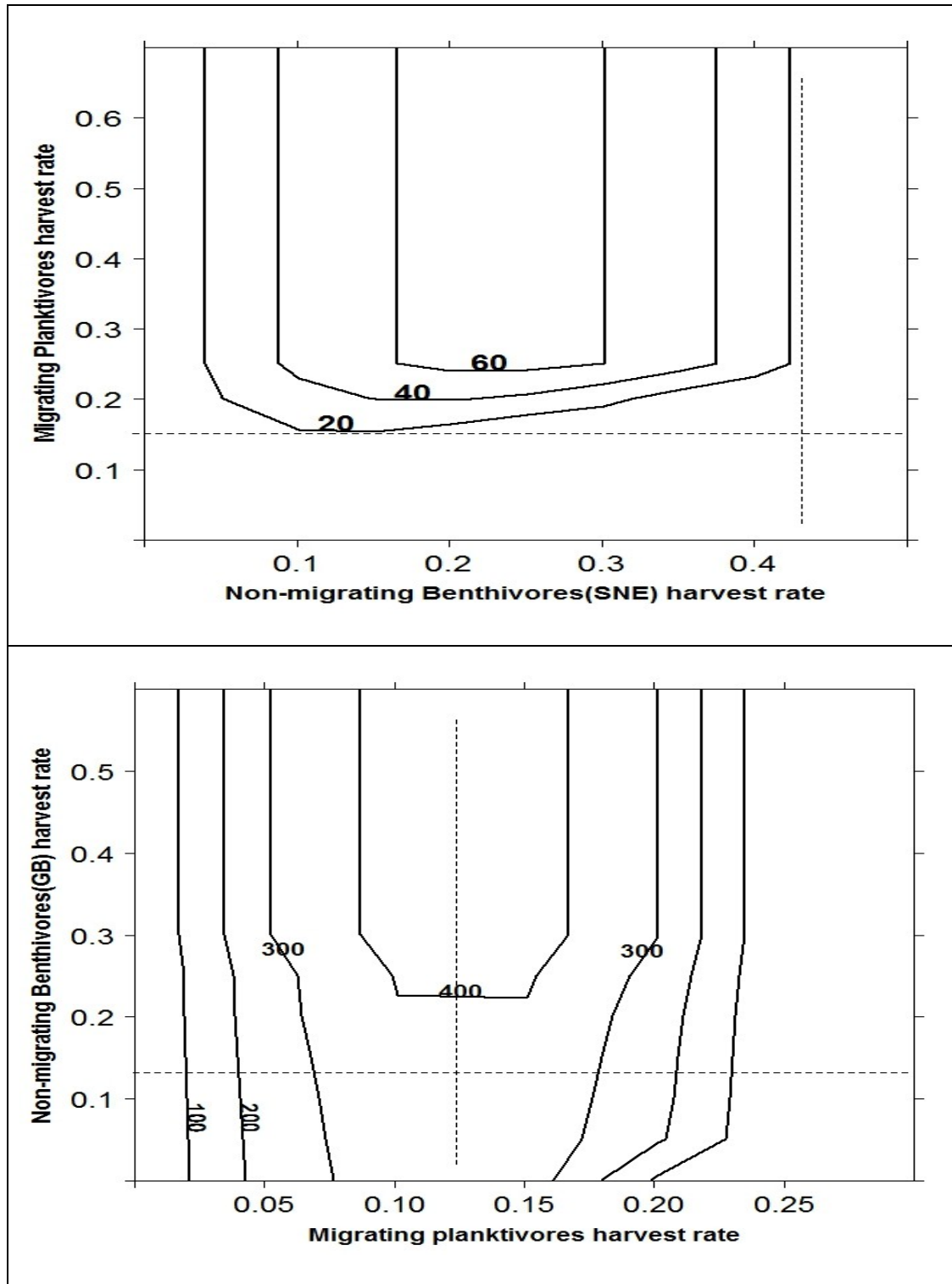


Figure 18. Non-migrating benthivores (above) and migrating planktivores (below) equilibrium yield (kt) obtained for pairs of harvest rates in the SNE and GB areas. Broken lines indicate  $h_{msy}$  from single-species model.

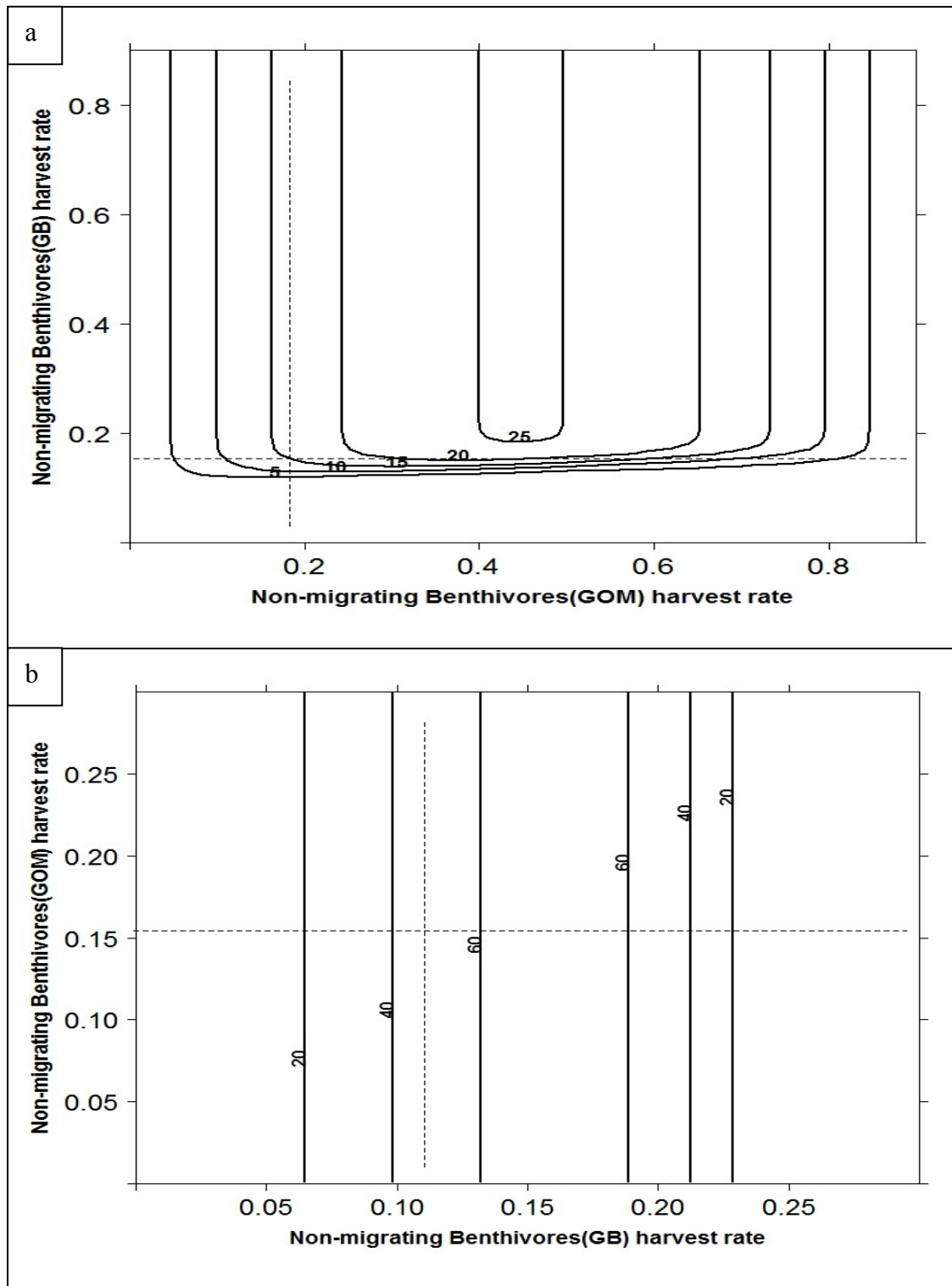


Figure 19. Non-migrating benthivores equilibrium yield (kt) obtained for pairs of harvest rates in the Gulf of Maine (a) and Georges Bank (b) areas. Broken lines indicate  $h_{msy}$  from single-species model.

## DISCUSSION

In this study we extended multispecies biomass-dynamics models to multiple spatial areas to account for patterns of connectivity. The spatial distribution of each group was determined from trawl-survey data, taking into account distributional shifts. One of the benefits of the multi-species models approach considered spatially is its capacity for examining the translation of species interactions across multiple areas. To account for the question of spatial overlap between the predator and prey species, which has been demonstrated in many ecosystems to be highly variable, resulting in widely varying predation mortality, the multi-species model needs to be spatially disaggregated (Bogstad et al. 1994, Bogstad and Tjelmeland 1990).

Even though some of changes in fish community structures may be related to fishing impacts (Atkinson et al. 1997, Garrison and Link 2000), there is a broad body of evidence that climate fluctuations are playing an important role. During the warm period of the 1920s to 1950s, the distribution of fish species such as cod, haddock and herring expanded northward and eastward in the North Atlantic (Drinkwater 2006). There have been clear poleward shifts in many stocks on the northeast Atlantic continental shelf consistent with a warming trend since the mid 1960s (Murawski 1993, Nye et al. 2009, Rose 2005): During warmer periods, “southern” species have tended to become more prominent and “northern” species less abundant.

Nye et al. (2009) reported that the center of biomass for little and winter skate appeared to shift southward, and poleward shifts occurred in alewife, American shad, silver hake, red hake (southern stock), and yellowtail flounder (southern stock) during the warm periods of the 1980s and 1990s. The trend analysis in our study from the

bottom trawl-survey data showed similar trends with symmetric responses to climate variations among species. For example, three fish species including Atlantic herring, silver hake, and white hake showed a significant decrease in the Southern New England and an increasing trend in the Gulf of Maine. On the other hand, little and winter skate showed a significant increase in the Southern New England and a significant decrease in the Georges Bank region (Figure 1a-1c and Table 1), which corresponds to previous results from Nye et al. (2009).

If the data from a fishing survey using research vessel can be disaggregated into age groups, much more information can be extracted (Doubleday 1981, Doubleday and Rivard 1981). Still, the catch-at-age data are quite sensitive to any errors such as sampling and measurement errors (Doubleday and Rivard 1981). Apart from sampling and measurement errors, variation can also occur in data sets due to variations in the ecological system, such as climatic, seasonal, or topographic variation. In a time series of bottom-trawl surveys, for example, environmental variation from year to year may cause fluctuations in catch rates, which often fails to produce reliable estimates for management purposes (Hilborn and Walters 1992). However, biased indices of abundance from the survey data can be calibrated from other sources of information through many current methods of stock analysis including VPA or tuned VPA based on the long-term stock assessment (Gulland 1988).

We used such estimates of biomass from recent stock assessments for our model analysis. Fitting the biomass dynamics models to the stock assessment biomass estimates instead of fitting directly to the survey data is straightforward if biomass is assumed to be known without error. In addition, this approach is suitable for the

specific cases where no data series of effort or age are available and where the only estimates available are the total catch and biomass from stock assessments to obtain the MSY of the fish stocks (Garcia et al. 1989).

Overholtz et al. (2000) found that pelagic fish community in the northeast Atlantic continental shelf is heavily consumed by predatory fishes and the consumption by predatory fish was important during 1973-1997 in the region. In our study, Atlantic mackerel showed a decreasing trend in the Gulf of Maine, even though there were no significant trends in the Southern New England and Georges Bank (Figure 1a and Table 1). Spiny dogfish is an important predator of mackerel, removing significant quantities of the species during the 1990s in the region (NEFSC 2006).

Our results showed that the Type-III predation effects of migrating piscivores (F) on non-migrating benthivores (B) were important and statistically significant in the Georges Bank and Gulf of Maine areas, suggesting that the largest removal of non-migrating benthivores production can be explained due to predation by migrating piscivores (F) (Model 1 in Table 20).

Furthermore, migrating groups played a spatially essential role in species interactions across multiple areas, indicating that the three spatial areas are functionally connected through the high degree of connectivity and direct linkages between migrating groups (F and P) and non-migrating groups (B and S) in Table 20. In addition, the estimated trophic interactions for predation and competition effects are the same order of magnitude as the observed catch, suggesting that species interactions over the study areas were also significant when commercial catch was accounted for in the models.

Atlantic herring and mackerel are known to be important prey species consumed by predators including silver hake, spiny dogfish, winter skate, and cod (Overholtz et al. 1991, Tsou and Collie 2001). Predation is a dominant source of mortality for prey species (herring and mackerel) over the entire study area as indicated by the negative effect (predation) of migrating piscivores (F) on migrating planktivores (P) (Model 7 in Table 20). The relatively strong impact of predation by migrating piscivores (F) on prey groups (P) can partly explain the change of fish community structure in the study areas, reflecting shifts in the dominant piscivores from cod to spiny dogfish or goosefish (Link and Garrison 2002, Link 2007, Overholtz and Link 2007). However, we could not find any significant predation effect of cod on migrating planktivores in all the regions (Table 20). Note that non-migrating piscivores (S) in the Gulf of Maine and Georges Bank (Table 2 and Table 3) consist of two fish species (summer flounder and cod) but the S group does not include cod in the Southern New England (Table 4 and Table 20). The Atlantic cod are assessed and managed as two stocks: the Gulf of Maine and Georges Bank cod stocks (NEFSC 2012).

The interactions with non-migrating piscivores (S) were not important in multi-species models considered spatially, except for Southern New England (Table 17). The Southern New England area had a strong predation effect of non-migrating piscivores (summer flounder) on migrating planktivores: negative effect of S on P (Model 4 in Table 20). The strong impact of predation by non-migrating piscivores (S) on migrating planktivores (P) in the Southern New England area could reflect the relatively higher abundance of longfin squid consumed by summer flounder, which

corresponds to previous diet analysis results from Bowman et al. (2000). The diet of summer flounder sampled in Southern New England during 1977-1980 contained on average > 50% squid by weight (23.7% for northern shortfin squids and 24.4% for longfin squids), and longfin squids have still remained the main prey species (10-25%) for summer flounder since 1970s in the area (Bowman et al. 2000, Smith and Link 2010).

The prevalence of trophic asymmetry, having an unsymmetrical intensity of competition or predation between two organisms, as a response to stress is not well-established. Dispersal limitation, reduced functional redundancy, or increased physiological sensitivity to environmental stress for species in higher trophic levels may result in trophic asymmetry. In our study, the predation interactions between migrating piscivores (F) and non-migrating benthivores (B) work in both directions (Model 1-2 in Table 20). On the other hand, unidirectional negative interactions are also detected in the other species interactions over the study areas (Table 20). In Southern New England, there appear to be more top-down (negative) interactions, suggesting that predators (S group) are not food limited.

We interpreted the (reciprocal) negative interaction between migrating piscivores (F) and non-migrating piscivores (S) as competition (results not shown) based on the diet overlap between these two groups (Grosslein et al. 1980, Bowman et al. 2000, Smith and Link 2010). In addition, the negative interaction between migrating planktivores (P) and non-migrating benthivores (B) was regarded as competition through pathways of energy flow in benthic-pelagic linkages. Migrating planktivores (P), for example, are known to prey on primarily planktonic organisms

(e.g. chaetognaths, copepods, pelagic amphipods, mysids, euphausiids, or salps), and non-migrating benthivores (B) typically eat some combination of small benthic crustaceans, echinoderms, cnidarians, or polychaetes (Bowman et al. 2000, Smith and Link 2010). We used Type-I functional responses for the competition effects so as not to estimate additional parameters ( $\alpha$  coefficients).

The influence of species interactions on the change of fish community structure in the study areas was explained by direct predator-prey interactions, mostly predation. However, the consequence of indirect effects to communities or ecosystems could also result in fish populations increasing or declining in the food web. One of example of an indirect interaction was evident between non-migrating benthivores residing in the Gulf of Maine and Georges Bank (Model 2 in Table 20). The equilibrium yields of migrating piscivores (F) depend on the harvest of non-migrating benthivores in the both areas due to predation. As non-migrating benthivore harvest rates in the Georges Bank increase, the yields of migrating piscivores decline in the area (direct effect) (Figure 17). The decline would remove their consumption of non-migrating benthivores in the Gulf of Maine and, as an indirect effect, the yields of benthivores in the Gulf of Maine are maximized (Figure 19a). However, the change of non-migrating benthivore harvest rates in the Gulf of Maine does not greatly affect the equilibrium yields of non-migrating benthivores in the Georges Bank, which may be due to the low levels of current stock biomass in the area (Figure 19b).

Still, the use of multi-species biomass dynamics model across multiple domains demonstrated trade-off in species abundance and community compositions that arose from different fishing patterns (Figures 16-19). The harvesting of one

species or group may affect the harvest of another. Therefore, fish population responses were a function of not only the rate of fishing, but also of both direct and indirect interactions among species.

Our results showed that accounting for trophic interactions improves the model fit and that the strength and direction of these interactions vary among spatial domains. Based on the area-specific interaction effects, this approach can help us understand the functional connections among multiple areas and thus inform current fisheries management.

APPENDIX A

Table A1. Summary of biomass data sources and methods.

Species name	Stock structure	Year	Assessment Method	Assessment estimates available	Data sources
Haddock	GB stock	1960-2011	VPA and Swept Area Abundances	Stock Biomass (January 1)	NEFSC Reference Doc. 12-06 (Table B16)
	GOM stock	1977-2011	VPA	Stock Biomass (January 1)	NEFSC Reference Doc. 12-06 (Table C.17 and Table C.30)
Yellowtail flounder	GB stock	1963-1972	Catch-Survey Analysis (CSA) method	Total Biomass	Data from Erin's MS thesis
		1973-2008	VPA	Stock Biomass (January 1)	NEFSC Reference Doc. 08-15 (Table C12b) and 08-16 (page 318)
	CC/GOM stock	1985-2008	VPA	Stock Biomass (January 1)	NEFSC Reference Doc. 08-16 (page 468-478)
	CC/GOM stock	1985-2005	VPA	Population numbers at age (Jan 1)	NEFSC Reference Doc. 12-06 (Table D14 and 17)
	SNE/MA stock	1973-2008	VPA	Stock Biomass (January 1)	NEFSC Reference Doc. 08-16 (page 404)
Winter flounder	GB stock	1964-2000	Age-structured assessment model	Total Biomass	NEFSC Reference Doc. 02-03 (Table 1)
	GB stock	2001-2005	VPA	Mean stock weights (2003-2007)	NEFSC Reference Doc. 08-15 (Table K24)

Species name	Stock structure	Year	Assessment Method	Assessment estimates available	Data sources
Winter flounder	GB stock	2006-2011	VPA	Mean stock weights (2006-2010)	NEFSC Reference Doc. 11-17 (Table B31)
	GB stock	1982-2011	VPA	Population numbers at age (Jan 1)	NEFSC Reference Doc. 11-17 (Table B24)
	GOM stock	1982-2010		January 1 Mean stock weights-at-age	NEFSC Reference Doc. 11-17 (page 951)
	GOM stock	1982-2008	VPA	Population numbers at age (January 1)	NEFSC Reference Doc. 08-15 (Table I19)
	SNE/MA stock	1981-2010		January 1 Mean stock weights-at-age	NEFSC Reference Doc. 11-17 (page 914)
	SNE/MA stock	1981-2008	VPA	Population numbers at age (January 1)	NEFSC Reference Doc. 08-15 (Table J29)

Species name	Stock structure	Year	Assessment Method	Assessment estimates available	Data sources
Atlantic cod	GB stock	1963-1977	Modified catch survey analysis (CSA)	Total Biomass	Data from Erin's thesis
		1978-2005	VPA using ADAPT	January 1 stock numbers, January 1 stock weight at age	NEFSC Reference Doc. 06-10 (Table 12) and NEFSC Reference Doc. 08-05 (Table A6 and Table A17a)
		1978-2008	VPA	Stock Biomass (January 1)	NEFSC Reference Doc. 08-16 (page 41)
		1978-2011	VPA using ADAPT	Stock Biomass (January 1)	NEFSC Reference 12-06 (Table A13c)
	GOM stock	1963-1982	VPA	Population numbers (January 1)	SAW 33 (NEFSC 01-18) & GRAM 2 and GRAM 3 (p 529)
		1982-2005	VPA	Population numbers (January 1)	NEFSC Reference Doc. 05-13 (Table F5a and Table F11)
		1982-2010	ASAP base model	Stock Biomass (January 1)	NEFSC Reference Doc. 12-05 (Table A.39, A.42 and A.64)

Species name	Stock structure	Year	Assessment Method	Assessment estimates available	Data sources
Summer flounder	Managed as a unit stock	1982-2007	Two model approaches: VPA + Surplus Production analysis	Stock Biomass (January 1)	NEFSC Reference Doc. 08-12 (page 214-215)
		1979-1981		Catch numbers & Mean stock weights at age	NEFSC Reference Doc. 11-20 (Table 26-27)
		2008-2010		Mean stock weights (January 1)	NEFSC Reference Doc. 08-12 (page 249)
		1982-2010		Population numbers (January 1)	NEFSC Reference Doc. 11-20 (Table 57)
Silver Hake	Northern stock	1963-1999	Bayesian Surplus Production (BSP) method	Total Biomass	NEFSC Reference Doc. 01-03 (Appendix 1; page 125), NEFSC Reference Doc. 11-02 (Table A37 and A40)
	Southern stock	1963-1999	Bayesian Surplus Production (BSP) method	Total Biomass	NEFSC Reference Doc. 01-03 (Appendix 1; page 131), NEFSC Reference Doc. 11-02 (Table A38 and A41)
Spiny Dogfish	Managed as a unit stock	1963-1967	Catch-Survey Analysis (CSA) method	Total Biomass	Data from Erin's thesis
	Managed as a unit stock	1968-2006	Swept Area method	Total Biomass	NEFSC Reference Doc. 06-25 (Table B6.2 )
	Managed as a unit stock	1968-2009	Swept Area method	Total Biomass	NEFSC Reference Doc. 10-06 (Table 8)

Species name	Stock structure	Year	Assessment Method	Assessment estimates available	Data sources
Winter & Little Skate	Stock complex	1963-2008	Swept Area method	Fall survey & stock biomass	Data from Erin's thesis and NEFSC Reference Doc. 09-02
Goosefish	Northern stock	1980-2009	Statistical Catch-At-Length Analysis (Scale model)	Total Biomass	NEFSC Reference Doc. 10-17 (Table A35)
	Southern stock	1980-2009	Statistical Catch-At-Length Analysis (Scale model)	Total Biomass	NEFSC Reference Doc. 10-17 (Table A35)
Pollock	Gulf of Maine/Georges Bank stock	1970-2009	Age Structured Assessment Program (ASAP)	Stock Biomass (January 1)	NEFSC Reference Doc. 10-17 (C11)
White hake	Gulf of Maine/Georges Bank stock	1985-1993	Two model approaches: Modified DeLury model and Surplus Production model	Stock Biomass	NEFSC Reference Doc. 95-08 (page 80)
		1979-1988	Average value were calculated using the Rivard estimates 1989-2007	Mean stock weights at age	NEFSC Reference Doc. 95-08 (page 80)
		1989-2007	Rivard Jan-1 weights-at-age	January 1 weight-at-age	NEFSC Reference Doc. 08-15 (Table L14)
		1963-2007	ASPM	Population abundance	NEFSC Reference Doc. 08-15 (Table L23) and NEFSC Reference Doc. 12-06 (Table H1, H4, H10)

Species name	Stock structure	Year	Assessment Method	Assessment estimates available	Data sources
Atlantic herring	Combined Gulf of Maine-Georges Bank stock	1961-1966	Forward Projection Approach model (FPA)	Stock Biomass (January 1)	NEFSC Reference Doc. 04-06 (page 239 )
		1967-2002	VPA: un-tuned VPA method	Population numbers (January 1)	NEFSC Reference Doc. 04-06 (Page 272)
		1967-2002		Mean Weight at age	NEFSC Reference Doc. 04-06 ( Table 3.3)
		2003-2008	Age Structured Assessment Program (ASAP)	Total biomass (age 2+, January 1)	TRAC Reference Doc. 2009-04 (Table 17)
Atlantic mackerel	Managed as a unit stock	1963-2003	VPA (From Erin's estimates)	Total Biomass	Data from Erin's thesis and NEFSC 06-09
		2000-2008	Catch-Survey Analysis (CSA) method	Catch abundance and Mean weight	TRAC Reference Doc. 2010-13 (Table 1 and Table 3)
		2000-2008		Survey abundance	TRAC Reference Doc. 2010-01 (Table 5)
Longfin squid	Managed as a unit stock	1976-2009		Stock Biomass	NEFSC Reference Doc. 11-02 (Table B25)

Table A2. Summary of catch data sources.

Species name	Stocks	Year	Data (available)	Data sources
Haddock	GB stock	1960-2010	landings	NEFSC Reference Doc. 08-15 (Table B3) and 12-06 (Table B1 and Table B3)
	GOM stock	1964-2010	commercial & recreational landings with discards	NEFSC Reference Doc. 12-06 (Table C.1)
Yellowtail flounder	GB stock	1935-2007	commercial landings & discards	NEFSC Reference Doc. 08-15 (Table C1)
	CC/GOM stock	1935-2010	commercial landings & discards	NEFSC Reference Doc. 12-06 (Table D1)
	SNE/MA stock	1935-2007	commercial landings & discards	NEFSC Reference Doc. 08-15 (Table D1)
Winter flounder	GB stock	1964-2010	commercial landings & discards	NEFSC Reference Doc. 11-17 (Table B3)
	GOM stock	1964-2010	commercial & recreational landings with discards	NEFSC Reference Doc. 11-17 (Table C1 and C13)
	SNE/MA stock,	1964-2010	commercial & recreational landings with discards	NEFSC Reference Doc. 11-17 (Table A1, A4, A5, Appendix A)
Little skate	Stock complex	1964-2007	commercial landings & discards (regional proportions)	NEFSC Reference Doc. 09-02 (Table 1 and Table 10)
Atlantic cod	GB stock	1960-2010	commercial & recreational landings with discards	NEFSC Reference Doc. 12-06 (Table A1 and A5)
	GOM stock	1964-2010	commercial & recreational landings with discards	NEFSC Reference Doc. 12-05 (Table A.6)
Summer flounder	Managed as a unit stock	1940-2010	commercial & recreational landings with discards (regional proportions)	NEFSC Reference Doc. 11-20 (Table 1 and Table 28)
Silver Hake	Northern stock	1955-2009	commercial landings & discards (regional proportions)	NEFSC Reference Doc. 11-02 (Table A1 and Table A28)
	Southern stock	1955-2009	commercial landings & discards (regional proportions)	NEFSC Reference Doc. 11-02 (Table A1 and Table A29)

Species name	Stocks	Year	Data (available)	Data sources
Spiny Dogfish	Stock complex	1962-2005	commercial & recreational landings with discards	NEFSC Reference Doc. 06-25 (Table B4.1, B4.8, B4.13)
		2005-2008	commercial & recreational landings with discards	TRAC Reference Doc. 2010-02 (Page 2) & NEFSC 10-06
Winter Skate	Stock complex	1964-2007	commercial landings & discards (regional proportions)	NEFSC Reference Doc. 09-02 (Table 1 and Table 10)
Goosefish	Northern stock	1964-2009	commercial landings & discards (regional proportions)	NEFSC Reference Doc. 10-17 (Table A3 and Table A10)
	Southern stock	1964-2009	commercial landings & discards (regional proportions)	NEFSC Reference Doc. 10-17 (Table A3 and Table A10)
Pollock	A unit stock: Gulf of Maine/Georges Bank stock	1960-2009	commercial & recreational landings with discards (regional proportions)	NEFSC Reference Doc. 10-17 (Table C2)
White hake	A unit stock: Gulf of Maine/Georges Bank stock	1964-2010	commercial & recreational landings with discards (regional proportions)	NEFSC Reference Doc. 12-06 (Table H1 and Table H4)
Atlantic herring	Stock complex: Combined Gulf of Maine-Georges Bank stock	1960-2008	commercial landings (regional proportions)	NEFSC Reference Doc. 04-06 (Table 3.2) TRAC Reference Doc. 2009-04 (Table 1)
Atlantic mackerel	Managed as a unit stock	1960-2005	commercial & recreational landings (regional proportions)	NEFSC Reference Doc. 06-09 (Table B1)
		2005-2008	commercial & recreational landings (regional proportions)	TRAC Reference Doc. 2010-13 (Table 5)
Longfin squid	Managed as a unit stock	1963-2010	commercial landings & discards (regional proportions)	NEFSC Reference Doc. 11-02 (Table B3 and Table B7)

## APPENDIX B

The ADMB .tpl file code for multi-species biomass dynamics model in multiple areas (model M1 in Table 20).

### DATA\_SECTION

```
init_int nyrs;           //first entry in .dat is the number of yrs of // data
init_matrix Data(1,nyrs,1,87); // .dat is a matrix with nyr rows and 87 columns

    vector Year(1,nyrs); //1. column number in .dat file
// Georges Bank biomass and catch data
vector obs_bio_GB_HAD(1,nyrs); //2.
vector obs_bio_GB_YTL(1,nyrs); //3.
vector obs_bio_GB_WFL(1,nyrs); //4.
vector obs_bio_GB_LSK(1,nyrs); //5.
vector obs_bio_GB_COD(1,nyrs); //6.
vector obs_bio_GB_SFL(1,nyrs); //7.
vector obs_bio_GB_SHK(1,nyrs); //8.
vector obs_bio_GB_SPD(1,nyrs); //9.
vector obs_bio_GB_WSK(1,nyrs); //10.
vector obs_bio_GB_GOS(1,nyrs); //11.
vector obs_bio_GB_POL(1,nyrs); //12.
vector obs_bio_GB_WHK(1,nyrs); //13.
vector obs_bio_GB_HER(1,nyrs); //14.
vector obs_bio_GB_MCK(1,nyrs); //15.
vector obs_bio_GB_SQD(1,nyrs); //16.
vector obs_cat_GB_HAD(1,nyrs); //17.
vector obs_cat_GB_YTL(1,nyrs); //18.
vector obs_cat_GB_WFL(1,nyrs); //19.
vector obs_cat_GB_LSK(1,nyrs); //20.
vector obs_cat_GB_COD(1,nyrs); //21.
vector obs_cat_GB_SFL(1,nyrs); //22.
vector obs_cat_GB_SHK(1,nyrs); //23.
vector obs_cat_GB_SPD(1,nyrs); //24.
vector obs_cat_GB_WSK(1,nyrs); //25.
vector obs_cat_GB_GOS(1,nyrs); //26.
vector obs_cat_GB_POL(1,nyrs); //27.
vector obs_cat_GB_WHK(1,nyrs); //28.
vector obs_cat_GB_HER(1,nyrs); //29.
vector obs_cat_GB_MCK(1,nyrs); //30.
vector obs_cat_GB_SQD(1,nyrs); //31.

// Gulf of Maine biomass and catch data
vector obs_bio_GOM_HAD(1,nyrs); //32.
vector obs_bio_GOM_YTL(1,nyrs); //33.
vector obs_bio_GOM_WFL(1,nyrs); //34.
vector obs_bio_GOM_LSK(1,nyrs); //35.
vector obs_bio_GOM_COD(1,nyrs); //36.
vector obs_bio_GOM_SFL(1,nyrs); //37.
vector obs_bio_GOM_SHK(1,nyrs); //38.
vector obs_bio_GOM_SPD(1,nyrs); //39.
vector obs_bio_GOM_WSK(1,nyrs); //40.
vector obs_bio_GOM_GOS(1,nyrs); //41.
vector obs_bio_GOM_POL(1,nyrs); //42
```

```

vector obs_bio_GOM_WHK(1,nyrs); //43.
vector obs_bio_GOM_HER(1,nyrs); //44.
vector obs_bio_GOM_MCK(1,nyrs); //45.
vector obs_bio_GOM_SQD(1,nyrs); //46.
vector obs_cat_GOM_HAD(1,nyrs); //47
vector obs_cat_GOM_YTL(1,nyrs); //48.
vector obs_cat_GOM_WFL(1,nyrs); //49.
vector obs_cat_GOM_LSK(1,nyrs); //50.
vector obs_cat_GOM_COD(1,nyrs); //51.
vector obs_cat_GOM_SFL(1,nyrs); //52.
vector obs_cat_GOM_SHK(1,nyrs); //53.
vector obs_cat_GOM_SPD(1,nyrs); //54.
vector obs_cat_GOM_WSK(1,nyrs); //55.
vector obs_cat_GOM_GOS(1,nyrs); //56.
vector obs_cat_GOM_POL(1,nyrs); //57
vector obs_cat_GOM_WHK(1,nyrs); //58.
vector obs_cat_GOM_HER(1,nyrs); //59.
vector obs_cat_GOM_MCK(1,nyrs); //60.
vector obs_cat_GOM_SQD(1,nyrs); //61.

// Southern New England biomass and catch data
vector obs_bio_SNE_YTL(1,nyrs); //62.
vector obs_bio_SNE_WFL(1,nyrs); //63.
vector obs_bio_SNE_LSK(1,nyrs); //64.
vector obs_bio_SNE_SFL(1,nyrs); //65.
vector obs_bio_SNE_SHK(1,nyrs); //66.
vector obs_bio_SNE_SPD(1,nyrs); //67.
vector obs_bio_SNE_WSK(1,nyrs); //68.
vector obs_bio_SNE_GOS(1,nyrs); //69.
vector obs_bio_SNE_POL(1,nyrs); //61.
vector obs_bio_SNE_WHK(1,nyrs); //71.
vector obs_bio_SNE_HER(1,nyrs); //72.
vector obs_bio_SNE_MCK(1,nyrs); //73.
vector obs_bio_SNE_SQD(1,nyrs); //74.
vector obs_cat_SNE_YTL(1,nyrs); //75.
vector obs_cat_SNE_WFL(1,nyrs); //76.
vector obs_cat_SNE_LSK(1,nyrs); //77.
vector obs_cat_SNE_SFL(1,nyrs); //78.
vector obs_cat_SNE_SHK(1,nyrs); //79.
vector obs_cat_SNE_SPD(1,nyrs); //80.
vector obs_cat_SNE_WSK(1,nyrs); //81.
vector obs_cat_SNE_GOS(1,nyrs); //82.
vector obs_cat_SNE_POL(1,nyrs); //83
vector obs_cat_SNE_WHK(1,nyrs); //84.
vector obs_cat_SNE_HER(1,nyrs); //85.
vector obs_cat_SNE_MCK(1,nyrs); //86.
vector obs_cat_SNE_SQD(1,nyrs); //87.

//observed biomass and catch for each group
vector obs_bio_B_GB(1,nyrs);
vector obs_cat_B_GB(1,nyrs);
vector obs_bio_S_GB(1,nyrs);
vector obs_cat_S_GB(1,nyrs);
vector obs_bio_F_GB(1,nyrs);
vector obs_cat_F_GB(1,nyrs);
vector obs_bio_P_GB(1,nyrs);

```

```

vector obs_cat_P_GB(1,nyrs);
vector obs_bio_B_GOM(1,nyrs);
vector obs_cat_B_GOM(1,nyrs);
vector obs_bio_S_GOM(1,nyrs);
vector obs_cat_S_GOM(1,nyrs);
vector obs_bio_F_GOM(1,nyrs);
vector obs_cat_F_GOM(1,nyrs);
vector obs_bio_P_GOM(1,nyrs);
vector obs_cat_P_GOM(1,nyrs);
vector obs_bio_B_SNE(1,nyrs);
vector obs_cat_B_SNE(1,nyrs);
vector obs_bio_S_SNE(1,nyrs);
vector obs_cat_S_SNE(1,nyrs);
vector obs_bio_F_SNE(1,nyrs);
vector obs_cat_F_SNE(1,nyrs);
vector obs_bio_P_SNE(1,nyrs);
vector obs_cat_P_SNE(1,nyrs);
vector obs_bio_F_tot(1,nyrs);
vector obs_cat_F_tot(1,nyrs);
vector obs_bio_P_tot(1,nyrs);
vector obs_cat_P_tot(1,nyrs);

```

```

int i; //declaring an integer i for loops
int j;

```

#### LOCAL\_CALC

```

Year=column(Data,1);

```

```

// Georges Bank

```

```

//Migrating Piscivores(F) = Silver hake, spiny dogfish, Winter skate, Goosefish, Pollock, White hake
obs_bio_F_tot = column(Data,8) + column(Data,9) + column(Data,10) + column(Data,11) +
column(Data,12) + column(Data,13) + column(Data,38) + column(Data,39) + column(Data,40) +
column(Data,41) + column(Data,42) + column(Data,43) + column(Data,66) + column(Data,67) +
column(Data,68) + column(Data,69) + column(Data,70) + column(Data,71);

```

```

obs_cat_F_tot = column(Data,23) + column(Data,24) + column(Data,25) + column(Data,26) +
column(Data,27) + column(Data,28) + column(Data,53) + column(Data,54) + column(Data,55)+
column(Data,56) + column(Data,57) + column(Data,58) + column(Data,79) + column(Data,80) +
column(Data,81) + column(Data,82) + column(Data,83) + column(Data,84);

```

```

//Migrating Planktivores(P) = Atlantic herring, Mackerel, Longfin squid

```

```

obs_bio_P_tot=column(Data,14)+column(Data,15)+column(Data,16)+column(Data,44)+column(Data,45)+column(Data,46)+column(Data,72)+column(Data,73)+column(Data,74);

```

```

obs_cat_P_tot=column(Data,59)+column(Data,60)+column(Data,61)+column(Data,29)+column(Data,30)+column(Data,31)+column(Data,85)+column(Data,86)+column(Data,87);

```

```

obs_bio_P_GB = column(Data,14)+column(Data,15)+column(Data,16);
obs_cat_P_GB = column(Data,29)+column(Data,30)+column(Data,31) ;

```

```

obs_bio_P_GOM = column(Data,44)+column(Data,45)+column(Data,46);
obs_cat_P_GOM = column(Data,59)+column(Data,60)+column(Data,61) ;

```

```

obs_bio_P_SNE = column(Data,72)+column(Data,73)+column(Data,74);
obs_cat_P_SNE = column(Data,85)+column(Data,86)+column(Data,87) ;

```

```

obs_bio_F_GB = column(Data,8) + column(Data,9) + column(Data,10) + column(Data,11)
+column(Data,12) + column(Data,13);
obs_cat_F_GB = column(Data,23) + column(Data,24) + column(Data,25) + column(Data,26) +
column(Data,27) + column(Data,28);

obs_bio_F_GOM = column(Data,38) + column(Data,39) + column(Data,40)+ column(Data,41)+
column(Data,42)+ column(Data,43);
obs_cat_F_GOM = column(Data,53) + column(Data,54) + column(Data,55)+ column(Data,56)+
column(Data,57)+ column(Data,58);

obs_bio_F_SNE = column(Data,66) + column(Data,67) + column(Data,68)+ column(Data,69)+
column(Data,70)+ column(Data,71);
obs_cat_F_SNE = column(Data,79) + column(Data,80) + column(Data,81)+ column(Data,82)+
column(Data,83)+ column(Data,84);

obs_bio_B_GB = column(Data,2) + column(Data,3) + column(Data,4) + column(Data,5);
obs_cat_B_GB = column(Data,17) + column(Data,18) + column(Data,19) + column(Data,20);

obs_bio_B_GOM = column(Data,32) + column(Data,33) + column(Data,34) + column(Data,35);
obs_cat_B_GOM = column(Data,47) + column(Data,48) + column(Data,49) + column(Data,50);

obs_bio_B_SNE = column(Data,62) + column(Data,63) + column(Data,64);
obs_cat_B_SNE = column(Data,75) + column(Data,76) + column(Data,77);

//Non-migrating Piscivores(S) = Atlantic cod, Summer flounder
obs_bio_S_GB = column(Data,6) + column(Data,7);
obs_cat_S_GB = column(Data,21)+ column(Data,22);

obs_bio_S_GOM = column(Data,36) + column(Data,37);
obs_cat_S_GOM = column(Data,51) + column(Data,52);

obs_bio_S_SNE = column(Data,65);
obs_cat_S_SNE = column(Data,78);

END_CALCUS
// Penalty function with pseudocode by defining a target value for carrying capacity (K)
number k_pseudo_B_GB;
!!k_pseudo_B_GB=max(obs_bio_B_GB)*3;
number k_pseudo_B_GOM;
!!k_pseudo_B_GOM=max(obs_bio_B_GOM)*2;
number k_pseudo_B_SNE;
!!k_pseudo_B_SNE=max(obs_bio_B_SNE)*2;
number k_pseudo_F_tot;
!!k_pseudo_F_tot=max(obs_bio_F_tot)*1.5;
number k_pseudo_P_tot;
!!k_pseudo_P_tot=max(obs_bio_P_tot)*1.5;

//!!cout<<"k_pseudo_F_tot = "<<k_pseudo_F_tot<<endl;
//!!cout<<"log(k_pseudo_B_GB) = "<<log(k_pseudo_B_GB)<<endl;
//!!exit(55);

PARAMETER_SECTION
//"single-species" parameters:
init_bounded_number log_r_P_tot(-4.6,-0.11);
number r_P_tot;

```

```

init_bounded_number log_k_P_tot(1.0,10.0);
number k_P_tot;
init_bounded_number log_B0_P_tot(1.0,10.0);
number B0_P_tot;

init_bounded_number log_r_F_tot(-4.6,-0.11);
number r_F_tot;
init_bounded_number log_k_F_tot(1.0,10.0);
number k_F_tot;
init_bounded_number log_B0_F_tot(1.0,10.0);
number B0_F_tot;

init_bounded_number log_r_B_GB(-4.6,-0.11);
number r_B_GB;
init_bounded_number log_k_B_GB(1.0,10.0);
number k_B_GB;
init_bounded_number log_B0_B_GB(1.0,10.0);
number B0_B_GB;

init_bounded_number log_r_B_GOM(-4.6,-0.11);
number r_B_GOM;
init_bounded_number log_k_B_GOM(1.0,10.0);
number k_B_GOM;
init_bounded_number log_B0_B_GOM(1.0,10.0);
number B0_B_GOM;

init_bounded_number log_r_B_SNE(-4.6,-0.11);
number r_B_SNE;
init_bounded_number log_k_B_SNE(1.0,10.0);
number k_B_SNE;
init_bounded_number log_B0_B_SNE(1.0,10.0);
number B0_B_SNE;

init_bounded_number log_r_S_GB(-4.6,-0.11);
number r_S_GB;
init_number k_S_GB(-1); //fixed value for carrying capacity
init_number log_B0_S_GB;
number B0_S_GB;

init_bounded_number log_r_S_GOM(-4.6,-0.11);
number r_S_GOM;
init_number k_S_GOM(-1); //fixed value for carrying capacity
init_number log_B0_S_GOM;
number B0_S_GOM;

init_bounded_number log_r_S_SNE(-4.6,-0.11);
number r_S_SNE;
init_number k_S_SNE(-1); //fixed value for carrying capacity
init_number log_B0_S_SNE;
number B0_S_SNE;

// Type 1 for P and B group
init_bounded_number log_n_PB_GB(-16.0,-2.3,2);
number n_PB_GB;

```

```

init_bounded_number log_n_BP_SNE(-16.0,-2.3,2);
number n_BP_SNE;

// Type 3 for F and B group in Georges Bank
init_bounded_number log_c_fb_GB(-16.0,-2.3,3);
number c_fb_GB;
init_bounded_number log_d_fb_GB(-16.0,-2.3,3);
number d_fb_GB;
init_bounded_number log_alpha_fb_GB(-16.0,-2.3,3);
number alpha_fb_GB;
init_bounded_number log_alpha_fp_GB(-16.0,-2.3,3);
number alpha_fp_GB;

// Type 3 for F and B group in Gulf of Maine
init_bounded_number log_c_fb_GOM(-16.0,-2.3,3);
number c_fb_GOM;
//init_bounded_number log_d_fb_GOM(-16.0,-2.3,3);
//number d_fb_GOM;
init_bounded_number log_alpha_fb_GOM(-16.0,-2.3,3);
number alpha_fb_GOM;
init_bounded_number log_alpha_fp_GOM(-16.0,-2.3,3);
number alpha_fp_GOM;

//predicted biomass for each group
vector pred_bio_P_tot(1,nyrs);
vector pred_bio_F_tot(1,nyrs);
vector prop_GB_P(1,nyrs);
vector prop_GOM_P(1,nyrs);
vector prop_SNE_P(1,nyrs);
vector pred_bio_P_GB(1,nyrs);
vector pred_bio_P_GOM(1,nyrs);
vector pred_bio_P_SNE(1,nyrs);
vector prop_GB_F(1,nyrs);
vector prop_GOM_F(1,nyrs);
vector prop_SNE_F(1,nyrs);
vector pred_bio_F_GB(1,nyrs);
vector pred_bio_F_GOM(1,nyrs);
vector pred_bio_F_SNE(1,nyrs);
vector pred_bio_B_GB(1,nyrs);
vector pred_bio_B_GOM(1,nyrs);
vector pred_bio_B_SNE(1,nyrs);
vector pred_bio_B_tot(1,nyrs);
vector pred_bio_S_SNE(1,nyrs);
vector pred_bio_S_GOM(1,nyrs);
vector pred_bio_S_GB(1,nyrs);

//make numbers to use in f penalty (fpens)
number fpenP_tot;
number fpenF_tot;
number fpenB_GB;
number fpenB_GOM;
number fpenB_SNE;
number fpenS_SNE;
number fpenS_GOM;
number fpenS_GB;
number p;

```

```

number y;
  number AIC;

// Define p and y to calculate AIC & sum of squared residuals (SSR)
!!p = 30; // number of parameters
!!y = nyrs*8; // number of guilds: 8

// create sdreport numbers (puts all parameters in .std file)
sdreport_number sd_r_P_tot;
sdreport_number sd_k_P_tot;
sdreport_number sd_B0_P_tot;
sdreport_number sd_r_F_tot;
sdreport_number sd_k_F_tot;
sdreport_number sd_B0_F_tot;
sdreport_number sd_r_B_GB;
sdreport_number sd_B0_B_GB;
sdreport_number sd_r_B_GOM;
sdreport_number sd_k_B_GOM;
sdreport_number sd_B0_B_GOM;
sdreport_number sd_r_B_SNE;
sdreport_number sd_k_B_SNE;
sdreport_number sd_B0_B_SNE;
sdreport_number sd_r_S_SNE;
sdreport_number sd_B0_S_SNE;
sdreport_number sd_r_S_GOM;
sdreport_number sd_B0_S_GOM;
sdreport_number sd_r_S_GB;
sdreport_number sd_B0_S_GB;

objective_function_value f;

INITIALIZATION_SECTION
  log_r_P_tot -1.29
  log_k_P_tot 8.44
  log_B0_P_tot 6.88

  log_r_F_tot -1.98
  log_k_F_tot 8.29
  log_B0_F_tot 7.6

  log_r_B_GB -1.34
  log_k_B_GB 6.05
  log_B0_B_GB 5.3

  log_r_B_GOM -0.93
  log_k_B_GOM 4.39
  log_B0_B_GOM 3.95

  log_r_B_SNE -0.62
  log_k_B_SNE 5.4
  log_B0_B_SNE 4.84

  log_r_S_GB -0.49
  log_B0_S_GB 4.87
  k_S_GB 300

```

```

log_r_S_GOM -0.246
log_B0_S_GOM 3.42
k_S_GOM 80

log_r_S_SNE -0.22
log_B0_S_SNE 4.1
k_S_SNE 100

// Type 1 functional response for interaction between B and P (GB & SNE)
log_n_PB_GB -6.6
log_n_BP_SNE -5.9

// Type 3 functional response for interaction between B and F in Georges Bank
log_c_fb_GB -4.7
log_d_fb_GB -4.8
log_alpha_fb_GB -4.4
log_alpha_fp_GB -2.5

// Type 3 functional response for interaction between B and F in Gulf of Maine
log_c_fb_GOM -4.8
//log_d_fb_GOM -5.4
log_alpha_fb_GOM -3.9
log_alpha_fp_GOM -3.1

PRELIMINARY_CALCS_SECTION
// proportion of each area to total area
prop_GB_P = elem_div(obs_bio_P_GB,obs_bio_P_tot);
prop_GOM_P = elem_div(obs_bio_P_GOM,obs_bio_P_tot);
prop_SNE_P = elem_div(obs_bio_P_SNE,obs_bio_P_tot);

prop_GB_F = elem_div(obs_bio_F_GB,obs_bio_F_tot);
prop_GOM_F = elem_div(obs_bio_F_GOM,obs_bio_F_tot);
prop_SNE_F = elem_div(obs_bio_F_SNE,obs_bio_F_tot);

PROCEDURE_SECTION
r_P_tot = mfexp(log_r_P_tot);
k_P_tot = mfexp(log_k_P_tot);
B0_P_tot = mfexp(log_B0_P_tot);

r_F_tot = mfexp(log_r_F_tot);
k_F_tot = mfexp(log_k_F_tot);
B0_F_tot = mfexp(log_B0_F_tot);

r_B_GB = mfexp(log_r_B_GB);
k_B_GB = mfexp(log_k_B_GB);
B0_B_GB = mfexp(log_B0_B_GB);

r_B_GOM = mfexp(log_r_B_GOM);
k_B_GOM = mfexp(log_k_B_GOM);
B0_B_GOM = mfexp(log_B0_B_GOM);

r_B_SNE = mfexp(log_r_B_SNE);
k_B_SNE = mfexp(log_k_B_SNE);
B0_B_SNE = mfexp(log_B0_B_SNE);

```

```

r_S_GB = mfexp(log_r_S_GB);
B0_S_GB = mfexp(log_B0_S_GB);

r_S_GOM = mfexp(log_r_S_GOM);
B0_S_GOM = mfexp(log_B0_S_GOM);

r_S_SNE = mfexp(log_r_S_SNE);
B0_S_SNE = mfexp(log_B0_S_SNE);

n_PB_GB = mfexp(log_n_PB_GB);
n_BP_SNE = mfexp(log_n_BP_SNE);

c_fb_GB = mfexp(log_c_fb_GB);
d_fb_GB = mfexp(log_d_fb_GB);
alpha_fb_GB = mfexp(log_alpha_fb_GB);
alpha_fp_GB = mfexp(log_alpha_fp_GB);

c_fb_GOM = mfexp(log_c_fb_GOM);
//d_fb_GOM = mfexp(log_d_fb_GOM);
alpha_fb_GOM = mfexp(log_alpha_fb_GOM);
alpha_fp_GOM = mfexp(log_alpha_fp_GOM);

//cout statements useful for viewing parameters
cout << "r_P_tot " << '\t' << r_P_tot << endl;
cout << "k_P_tot " << '\t' << k_P_tot << endl;
cout << "B0_P_tot" << '\t' << B0_P_tot << endl;

cout << "r_F_tot " << '\t' << r_F_tot << endl;
cout << "k_F_tot " << '\t' << k_F_tot << endl;
cout << "B0_F_tot" << '\t' << B0_F_tot << endl;

cout << "r_B_GB " << '\t' << r_B_GB << endl;
cout << "k_B_GB " << '\t' << k_B_GB << endl;
cout << "B0_B_GB " << '\t' << B0_B_GB << endl;

cout << "r_B_GOM " << '\t' << r_B_GOM << endl;
cout << "k_B_GOM " << '\t' << k_B_GOM << endl;
cout << "B0_B_GOM " << '\t' << B0_B_GOM << endl;

cout << "r_B_SNE " << '\t' << r_B_SNE << endl;
cout << "k_B_SNE " << '\t' << k_B_SNE << endl;
cout << "B0_B_SNE " << '\t' << B0_B_SNE << endl;

cout << "r_S_GB " << '\t' << r_S_GB << endl;
cout << "k_S_GB " << '\t' << k_S_GB << endl;
cout << "B0_S_GB " << '\t' << B0_S_GB << endl;

cout << "r_S_GOM " << '\t' << r_S_GOM << endl;
cout << "k_S_GOM " << '\t' << k_S_GOM << endl;
cout << "B0_S_GOM " << '\t' << B0_S_GOM << endl;

cout << "r_S_SNE " << '\t' << r_S_SNE << endl;
cout << "k_S_SNE " << '\t' << k_S_SNE << endl;
cout << "B0_S_SNE " << '\t' << B0_S_SNE << endl;

```

```

cout << "n_PB_GB  " << '\t' << n_PB_GB << endl;
cout << "n_BP_SNE  " << '\t' << n_BP_SNE << endl;

cout << "c_fb_GB  " << '\t' << c_fb_GB << endl;
cout << "d_fb_GB  " << '\t' << d_fb_GB << endl;
cout << "alpha_fb_GB" << '\t' << alpha_fb_GB << endl;
cout << "alpha_fp_GB" << '\t' << alpha_fp_GB << endl;

    cout << "c_fb_GOM  " << '\t' << c_fb_GOM << endl;
//cout << "d_fb_GOM  " << '\t' << d_fb_GOM << endl;
cout << "alpha_fb_GOM" << '\t' << alpha_fb_GOM << endl;
cout << "alpha_fp_GOM" << '\t' << alpha_fp_GOM << endl;

//reset fpens to 0.0
fpenP_tot = 0.0;
fpenF_tot = 0.0;

fpenB_GB = 0.0;
fpenB_GOM = 0.0;
fpenB_SNE = 0.0;

fpenS_SNE = 0.0;
fpenS_GOM = 0.0;
fpenS_GB = 0.0;

//define sdreport numbers
sd_r_P_tot = r_P_tot;
sd_k_P_tot = k_P_tot;
sd_B0_P_tot = B0_P_tot;

sd_r_F_tot = r_F_tot;
sd_k_F_tot = k_F_tot;
sd_B0_F_tot = B0_F_tot;

sd_r_B_GB = r_B_GB;
sd_k_B_GB = k_B_GB;
sd_B0_B_GB = B0_B_GB;

sd_r_B_GOM = r_B_GOM;
sd_k_B_GOM = k_B_GOM;
sd_B0_B_GOM = B0_B_GOM;

sd_r_B_SNE = r_B_SNE;
sd_k_B_SNE = k_B_SNE;
sd_B0_B_SNE = B0_B_SNE;

sd_r_S_GB = r_S_GB;
sd_B0_S_GB = B0_S_GB;

sd_r_S_GOM = r_S_GOM;
sd_B0_S_GOM = B0_S_GOM;

sd_r_S_SNE = r_S_SNE;

```

```

sd_B0_S_SNE = B0_S_SNE;

sd_n_PB_GB = n_PB_GB;
sd_n_BP_SNE = n_BP_SNE;

sd_c_fb_GB = c_fb_GB;
sd_d_fb_GB = d_fb_GB;
sd_alpha_fb_GB = alpha_fb_GB;
sd_alpha_fp_GB = alpha_fp_GB;

sd_c_fb_GOM = c_fb_GOM;
//sd_d_fb_GOM = d_fb_GOM;
sd_alpha_fb_GOM = alpha_fb_GOM;
sd_alpha_fp_GOM = alpha_fp_GOM;

//initial biomass
pred_bio_P_tot(1) = B0_P_tot;
pred_bio_F_tot(1) = B0_F_tot;
pred_bio_B_GB(1) = B0_B_GB;
pred_bio_B_GOM(1) = B0_B_GOM;
pred_bio_B_SNE(1) = B0_B_SNE;

pred_bio_S_SNE(1) = B0_S_SNE;
pred_bio_S_GOM(1) = B0_S_GOM;
pred_bio_S_GB(1) = B0_S_GB;
pred_bio_P_GB(1) = prop_GB_P(1)*pred_bio_P_tot(1);
pred_bio_P_GOM(1) = prop_GOM_P(1)*pred_bio_P_tot(1);
pred_bio_P_SNE(1) = prop_SNE_P(1)*pred_bio_P_tot(1);
pred_bio_F_GB(1) = prop_GB_F(1)*pred_bio_F_tot(1);
pred_bio_F_GOM(1) = prop_GOM_F(1)*pred_bio_F_tot(1);
pred_bio_F_SNE(1) = prop_SNE_F(1)*pred_bio_F_tot(1);
pred_bio_B_tot(1)=pred_bio_B_GB(1)+pred_bio_B_GOM(1)+pred_bio_B_SNE(1);

//loop through all years to calculate predicted biomass
for (i = 1; i<= nyrs-1; i++)
{
pred_bio_P_tot(i+1)=posfun(pred_bio_P_tot(i)+r_P_tot*pred_bio_P_tot(i)*(1-
pred_bio_P_tot(i)/k_P_tot)-obs_cat_P_tot(i)-
n_PB_GB*(prop_GB_P(i)*pred_bio_P_tot(i))*pred_bio_B_GB(i),0.01,fpenP_tot);

pred_bio_F_tot(i+1)=posfun(pred_bio_F_tot(i)+r_F_tot*pred_bio_F_tot(i)*(1-
pred_bio_F_tot(i)/k_F_tot)-obs_cat_F_tot(i)+
(d_fb_GB*(prop_GB_F(i)*pred_bio_F_tot(i))*(pred_bio_B_GB(i)*pred_bio_B_GB(i)))/
(1+alpha_fb_GB*(pred_bio_B_GB(i)*pred_bio_B_GB(i))+alpha_fp_GB*((prop_GB_P(i)*pred_bio
_P_tot(i))*(prop_GB_P(i)*pred_bio_P_tot(i)))) ,0.01,fpenF_tot);

pred_bio_B_GB(i+1)=posfun(pred_bio_B_GB(i)+r_B_GB*pred_bio_B_GB(i)*(1-
pred_bio_B_GB(i)/k_B_GB)-obs_cat_B_GB(i)-
(c_fb_GB*(prop_GB_F(i)*pred_bio_F_tot(i))*(pred_bio_B_GB(i)*pred_bio_B_GB(i)))/
(1+alpha_fb_GB*(pred_bio_B_GB(i)*pred_bio_B_GB(i))+alpha_fp_GB*((prop_GB_P(i)*pred_bio
_P_tot(i))*(prop_GB_P(i)*pred_bio_P_tot(i)))) ,0.01,fpenB_GB);

pred_bio_B_GOM(i+1)=posfun(pred_bio_B_GOM(i)+r_B_GOM*pred_bio_B_GOM(i)*(1-
pred_bio_B_GOM(i)/k_B_GOM)-obs_cat_B_GOM(i)

```

```

- (c_fb_GOM*(prop_GOM_F(i)*pred_bio_F_tot(i))*(pred_bio_B_GOM(i)*pred_bio_B_GOM(i))/
(1+alpha_fb_GOM*(pred_bio_B_GOM(i)*pred_bio_B_GOM(i))+
alpha_fp_GOM*( (prop_GOM_P(i)*pred_bio_P_tot(i))*(prop_GOM_P(i)*pred_bio_P_tot(i))))
,0.01,fpenB_GOM);

pred_bio_B_SNE(i+1)=posfun(pred_bio_B_SNE(i)+r_B_SNE*pred_bio_B_SNE(i)*(1-
pred_bio_B_SNE(i)/k_B_SNE)-obs_cat_B_SNE(i)
-n_BP_SNE*pred_bio_B_SNE(i)*(prop_SNE_P(i)*pred_bio_P_tot(i))
,0.01,fpenB_SNE);

pred_bio_S_GOM(i+1)=posfun(pred_bio_S_GOM(i)+r_S_GOM*pred_bio_S_GOM(i)*(1-
pred_bio_S_GOM(i)/k_S_GOM)-obs_cat_S_GOM(i)
,0.01,fpenS_GOM);

pred_bio_S_SNE(i+1)=posfun(pred_bio_S_SNE(i)+r_S_SNE*pred_bio_S_SNE(i)*(1-
pred_bio_S_SNE(i)/k_S_SNE)-obs_cat_S_SNE(i)
,0.01,fpenS_SNE);

pred_bio_S_GB(i+1)=posfun(pred_bio_S_GB(i)+r_S_GB*pred_bio_S_GB(i)*(1-
pred_bio_S_GB(i)/k_S_GB)-obs_cat_S_GB(i)
,0.01,fpenS_GB);
}

//tell us about fpens
if(fpenP_tot>0) cout << "FPEN P_tot=" << endl << fpenP_tot << endl;
if(fpenF_tot>0) cout << "FPEN F_tot=" << endl << fpenF_tot << endl;

if(fpenB_GB>0) cout << "FPEN B_GB=" << endl << fpenB_GB << endl;
if(fpenB_GOM>0) cout << "FPEN B_GOM=" << endl << fpenB_GOM << endl;
if(fpenB_SNE>0) cout << "FPEN B_SNE=" << endl << fpenB_SNE << endl;

if(fpenS_GOM>0) cout << "FPEN S_GOM=" << endl << fpenS_GOM << endl;
if(fpenS_SNE>0) cout << "FPEN S_SNE=" << endl << fpenS_SNE << endl;
if(fpenS_GB>0) cout << "FPEN S_GB=" << endl << fpenS_GB << endl;

//the objective function for total biomass of migrating Planktivores and Piscivores
dvar_vector resid_P_tot = (log(pred_bio_P_tot(1,nyrs)+1.e-3) - log(obs_bio_P_tot(1,nyrs)+1.e-3));
dvariable ssq_P_tot = norm2(resid_P_tot) + square(log(k_pseudo_P_tot) - log(k_P_tot));

dvar_vector resid_F_tot = (log(pred_bio_F_tot(1,nyrs)+1.e-3) - log(obs_bio_F_tot(1,nyrs)+1.e-3));
dvariable ssq_F_tot = norm2(resid_F_tot) + square(log(k_pseudo_F_tot) - log(k_F_tot));

// additional objective function of Benthivores (GB, GoM, SNE)
dvar_vector resid_B_GB = (log(pred_bio_B_GB(1,nyrs)+1.e-3) - log(obs_bio_B_GB(1,nyrs)+1.e-3));
dvariable ssq_B_GB = norm2(resid_B_GB) + square(log(k_pseudo_B_GB) - log(k_B_GB));

dvar_vector resid_B_GOM = (log(pred_bio_B_GOM(1,nyrs)+1.e-3) -
log(obs_bio_B_GOM(1,nyrs)+1.e-3));
dvariable ssq_B_GOM = norm2(resid_B_GOM) + square(log(k_pseudo_B_GOM) - log(k_B_GOM));

dvar_vector resid_B_SNE = (log(pred_bio_B_SNE(1,nyrs)+1.e-3) - log(obs_bio_B_SNE(1,nyrs)+1.e-
3));
dvariable ssq_B_SNE = norm2(resid_B_SNE) + square(log(k_pseudo_B_SNE) - log(k_B_SNE));

```

```

dvar_vector resid_S_GOM = (log(pred_bio_S_GOM(1,nyrs)+1.e-3) -
  log(obs_bio_S_GOM(1,nyrs)+1.e-3));
dvariable ssq_S_GOM = norm2(resid_S_GOM);

dvar_vector resid_S_SNE = (log(pred_bio_S_SNE(1,nyrs)+1.e-3) - log(obs_bio_S_SNE(1,nyrs)+1.e-
3));
dvariable ssq_S_SNE = norm2(resid_S_SNE);

dvar_vector resid_S_GB = (log(pred_bio_S_GB(1,nyrs)+1.e-3) - log(obs_bio_S_GB(1,nyrs)+1.e-3));
dvariable ssq_S_GB = norm2(resid_S_GB);

f = ssq_P_tot + ssq_F_tot + ssq_B_GB + ssq_B_GOM + ssq_B_SNE + ssq_S_GOM + ssq_S_SNE +
  ssq_S_GB;

cout << "obj func value - SSR" << "\t" << f << endl;
cout << "ssqP_tot" << "\t" << ssq_P_tot << endl;
cout << "ssqF_tot" << "\t" << ssq_F_tot << endl;
cout << "ssqB_GB " << "\t" << ssq_B_GB << endl;
cout << "ssqB_GOM " << "\t" << ssq_B_GOM << endl;
cout << "ssqB_SNE " << "\t" << ssq_B_SNE << endl;
cout << "ssqS_GOM" << "\t" << ssq_S_GB << endl;
cout << "ssqS_GOM" << "\t" << ssq_S_GOM << endl;
cout << "ssqS_GOM" << "\t" << ssq_S_SNE << endl;
cout << endl;

//calculate negative loglikelihood (nll) and AIC
dvariable nll = 0.5*y*log(f);
dvariable AIC = 2*nll + 2*p*(y/(y-p-1));

cout << "Negative Ln Likelihood (-Ln(L))" << "\t" << nll << endl;
cout << "AIC" << "\t" << AIC << endl << endl;

RUNTIME_SECTION
maximum_function_evaluations 40000;

REPORT_SECTION
  report<<"observed biomass_P_tot" << obs_bio_P_tot << endl;
  report<<"predicted biomass_P_tot" << pred_bio_P_tot << endl;
  report<<"obs_catch_P_tot" << obs_cat_P_tot << endl;
  report<<"<<endl;

  report<<"observed biomass_F_tot: " << obs_bio_F_tot << endl;
  report<<"predicted biomass_F_tot: " << pred_bio_F_tot << endl;
  report<<"obs_catch_F_tot: " << obs_cat_F_tot << endl;
  report<<"<<endl;

  report<<"observed biomass_B_GB"<<obs_bio_B_GB<<endl;
  report<<"predicted biomass_B_GB"<<pred_bio_B_GB<<endl;
  report<<"obs_catch_B_GB"<<obs_cat_B_GB<<endl;
  report<<"<<endl;

  report<<"observed biomass_B_GOM"<<obs_bio_B_GOM<<endl;
  report<<"predicted biomass_B_GOM"<<pred_bio_B_GOM<<endl;

```

```

report<<"obs_catch_B_GOM"<<obs_cat_B_GOM<<endl;
report<<"<<endl;

report<<"observed biomass_B_SNE"<<obs_bio_B_SNE<<endl;
report<<"predicted biomass_B_SNE"<<pred_bio_B_SNE<<endl;
report<<"obs_catch_B_SNE"<<obs_cat_B_SNE<<endl;
report<<"<<endl;

report<<"observed biomass_S_GB"<<obs_bio_S_GB<<endl;
report<<"predicted biomass_S_GB"<<pred_bio_S_GB<<endl;
report<<"obs_catch_S_GB"<<obs_cat_S_GB<<endl;
report<<"<<endl;

report<<"observed biomass_S_GOM"<<obs_bio_S_GOM<<endl;
report<<"predicted biomass_S_GOM"<<pred_bio_S_GOM<<endl;
report<<"obs_catch_S_GOM"<<obs_cat_S_GOM<<endl;
report<<"<<endl;

report<<"observed biomass_S_SNE"<<obs_bio_S_SNE<<endl;
report<<"predicted biomass_S_SNE"<<pred_bio_S_SNE<<endl;
report<<"obs_catch_S_SNE"<<obs_cat_S_SNE<<endl;
report<<"<<endl;

report<<" prop_GB_P= "<< prop_GB_P << endl;
report<<"<<endl;
report<<" prop_GOM_P= "<< prop_GOM_P << endl;
report<<"<<endl;
report<<" prop_SNE_P= "<< prop_SNE_P << endl;
report<<"<<endl;
report<<" prop_GB_F= "<< prop_GB_F << endl;
report<<"<<endl;
report<<" prop_GOM_F= "<< prop_GOM_F << endl;
report<<"<<endl;
report<<" prop_SNE_F= "<< prop_SNE_F << endl;
report<<"<<endl;

report<<"observed biomass_P_GB: " << obs_bio_P_GB << endl;
report<<"predicted biomass_P_GB="<<"prop_GB_P*pred_bio_P_tot"<<endl;
for (i = 1; i<= nyrs; i++)
{
  report << prop_GB_P(i)*pred_bio_P_tot(i) << endl;
}
report<<"obs_catch_P_GB: " << obs_cat_P_GB << endl;
report<<"<<endl;

report<<"observed biomass_P_GOM: " << obs_bio_P_GOM << endl;
report<<"predicted biomass_P_GOM="<<"prop_GOM_P*pred_bio_P_tot" <<endl;
for (i = 1; i<= nyrs; i++)
{
  report << prop_GOM_P(i)*pred_bio_P_tot(i) << endl;
}

report<<"obs_catch_P_GOM: " << obs_cat_P_GOM << endl;
report<<"<<endl;

```

```

report<<"observed biomass_P_SNE: " << obs_bio_P_SNE << endl;
report<<"predicted biomass_P_SNE="<< "prop_SNE_P*pred_bio_P_tot" <<endl;
for (i = 1; i<= nyrs; i++)
{
  report << prop_SNE_P(i)*pred_bio_P_tot(i) << endl;
}

report<<"obs_catch_P_SNE: " << obs_cat_P_SNE << endl;
report<<" "<<endl;

report<<"observed biomass_F_GB: " << obs_bio_F_GB << endl;
report<<"predicted biomass_F_GB="<< "prop_GB_F*pred_bio_F_tot" <<endl;
for (i = 1; i<= nyrs; i++)
{
  report << prop_GB_F(i)*pred_bio_F_tot(i) << endl;
}

report<<"obs_catch_F_GB: " << obs_cat_F_GB << endl;
report<<" "<<endl;

report<<"observed biomass_F_GOM: " << obs_bio_F_GOM << endl;
report<<"predicted biomass_F_GOM="<< "prop_GOM_F*pred_bio_F_tot" <<endl;
for (i = 1; i<= nyrs; i++)
{
  report << prop_GOM_F(i)*pred_bio_F_tot(i) << endl;
}

report<<"obs_catch_F_GOM: " << obs_cat_F_GOM << endl;
report<<" "<<endl;

report<<"observed biomass_F_SNE: " << obs_bio_F_SNE << endl;
report<<"predicted biomass_F_SNE="<< "prop_SNE_F*pred_bio_F_tot" <<endl;
for (i = 1; i<= nyrs; i++)
{
  report << prop_SNE_F(i)*pred_bio_F_tot(i) << endl;
}

report<<"obs_catch_F_SNE: " << obs_cat_F_SNE << endl;
report<<" "<<endl;

```

## BIBLIOGRAPHY

- Atkinson, D. B., G. A. Rose, E. F. Murphy, and C. A. Bishop. 1997. Distribution changes and abundance of northern cod (*Gadus morhua*), 1981-1993. *Canadian Journal of Fisheries and Aquatic Sciences*, 54 (Suppl. 1): 132-138.
- Bohaboy, E. C. 2010. Multi-species fish population biomass dynamics of Georges Bank. M. Sc. Thesis, Graduate School of Oceanography, University of Rhode Island, Rhode Island.
- Brodziak, J. K. T., E. M. Holmes, K. A. Sosebee, and R. K. Mayo. 2001. Assessment of the silver hake resource in the Northwest Atlantic in 2000. *Northeast Fisheries Science Center Reference Document* 01-03; 134 p. Northeast Fisheries Science Center, Woods Hole, Massachusetts.
- Brodziak, J. K. T. 2002. An age-structured assessment model for Georges Bank winter flounder. *Northeast Fisheries Science Center Reference Document* 02-03; 54 p.
- Buckland, S. T., K. P. Burnham, and N. H. Augustin. 1997. Model selection: an integral part of inference. *Biometrics*, 53: 603-618.
- Burnham, K. P. and D. R. Anderson. 2002. *Model Selection and Multimodel Inference: A Practical Information-Theoretic Approach*. Springer Verlag, New York.
- Burnham, K. P. and D. R. Anderson. 2004. Multimodel Inference: understanding AIC and BIC in model selection. *Sociological Methods and Research*, 33: 261-304.
- Collie, J. S. and A.K. DeLong. 1999. Multispecies interactions in the Georges Bank fish community. In *Ecosystem approaches for fisheries management*. Alaska Sea Grant College Program, AK-SG-99-01, Fairbanks, Alaska. pp. 187-210.

- Collie, J. S. and G. H. Kruse. 1998. Estimating king crab (*Paralithodes camtschaticus*) abundance from commercial catch and research survey data. Proceedings of the North Pacific Symposium on Invertebrate Stock Assessment and Management. G.S. Jamieson and A. Campbell, *editors*. *Canadian Special Publication of Fisheries and Aquatic Sciences*, 125: 73-83.
- Collie, J. S. and P. D. Spencer. 1994. Modeling predator-prey dynamics in a fluctuating environment. *Canadian Journal of Fisheries and Aquatic Sciences*, 51: 2665-2672.
- Curti, K. L., J. S. Collie, C. M. Legault, and J. S. Link. 2013. Evaluating the performance of a multispecies statistical catch-at-age model. *Canadian Journal of Fisheries and Aquatic Sciences*, 70: 1-15.
- DFO (Fisheries and Oceans Canada). 2010. *Transboundary Resources Assessment Committee Status Report 2010/02*. Transboundary Resources Assessment Committee, Fisheries and Oceans Canada.
- Doubleday, W. G. 1981. A method for estimating the abundance of survivors of an exploited fish population using commercial catch-at-age and research vessel abundance indices. *Canadian Special Publication of Fisheries and Aquatic Sciences*, 58: 164-178.
- Doubleday, W. G. and D. Rivard. 1981. Bottom trawl surveys. *Canadian Special Publication of Fisheries and Aquatic Sciences*, 58: 273 pp.
- Drinkwater, K. F. 2006. The regime shift of the 1920s and 1930s in the North Atlantic. *Progress in Oceanography*. 68: 134-151.

- Fogarty, M. J. and S. A. Murawski. 1998. Large-scale disturbance and the structure of marine systems: fishery impacts on Georges Bank. *Ecological Applications*, 8(1): S6-S22.
- Gabriel, W. L. 1992. Persistence of Demersal Fish Assemblages Between Cape Hatteras and Nova Scotia, Northwest Atlantic. *Journal of Northwest Atlantic Fishery Science*, 14: 29-46.
- Garcia, S., P. Sparre, and J. Csirke. 1989. Estimating surplus production and maximum sustainable yield from biomass data when catch and effort time series are not available. *Fishery Research*, 8: 13-23.
- Garrison, L. P. and J. Link. 2000. Fishing effects on spatial distribution and trophic guild structure of the fish community in the Georges Bank region. *ICES Journal of Marine Science*, 57: 723-730.
- Grosslein, M. D., R. W. Langton, and M. P. Sissenwine. 1980. Recent fluctuations in pelagic fish stocks of the northwest Atlantic, Georges Bank Region, in relation to species interactions. *Conseil Permanent International pour L'Exploration de la Mer* 177:374-404.
- Gulland, J. A. 1988. *Fish population dynamics: the implications for management*. 2<sup>nd</sup> edition. Wiley-Interscience Publication, 63-82.
- Hastings, N. A. J. and J. B. Peacock. 1975. *Statistical distributions*. London: Butterworths and Co.
- Hilborn, R. and C. J. Walters. 1992. *Quantitative Fisheries Stock Assessment: Choice, Dynamics & Uncertainty*. Chapman and Hall, New York.

- Holling, C. S. 1959. The components of predation as revealed by a study of small mammal predation of the European pine sawfly. *The Canadian Entomologist*, 91: 293-320.
- Johnson, J. B. and K. S. Omland. 2004. Model selection in ecology and evolution. *Trends in Ecology and Evolution*, 19: 101-108.
- Livingston, P. A. and Jurado-Molina, J. 2000. A multispecies virtual population analysis of the eastern Bering Sea. *Ices Journal of Marine Science*. 57(2): 294-299.
- Mahon, R. S. K. Brown, K. C. T. Zwanenburg, D. B, Atkinson, K. R. Buja, L. Clafin, G. D. Howell, M. E. Monaco, R. N. O'Boyle, and M. Sinclair. 1998. Assemblages and biogeography of demersal fishes of the east coast of North America. *Canadian Journal of Fisheries and Aquatic Sciences*, 55(7): 1704-1738.
- Magnusson, K. G. 1995. An overview of the multispecies VPA – theory and applications. *Reviews in Fish Biology and Fisheries*, 5: 195-212.
- Matsuda, H. and T. Katsukawa. 2002. Fisheries management based on ecosystem dynamics and feedback control. *Fisheries Oceanography*, 11: 366-370.
- May, R. M., J. R. Beddington, C. W. Clark, S. J. Holt, R. M. Laws. 1979. Management of multispecies fisheries. *Science*, 205: 267-275.
- Mayo, R. K., M. J. Fogarty, and F. M. Serchuk. 1992. Aggregate Fish Biomass and Yield on Georges Bank, 1960-87. *Journal of Northwest Atlantic Fishery Science*, 14: 59-78.

- Moustahfid, H., M. C. Tyrrell, J. S. Link, J. A. Nye, B. E. Smith, and R. J. Gamble. 2010. Functional feeding responses of piscivorous fishes from the northeast US continental shelf. *Ecosystem Ecology*, 163: 1059-1067.
- Murawski, S. A. 1993. Climate change and marine fish distributions: forecasting from historical analogy. *Transactions of the American Fisheries Society*, 122: 647-658.
- Northeast Fisheries Science Center (NEFSC). 2008a. 47<sup>th</sup> Northeast Regional Stock Assessment Workshop (47<sup>th</sup> SAW) Assessment Report. U.S. Dept. Commer., *Northeast Fisheries Science Center Reference Document*, 08-12.
- Northeast Fisheries Science Center (NEFSC). 2008b. Assessment of 19 Northeast Groundfish Stocks through 2007: Report of the 3<sup>rd</sup> Groundfish Assessment Review Meeting (GRAM III), Northeast Fisheries Science Center, Woods Hole, Massachusetts, August 4-8, 2008. U.S. Dept. Commer., *Northeast Fisheries Science Center Reference Document*, 08-15.
- Northeast Fisheries Science Center (NEFSC). 2009. The Northeast Data Poor Stocks Working Group Report, December 8-12, 2008 Meeting. Part A. Skate species complex, deep sea red crab, Atlantic wolfish, scup, and black sea bass. U.S. Dept. Commer., *Northeast Fisheries Science Center Reference Document*, 09-02.
- Northeast Fisheries Science Center (NEFSC). 2010. 50<sup>th</sup> Northeast Regional Stock Assessment Workshop (50<sup>th</sup> SAW) Assessment Report. U.S. Dept. Commer., *Northeast Fisheries Science Center Reference Document*, 10-17.

- Northeast Fisheries Science Center (NEFSC). 2011a. 51<sup>st</sup> Northeast Regional Stock Assessment Workshop (51<sup>st</sup> SAW) Assessment Report. U.S. Dept. Commer, *Northeast Fisheries Science Center Reference Document*, 11-02.
- Northeast Fisheries Science Center (NEFSC). 2011b. 52<sup>nd</sup> Northeast Regional Stock Assessment Workshop (52<sup>nd</sup> SAW) Assessment Report. U.S. Dept. Commer, *Northeast Fisheries Science Center Reference Document*, 11-17.
- Northeast Fisheries Science Center (NEFSC). 2012a. 53<sup>rd</sup> Northeast Regional Stock Assessment Workshop (53<sup>rd</sup> SAW) Assessment Report. U.S. Dept. Commer., *Northeast Fisheries Science Center Reference Document*, 12-05.
- Northeast Fisheries Science Center (NEFSC). 2012b. Assessment or Data Updates of 13 Northeast Groundfish Stocks through 2010. U.S. Dept. Commer., *Northeast Fisheries Science Center Reference Document*, 12-06.
- Northeast Fisheries Science Center (NEFSC). 2012c. 54<sup>th</sup> Northeast Regional Stock Assessment Workshop (54<sup>th</sup> SAW) Assessment Report. U.S. Dept. Commer., *Northeast Fisheries Science Center Reference Document*, 12-18.
- Nye, J. A., J. S. Link, J. A. Hare, and W. J. Overholtz. 2009. Changing spatial distribution of fish stocks in relation to climate and population size on the Northeast US continental shelf. *Marine Ecology Progress Series*. 393: 111-129.
- Quinn, T. J. and R. B. Deriso. 1999. *Quantitative Fish Dynamics*. Oxford University Press. 542 pp.
- Overholtz, W. J. and A. V. Tyler. 1985. Long-term responses of the demersal fish assemblages of Georges Bank. *Fishery Bulletin U.S.*, 83: 507-520.

- Overholtz, W. J., J. S. Link, and L. E. Suslowicz. 2000. Consumption of important pelagic fish and squid by predatory fish in the northeastern USA shelf ecosystem with some fishery comparisons. *Ices Journal of Marine Science*. 57:1147-1159.
- Pincin, J. S. and M. J. Wilberg. 2012. Surplus Production Model Accuracy in Populations Affected by a No-Take Marine Protected Area. *Marine and Coastal Fisheries: Dynamics, Management, and Ecosystem Science*, 4(1): 511-525.
- Planque, B., J. M. Fromentin, P. Cury, K. F. Drinkwater, S. Jennings, R.I. Perry, and S. Kifani. 2010. How does fishing alter marine populations and ecosystems sensitivity to climate? *Journal of Marine Systems*, 79: 403-417.
- Punt, A. E. and R. D. Methot. 2004. Effects of marine protected areas on the assessment of marine fisheries. Pages 133-154 in J. B. Shipley, editor. Aquatic protected areas as fisheries management tools. American Fisheries Society, Symposium 42, Bethesda, Maryland.
- Rago, P. J. and K. A. Sosebee. 2010. Biological Reference Points for Spiny Dogfish. *Northeast Fisheries Science Center Reference Document*. 10-06; 52p.
- Rose, G. A. 2005. On distributional responses of North Atlantic fish to climate change. *ICES Journal of Marine Science*, 62: 1360-1374.
- Rose K. A., J. A. Tyler, D. SinghDermot, and E. S. Rutherford. 1996. Multispecies modeling of fish populations. In: Megrey B. A. and E. Moksness. Computers in fisheries research. Chapman and Hall, New York, pp 194-222.

- Schaefer, M. B. 1954. Some aspects of the dynamics of populations important to the management of the commercial marine fisheries. *Inter-American Tropical Tuna Commission Bulletin*, 1(2): 27-56.
- Sissenwine, M. P. 1986. Perturbation of a predator-controlled continental shelf ecosystem. In *Variability and Management of Large Marine Ecosystems*, pp. 55-85. Ed. by K. Sherman, and L. M. Alexander. American Association for the Advancement of Science, Selected Symposium Series, no. 99.
- Sissenwine, M. P., E. B. Cohen, and M. D. Grosslein. 1984. Structure of the Georges Bank ecosystem. *Rapports et Process Verbaux des Reunions, Conseil International pour l'Exploration de la Mer*, 183: 243-254.
- Spencer, P. D. and J. S. Collie. 1995. A simple predator-prey model of exploited fish populations incorporating alternative prey. *ICES Journal of Marine Science*, 53: 615-628.
- Steele, J. H. and E. W. Henderson. 1981. A simple plankton model. *American Naturalist*, 117: 676-691.
- Terceiro, M. 2012. Stock Assessment of summer flounder for 2012. U.S. Dept. Commer., *Northeast Fisheries Science Center Reference Document*, 12-21; 148p.
- Tsou, T. S. and J. S. Collie. 2001a. Estimating predation mortality in the Georges Bank fish community. *Canadian Journal of Fisheries and Aquatic Sciences*, 58: 908-922.
- Tsou, T. S. and T. S. Collie. 2001b. Predation-mediated recruitment in the Georges Bank fish community. *ICES Journal of Marine Sciences*, 58: 994-1001.

- Tyrrell, M. C., H. Moustahfid, J. S. Link, and W. J. Overholtz. 2008. Evaluating the effect of predation mortality on forage species population dynamics in the Northeast US continental shelf ecosystem: an application using multispecies virtual population analysis. *ICES Journal of Marine Science*, 65: 1689-1700.
- Tyrrell, M. C., J. S. Link, and H. Moustahfid. 2011. The importance of including predation in fish population models: Implications for biological reference points. *Fisheries Research*, 108: 1-8.
- Yodzis, P. 1994. Predator-prey theory and the management of multispecies fisheries. *Ecological Applications*, 4: 51-58.